



POLITECNICO DI TORINO

DET - DEPARTMENT OF ELECTRONICS AND TELECOMMUNICATION

Master Degree Course in Biomedical Engineering

Master Degree Thesis

**Smart Glasses system for the  
maculopathy evaluation based on  
Pattern-Reversal Visual Evoked  
Potentials**

**Supervisors**

Prof. Eng. Danilo DEMARCHI  
Eng. Rossana TERRACCIANO  
Eng. Alessandro SANGINARIO

**Candidate**

Luana PULEO

October 2019



# Abstract

- *Objective:* this work aims to test the performance of the *Smart Glasses* system based on pattern-reversal Visual Evoked Potentials (pr-VEPs) in the *ophthalmological clinical context*, validating it through comparison with the commercial *Retimax CSO* system.
- *Materials & Methods:* the portable and cheap *Epson Moverio BT-200 Smart Glasses* are flanked by the *g.HIamp Research* bio-potential amplifier. The EEG signals, obtained by stimulation and taken by electrodes positioned according to International Standard 10/20, are sent to the bio-amplifier that records and processes them through the software *g.Recorder* associated with it. This is followed by further Matlab processing that highlights the characteristics of the waves obtained, in terms of amplitude and latency.
- *Results & Future Goals:* the results obtained through 10 healthy subjects and 30 subjects affected by maculopathy are therefore compared with the ones retrieved through a gold standard device Retimax CSO. Features extracted from time and frequency domain are evaluated by *statistical tools*. The results show a good correlation in both subjects categories. Nevertheless, several limitations emerged from this work, especially those age-related. The future objective is to improve the diagnostic valence of the device considering hardware and software enhancements of the current prototype proposed.

# Contents

|   |     |
|---|-----|
| <b>List of Tables</b>   | VI  |
| <b>List of Figures</b>  | VII |
| <b>1 Introduction</b>   | 1   |
| 1.1 Sensory Coding and Brain Electric Waves . . . . .               | 1   |
| 1.2 Neuroanatomy and Physiology of the Visual System . . . . .      | 2   |
| 1.3 Retina and Retinal diseases: Maculopathy . . . . .              | 5   |
| 1.3.1 Layers and components of the retina . . . . .                 | 5   |
| 1.3.2 Maculopathy disease . . . . .                                 | 6   |
| 1.4 VEPs: Visual Evoked Potentials . . . . .                        | 8   |
| 1.4.1 Flash VEPs . . . . .  | 9   |
| 1.4.2 Pattern VEPs . . . . .  | 10  |
| 1.5 Pattern Reversal VEP Physiological Interpretation . . . . .     | 13  |
| 1.6 Clinical Applications and State of Art . . . . .                | 14  |
| <b>2 Materials and Method</b>                                       | 16  |
| 2.1 Retimax CSO . . . . .   | 16  |
| 2.2 Epson Moverio BT-200 . . . . .                                  | 20  |
| 2.3 g.HIamp-Research . . . . .                                      | 21  |
| 2.3.1 g.HIamp-Research basic component . . . . .                    | 22  |
| 2.3.2 Technical specifications . . . . .                            | 23  |
| 2.4 Data Acquisition: Hardware and Software . . . . .               | 24  |
| 2.4.1 First prototype system for trigger generation . . . . .       | 24  |
| 2.4.2 Second and definitive prototype system for trigger generation | 29  |
| 2.4.3 g.Recorder Software . . . . .                                 | 35  |
| 2.5 Acquisition Protocol for the Experimental Tests . . . . .       | 37  |
| 2.6 Advice for the successful execution of an exam . . . . .        | 41  |
| 2.7 Data Post-processing . . . . .                                  | 43  |
| 2.8 An alternative visual stimulator: the Cardboard . . . . .       | 45  |

|          |   |            |
|----------|---|------------|
| <b>3</b> | <b>Results</b>  | <b>52</b>  |
| 3.1      | Calibration of our Prototype and Acquisitions on Healthy Subjects . | 52         |
| 3.2      | Acquisitions on Pathologic subjects: Experimental Tests . . . . .   | 59         |
| 3.3      | Power Spectral Density (PSD) . . . . .                              | 73         |
| 3.4      | Comparison between filtered 1-100 Hz and 1-30 Hz signals . . . . .  | 87         |
| 3.4.1    | Visual comparison . . . . .   | 88         |
| 3.4.2    | Comparison of the quantity of power . . . . .                       | 92         |
| <b>4</b> | <b>Statistic analysis</b>   | <b>95</b>  |
| 4.1      | Statistic analysis on healthy subjects . . . . .                    | 95         |
| 4.2      | Statistic analysis on pathological subjects . . . . .               | 106        |
| <b>5</b> | <b>Conclusions, Critical points and Future goals</b>                | <b>110</b> |
|          | <b>Bibliography</b>   | <b>116</b> |

# List of Tables

|     |   |     |
|-----|---|-----|
| 2.1 | g.HIamp-Research. . . . .   | 23  |
| 2.2 | Maximum voltages at the sockets. . . . .  | 23  |
| 2.3 | Amplifier Settings for all channels. . . . .  | 23  |
| 2.4 | Analog-digital converter (ADC). . . . .   | 23  |
| 2.5 | Power supply. . . . .   | 24  |
| 2.6 | Delayed P100 wave. . . . .  | 28  |
| 2.7 | Stimulation parameters. . . . .   | 41  |
| 3.1 | Clinical details of the healthy subjects. . . . .   | 52  |
| 3.2 | Left eye: differences between Retimax and Smart Glasses stimulations. . . . .                       | 57  |
| 3.3 | Right eye: differences between Retimax and Smart glasses stimulations. . . . .                      | 57  |
| 3.4 | Clinical details of the pathologic subjects: left eyes. . . . .                                     | 60  |
| 3.5 | Clinical details of the pathologic subjects: right eyes. . . . .                                    | 61  |
| 3.6 | Average of PSD of healthy subjects. . . . .   | 92  |
| 3.7 | Average of PSD of pathological subjects. . . . .  | 92  |
| 3.8 | Wet and Dry maculopathy: quantity of power. . . . .   | 94  |
| 4.1 | Pearson's Coefficients and p-values of the average of the signals, healthy subjects. . . . .        | 96  |
| 4.2 | Pearson's Coefficients and p-values of the signals components, healthy subjects. . . . .            | 97  |
| 4.3 | Pearson's Coefficients and p-values for the amount of signals power, healthy subjects. . . . .      | 98  |
| 4.4 | Average of the Pearson's Coefficients, healthy subjects. . . . .                                    | 98  |
| 4.5 | Left eye: CCC, $\chi_b$ and ICC. . . . .  | 105 |
| 4.6 | Right eye: CCC, $\chi_b$ and ICC. . . . .   | 105 |
| 4.7 | Pearson's Coefficient and p-values of the average of the signals, pathological subjects. . . . .    | 106 |
| 4.8 | Pearson's Coefficients and p-values for the amount of signals power, pathological subjects. . . . . | 106 |
| 4.9 | Average of the Pearson's Coefficients, pathological subjects. . . . .                               | 107 |

# List of Figures

|      |  |    |
|------|--|----|
| 1.1  | Human eye structure [4]. . . . .   | 3  |
| 1.2  | Accommodation mechanism [7]. . . . .   | 4  |
| 1.3  | (a)Light path flow chart;(b)Visual pathway [8]. . . . .  | 4  |
| 1.4  | Layers of the retina [10]. . . . .   | 5  |
| 1.5  | Visual effects of maculopathy progression [13]. . . . .  | 6  |
| 1.6  | (a)Healthy macula VS damage macula [15]; (b)Dry Macular Degeneration [16]. . . . .   | 6  |
| 1.7  | (a)Healthy macula VS damage macula [15]; (b)Wet Macular Degeneration [16]. . . . .   | 7  |
| 1.8  | Typical morphology of a flash VEP [23]. . . . .  | 10 |
| 1.9  | Typical morphology of a on/off pattern VEP [24]. . . . .   | 11 |
| 1.10 | Typical morphology of a pattern reversal VEP [24]. . . . .   | 12 |
| 1.11 | Healthy VS pathological subject. . . . .   | 13 |
| 2.1  | Components of the Retimax CSO system. . . . .  | 17 |
| 2.2  | Nuprep Skin Gel. . . . .   | 17 |
| 2.3  | Skin cup. . . . .  | 18 |
| 2.4  | KONIX EEG Paste. . . . .   | 18 |
| 2.5  | Retimax system while it is working. . . . .  | 19 |
| 2.6  | Retimax system screen. . . . .   | 19 |
| 2.7  | Smart glasses Epson Moverio BT-200 and external touchpad [27]. . . . .   | 20 |
| 2.8  | Features of our prototype. . . . .   | 21 |
| 2.9  | (a) g.HIamp-Research multi-channel biosignal amplifier; (b) 64-channel passive electrode driver box for g.HIampB [29]. . . . . | 22 |
| 2.10 | Audio signal before amplification. . . . .   | 25 |
| 2.11 | Amplification circuit and audio output signal. . . . .   | 25 |
| 2.12 | Arduino code for generating the square wave. . . . .   | 26 |
| 2.13 | First square wave model. . . . .   | 26 |
| 2.14 | Trigger signal by Arduino. . . . .   | 27 |
| 2.15 | First prototype for trigger generation. . . . .  | 27 |
| 2.16 | Result of the first prototype for trigger generation. . . . .  | 28 |
| 2.17 | On/off audio signal. . . . .   | 29 |
| 2.18 | On/off audio signal: oscilloscope. . . . .   | 30 |

|      |   |    |
|------|---|----|
| 2.19 | Op amp used as amplifier. . . . .   | 30 |
| 2.20 | Circuit power supply. . . . .   | 31 |
| 2.21 | Input audio signal, amplifier and output audio signal. . . . .                    | 31 |
| 2.22 | Rectifier and rectified signal. . . . .   | 32 |
| 2.23 | Op amp used as threshold comparator. . . . .                                      | 32 |
| 2.24 | Final prototype for trigger generation. . . . .                                   | 33 |
| 2.25 | Trigger signal: oscilloscope. . . . .   | 33 |
| 2.26 | (a)Op amp used as threshold comparator;(b)Supply voltage control circuit. . . . . | 34 |
| 2.27 | (a)Circuit on breadboard; (b)Circuit on matrix board. . . . .                     | 35 |
| 2.28 | (a)List of triggers; (b)Trigger 7 selected. . . . .                               | 36 |
| 2.29 | Main screen of g.Recorder. . . . .  | 36 |
| 2.30 | Settings and VEP section. . . . .   | 37 |
| 2.31 | Clinical acquisition protocol. . . . .  | 38 |
| 2.32 | International Standard 10/20. . . . .   | 39 |
| 2.33 | Impedance assessment tool. . . . .  | 39 |
| 2.34 | Our prototype while it's working. . . . .   | 40 |
| 2.35 | Stimulation pattern for pr-VEP tests [31]. . . . .                                | 40 |
| 2.36 | PSD of signals obtained via Retimax. . . . .                                      | 44 |
| 2.37 | PSD of signals obtained via g.HIamp. . . . .                                      | 44 |
| 2.38 | Cardboard. . . . .  | 46 |
| 2.39 | Developed application. . . . .  | 46 |
| 2.40 | Application blocks. . . . .   | 46 |
| 2.41 | Cardboard: subject MC. . . . .  | 47 |
| 2.42 | Cardboard: subject PC. . . . .  | 47 |
| 2.43 | Cardboard: subject MU. . . . .  | 47 |
| 2.44 | Cardboard: subject TR. . . . .  | 48 |
| 2.45 | Cardboard: subject VA. . . . .  | 48 |
| 2.46 | Cardboard: subject SP. . . . .  | 48 |
| 2.47 | Cardboard: subject SS. . . . .  | 49 |
| 2.48 | Cardboard: subject MG. . . . .  | 49 |
| 2.49 | Cardboard: subject BA. . . . .  | 49 |
| 2.50 | Cardboard: subject CG. . . . .  | 50 |
| 2.51 | Comparison Cardboard-Smart Glasses. . . . .                                       | 50 |
| 3.1  | Subject LP:(a)Left eye;(b) Right eye. . . . .                                     | 53 |
| 3.2  | Subject RT:(a)Left eye;(b) Right eye. . . . .                                     | 53 |
| 3.3  | Subject FC:(a)Left eye;(b) Right eye. . . . .                                     | 53 |
| 3.4  | Subject SS:(a)Left eye;(b) Right eye. . . . .                                     | 54 |
| 3.5  | Subject AV:(a)Left eye;(b) Right eye. . . . .                                     | 54 |
| 3.6  | Subject SS:(a)Left eye;(b) Right eye. . . . .                                     | 54 |
| 3.7  | Subject FP:(a)Left eye;(b) Right eye. . . . .                                     | 55 |
| 3.8  | Subject AT:(a)Left eye;(b) Right eye. . . . .                                     | 55 |

|      |   |    |
|------|---|----|
| 3.9  | Subject MN:(a)Left eye;(b) Right eye. . . . .                                 | 55 |
| 3.10 | Subject IT:(a)Left eye;(b) Right eye. . . . .                                 | 56 |
| 3.11 | Characteristics of the pr-VEPs. . . . .                                       | 56 |
| 3.12 | Average and standard deviation of all signals: healthy subjects. . . . .      | 58 |
| 3.13 | Patient AI:(a)Left eye;(b)Right eye. . . . .                                  | 62 |
| 3.14 | Patient BG:(a)Left eye;(b)Right eye. . . . .                                  | 62 |
| 3.15 | Patient LR:(a)Left eye;(b)Right eye. . . . .                                  | 62 |
| 3.16 | Patient MS:(a)Left eye;(b)Right eye. . . . .                                  | 63 |
| 3.17 | Patient CM:(a)Left eye;(b)Right eye. . . . .                                  | 63 |
| 3.18 | Patient DS:(a)Left eye;(b)Right eye. . . . .                                  | 63 |
| 3.19 | Patient LL:(a)Left eye;(b)Right eye. . . . .                                  | 64 |
| 3.20 | Patient PA:(a)Left eye;(b)Right eye. . . . .                                  | 64 |
| 3.21 | Patient BL:(a)Left eye;(b)Right eye. . . . .                                  | 64 |
| 3.22 | Patient BB:(a)Left eye;(b)Right eye. . . . .                                  | 65 |
| 3.23 | Patient MM:(a)Left eye;(b)Right eye. . . . .                                  | 65 |
| 3.24 | Patient ZV:(a)Left eye;(b)Right eye. . . . .                                  | 65 |
| 3.25 | Patient FC:(a)Left eye;(b)Right eye. . . . .                                  | 66 |
| 3.26 | Patient IA:(a)Left eye;(b)Right eye. . . . .                                  | 66 |
| 3.27 | Patient LS:(a)Left eye;(b)Right eye. . . . .                                  | 66 |
| 3.28 | Patient CN:(a)Left eye;(b)Right eye. . . . .                                  | 67 |
| 3.29 | Patient CE:Left eye. . . . .  | 67 |
| 3.30 | Patient LM:(a)Left eye;(b)Right eye. . . . .                                  | 67 |
| 3.31 | Patient PA:(a)Left eye;(b)Right eye. . . . .                                  | 68 |
| 3.32 | Patient CG:(a)Left eye;(b)Right eye. . . . .                                  | 68 |
| 3.33 | Patient GG:(a)Left eye;(b)Right eye. . . . .                                  | 68 |
| 3.34 | Patient MG:(a)Left eye;(b)Right eye. . . . .                                  | 69 |
| 3.35 | Patient BA:(a)Left eye;(b)Right eye. . . . .                                  | 69 |
| 3.36 | Patient SL:(a)Left eye;(b)Right eye. . . . .                                  | 69 |
| 3.37 | Patient BG:(a)Left eye;(b)Right eye. . . . .                                  | 70 |
| 3.38 | Patient CF:(a)Left eye;(b)Right eye. . . . .                                  | 70 |
| 3.39 | Patient GA:(a)Left eye;(b)Right eye. . . . .                                  | 70 |
| 3.40 | Patient SL:(a)Left eye;(b)Right eye. . . . .                                  | 71 |
| 3.41 | Patient GG:(a)Left eye;(b)Right eye. . . . .                                  | 71 |
| 3.42 | Patient BL:(a)Left eye;(b)Right eye. . . . .                                  | 71 |
| 3.43 | Average and standard deviation of all signals: pathological subjects. . . . . | 72 |
| 3.44 | Wet Maculopathy: average and standard deviation. . . . .                      | 72 |
| 3.45 | Dry Maculopathy: average and standard deviation. . . . .                      | 73 |
| 3.46 | PSD Subject LP. . . . .   | 74 |
| 3.47 | PSD Subject RT. . . . .   | 74 |
| 3.48 | PSD Subject FC. . . . .   | 74 |
| 3.49 | PSD Subject SS. . . . .   | 75 |
| 3.50 | PSD Subject AV. . . . .   | 75 |

|  |    |
|--|----|
| 3.51 PSD Subject SS. . . . .                                   | 75 |
| 3.52 PSD Subject FP. . . . .                                   | 76 |
| 3.53 PSD Subject AT. . . . .                                   | 76 |
| 3.54 PSD Subject MN. . . . .                                   | 76 |
| 3.55 PSD Subject IT. . . . .                                   | 77 |
| 3.56 PSD Patient AI. . . . .                                   | 77 |
| 3.57 PSD Patient BG. . . . .                                   | 77 |
| 3.58 PSD Patient LR. . . . .                                   | 78 |
| 3.59 PSD Patient MS. . . . .                                   | 78 |
| 3.60 PSD Patient CM. . . . .                                   | 78 |
| 3.61 PSD Patient DS. . . . .                                   | 79 |
| 3.62 PSD Patient LL. . . . .                                   | 79 |
| 3.63 PSD Patient PA. . . . .                                   | 79 |
| 3.64 PSD Patient BL. . . . .                                   | 80 |
| 3.65 PSD Patient BB. . . . .                                   | 80 |
| 3.66 PSD Patient MM. . . . .                                   | 80 |
| 3.67 PSD Patient ZV. . . . .                                   | 81 |
| 3.68 PSD Patient FC. . . . .                                   | 81 |
| 3.69 PSD Patient IA. . . . .                                   | 81 |
| 3.70 PSD Patient LS. . . . .                                   | 82 |
| 3.71 PSD Patient CN. . . . .                                   | 82 |
| 3.72 PSD Patient CE. . . . .                                   | 82 |
| 3.73 PSD Patient LM. . . . .                                   | 83 |
| 3.74 PSD Patient PA. . . . .                                   | 83 |
| 3.75 PSD Patient CG. . . . .                                   | 83 |
| 3.76 PSD Patient GG. . . . .                                   | 84 |
| 3.77 PSD Patient MG. . . . .                                   | 84 |
| 3.78 PSD Patient BA. . . . .                                   | 84 |
| 3.79 PSD Patient SL. . . . .                                   | 85 |
| 3.80 PSD Patient BG. . . . .                                   | 85 |
| 3.81 PSD Patient CF. . . . .                                   | 85 |
| 3.82 PSD Patient GA. . . . .                                   | 86 |
| 3.83 PSD Patient SL. . . . .                                   | 86 |
| 3.84 PSD Patient BL. . . . .                                   | 86 |
| 3.85 PSD Patient GG. . . . .                                   | 87 |
| 3.86 Filtering 1-30 HZ healthy subject. . . . .                | 87 |
| 3.87 Filtering 1-30 HZ pathological subject. . . . .           | 88 |
| 3.88 Overlapping filtered signals: Healthy Subject RT. . . . . | 88 |
| 3.89 Overlapping filtered signals: Healthy Subject SS. . . . . | 89 |
| 3.90 Overlapping filtered signals: Healthy Subject AV. . . . . | 89 |
| 3.91 Overlapping filtered signals: Healthy Subject FP. . . . . | 90 |
| 3.92 Overlapping filtered signals: Healthy Subject MN. . . . . | 90 |

|      |  |     |
|------|--|-----|
| 3.93 | Overlapping filtered signals: Patient AI. . . . .  | 90  |
| 3.94 | Overlapping filtered signals: Patient BL . . . . .   | 91  |
| 3.95 | Overlapping filtered signals: Patient FC . . . . .   | 91  |
| 3.96 | Overlapping filtered signals: Patient LM . . . . .   | 91  |
| 3.97 | Overlapping filtered signals: Patient LR . . . . .   | 92  |
| 3.98 | PSD of Wet Maculopathic signals. . . . .   | 93  |
| 3.99 | PSD of Dry Maculopathic signals. . . . .   | 93  |
| 4.1  | Linear Regression Line relative to the average of the signals, healthy subjects. . . . .         | 99  |
| 4.2  | Linear Regression Line relative to the signals components, healthy subjects. . . . .             | 100 |
| 4.3  | Linear Regression Line relative to the quantity of signals power, healthy subjects. . . . .      | 101 |
| 4.4  | Bland-Altman Plots of the average of the signals, healthy subjects. . . . .                      | 102 |
| 4.5  | Bland-Altman Plots of the signals components, healthy subjects. . . . .                          | 103 |
| 4.6  | Bland-Altman Plots of the quantity of signals power, healthy subjects. . . . .                   | 104 |
| 4.7  | Linear Regression Line relative to the average of the signals, pathological subjects. . . . .    | 107 |
| 4.8  | Linear Regression Line relative to the quantity of signals power, pathological subjects. . . . . | 108 |
| 4.9  | Bland-Altman Plots of the average of the signals, pathological subjects. . . . .                 | 108 |
| 4.10 | Bland-Altman Plots of the quantity of signals power, healthy subjects. . . . .                   | 109 |

# Chapter 1

## Introduction

### 1.1 Sensory Coding and Brain Electric Waves

The existence of recordable electric waves from the scalp was discovered in 1924 by Hans Berger. These waves, due to the complex electrochemical activity of the single cortical cells, have a maximum amplitude of  $100 \mu\text{V}$  [1]. During the recording of cerebral electrical potentials the dual neuronal activity is considered:

- **spontaneous**, commonly represented by the electroencephalographic signal (EEG), which records the fluctuations in time of the electrical potentials detected on the scalp in the absence of external stimuli;
- **related event**, *related event potential (ERP)*, neural activity triggered by specific events both internal to the subject, e.g. a movement, and external, e.g. sensory stimuli. The electrophysiological signals of response to sensory stimuli can be easily recorded at the sites where they are generated and in a non-invasive way. The response elicited by applying external stimuli is generally a low-intensity signal and it is therefore necessary to use particular techniques to extract the ERP from the current EEG. These techniques, called *averaging techniques* and used for the first time in 1947, require the repeatability of the stimulus over time in order to obtain answers that are as similar as possible to each other [1].

The evoked potentials are a typical example of ERP and provide numerical data that contribute objectively and reliably to the diagnosis of numerous neurological diseases affecting different sensory systems. Specific neuronal pathways transmit information from the sensory receptor to the central nervous system. It is interesting to understand how the nervous system, at the arrival of a stimulus on a sensory receptor, manages to identify it, perceive its strength and location. This task is made possible by *sensory coding* [2]:

- **coding of the type of stimulus:** the type of stimulus is encoded by the receptor and the information transport pathways are activated when the stimulus is applied to the receptor. For example, light waves activate photoreceptors that communicate through specific pathways with the visual cortex. The perception of stimuli is not necessarily based on the inputs coming from a single sensory pathway: often the brain must integrate information coming from different sensory systems;
- **coding of stimulus intensity:** the intensity of the stimulus is coded by the frequency of action potentials, *frequency codes*, and the number of activated receptors, *population code*. A more intense stimulus produces an increase in the discharge frequency of action potentials and activates a greater number of receptors;
- **coding of stimulus location:** the concept of localization is closely related to the existence of *receptive fields*. In fact, the stimulus must be located within the receptive field of the specific neuron. However, the size of the receptive fields varies greatly in the body: the location of the stimulus is better in those regions innervated by neurons with small receptive fields.

The different types of evoked responses (such as somatosensorial, auditory, visual ones) are characterized by latency, inter-peak latency, amplitude and morphology of the individual waves. In particular, the morphology varies according to the sensory stimulus used. The study of evoked potentials arose from the need to relate the response of the central nervous system to an external sensory stimulus, with the possibility of analyzing the reaction of individual organs with interesting clinical findings. For this reason, EPs are used for example in audiology or ophthalmology: in this latter field, VEPs, visual evoked potentials, represent an important electrophysiological tool for the diagnosis and study of neurological pathologies that can determine the involvement of the optic nerve, the optic pathways and the visual cortex [3].

## 1.2 Neuroanatomy and Physiology of the Visual System

The eye is an organ with a spherical shape, housed in the orbital cavity, protected by the eyelids and other ocular adnexa. Its function is to capture the light radiations coming from the external environment and transform them into nerve impulses that will be used to generate sight and reflexes. The eye guarantees vision by transforming light into information that, in the form of electrical impulses, reaches the brain where they are processed. The eyeball is essentially made up of an outer epidermis membrane that protects three inner chambers, as shown in *Figure 1.1.*

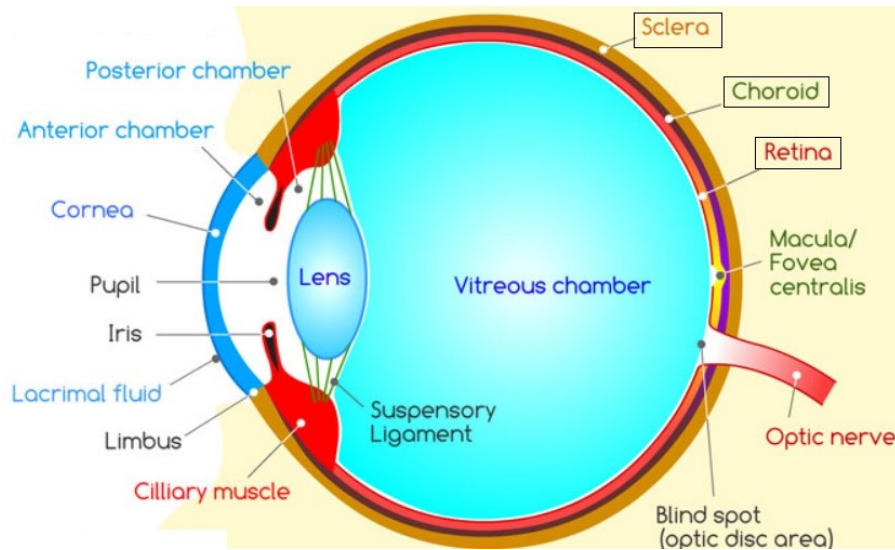


Figure 1.1: Human eye structure [4].

The two aqueous chambers on the front of the eye are the *anterior* and *posterior chambers*, separated by the *iris*. These chambers contain *aqueous humor*, secreted in the posterior chamber by a layer of cells that cover the *ciliary body* and intended to provide nutrients to the cornea and crystalline. This liquid passes into the anterior chamber through the *pupil*. The largest of the chambers is the *vitreous body*, containing *vitreous humor*, separated from the other chambers by the *crystalline lens* and the suspensory bonds, called *zonular fibers*, which connect the crystalline lens to the ciliary body. The vitreous humor is a gelatinous substance that helps to maintain the spherical structure of the eye [5]. The epidermis, on the other hand, consists of three different layers, each of which performs specific functions:

- *outer layer*, **sclera**: it is the ‘white part’ of the eye, resistant and with a protective function. Most of the sclera is opaque, but in the central part there is a transparent "window": the *cornea*, through which the light penetrates into the eye;
- *middle layer*, **choroid**: it is a layer of highly pigmented tissue, it is dark to avoid light reflections inside the eye and it is the most vascularized layer;
- *inner layer*, **retina**: its function is to collect the visual information that the main nerve of the eye, the *optic nerve*, must then send to the brain in the form of light impulses which are then transformed into images. In the retina there are two types of photosensitive cells that capture light: *rods* and *cones*. Rods are sensitive to light and movement and allow vision in low light conditions while cones are responsible for viewing colors and details. It is then the *lens*, transparent and flexible, which allows the light to be focused on the retina.

For more specific tasks, light is concentrated in the center of the retina, in an area called *macula*, which represents the most sensitive area to light stimuli [6]. The muscles around the lens alter its shape, allowing the vision of objects placed at different distances, according to the concept of *accommodation*.

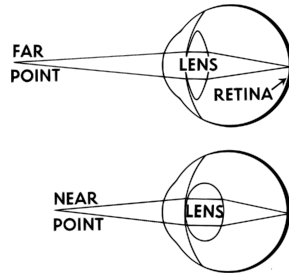


Figure 1.2: Accommodation mechanism [7].

The shape of the crystalline lens is controlled by the ciliary muscle which has fibers arranged concentrically, by means of the tension that it exerts on the zonular fibers that connect the ciliary muscle to the crystalline itself. The greater the contraction of a circular muscle, the smaller the inner diameter of the circle, which will correspond to a lower tension of the zonular fibers and a greater curvature of the crystalline lens. For the vision of distant objects the ciliary muscle is released, which increases the diameter of the muscle itself, tends the zonular fibers and reduces the curvature of the crystalline lens so that it takes on a more flattened shape [2].

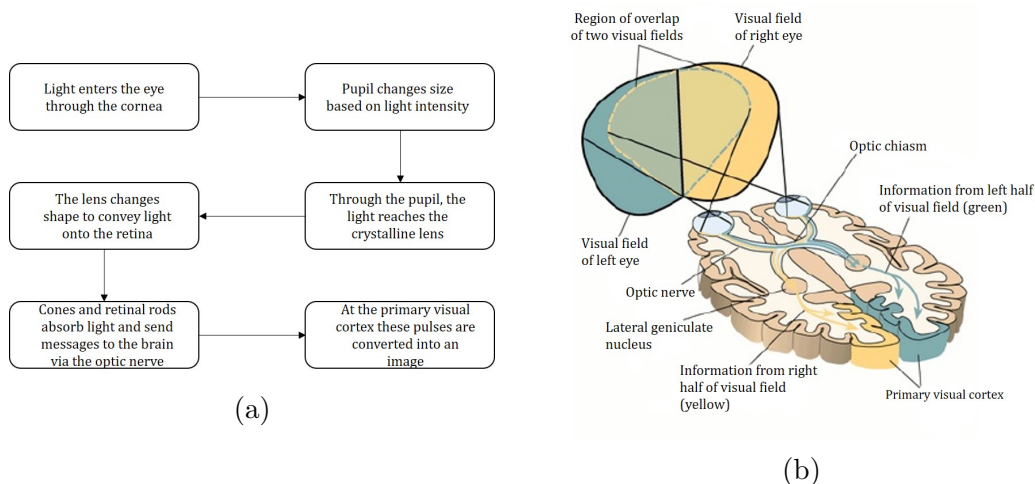


Figure 1.3: (a)Light path flow chart;(b)Visual pathway [8].

## 1.3 Retina and Retinal diseases: Maculopathy

### 1.3.1 Layers and components of the retina

The conversion of light energy into action potentials occurs at the level of the retina: this conversion is known as the *phototransduction process* [9]. The nerve components of the retina consist of three main layers of cells. Starting from the back of the eye to the front, these layers are composed of *photoreceptor cells*, called cones and rods, *bipolar cells* and *ganglion cells*:

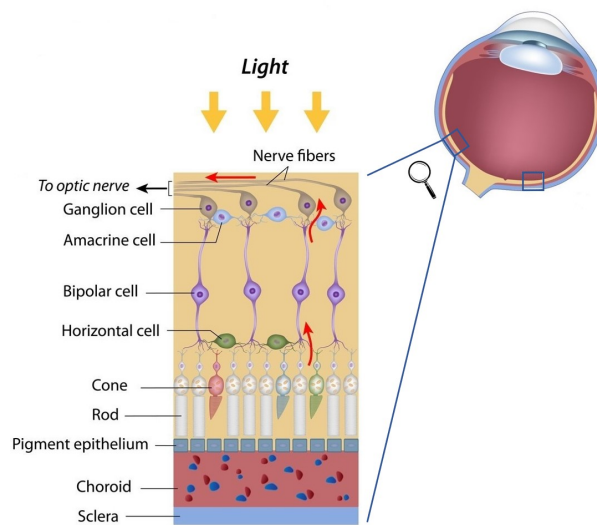


Figure 1.4: Layers of the retina [10].

- **cones and rods:** phototransduction phenomenon occurs at these photoreceptors, which transform the light energy into electrical signals. They are mainly concentrated in the centre of the macula, in an area called *fovea*, responsible for spatial resolution (*visual acuity*) and colour vision [11]. The remaining part of the retina is mainly used for viewing motion.
- **bipolar cells:** rods and cones contract synapses with the dendrites of bipolar cells, the neurons of the first order of the visual pathway. They in turn contract synapses with ganglion cells;
- **ganglion cells:** they are the largest neurons in the retina, organized in a single layer near the vitreous body. They represent the second-order neurons of the visual pathway. Their axons form the optic nerve. They do not contribute to visual images but only detect light intensity [9].

### 1.3.2 Maculopathy disease

One of the main causes of severe loss of visual acuity is *maculopathy*, a chronic degenerative disease with a tendency to become bilateral. Those suffering from macular pathology experience a loss of vision at the centre of the field of vision and distorted perception of the images [12].



Figure 1.5: Visual effects of maculopathy progression [13].

However, degenerative maculopathy never leads to complete blindness as lateral vision is usually preserved up to the terminal stages of retinal maculopathy. Maculopathy does not give pain. Indeed, initially the visual problem may not be noticed, because it is supplied with the good eye.

*Senile maculopathy*, or *age-related maculopathy* (AMD), is the most frequent form of maculopathy that usually affects people over 65 years of age [14]. There are two main kinds of AMD:

- **dry maculopathy:** it is the most frequent one and involves the thinning of the retina, the visual cells stop working and disappear. The transport of nutrient factors and the elimination of waste by retinal pigmented epithelium (RPE) are slowed down, resulting in yellowish or pigmented intra-retinal deposits;

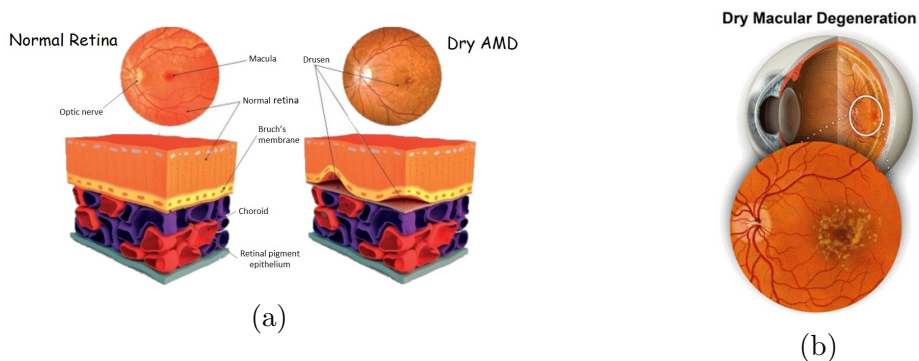


Figure 1.6: (a) Healthy macula VS damage macula [15]; (b) Dry Macular Degeneration [16].

- **wet maculopathy:** involves the proliferation of new vessels under the retina and this sometimes involves bleeding under the retina and lifting the pigmented epithelium. Some dry maculopathy can become wet maculopathy over time, so it is important to monitor its development [17].

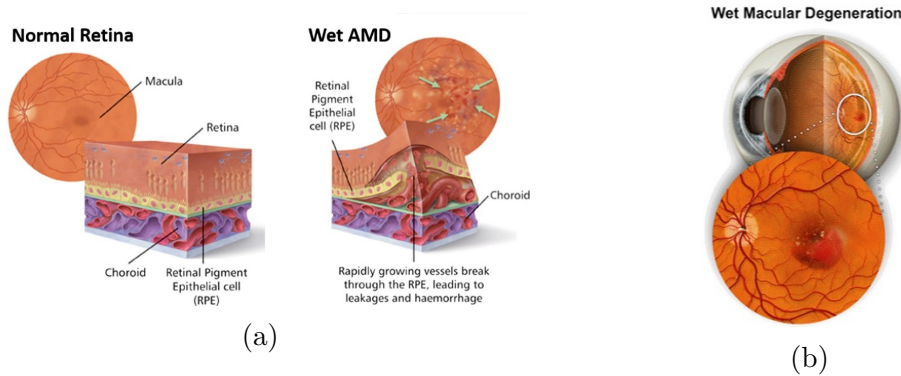


Figure 1.7: (a) Healthy macula VS damage macula [15]; (b) Wet Macular Degeneration [16].

The main risk factors can be classified as [18]:

- **demographic factors:** include *age*, *ethnicity* and *sex*. The risk of the onset of the disease increases with increasing age and it has been hypothesized that the ethnic differences in the prevalence of advanced AMD were due to a possible protective effect of iridescent pigmentation in colored subjects, in which the melanin can protect the EPR and the choroid with degenerative changes, which predispose the patient to choroidal neovascularization;
- **behavioral factors:** *smoking*, *alcohol consumption*, *diet*, *obesity*, *physical activity* and *exposure to sunlight*. Tobacco smoke is the main predictable risk factor for AMD due to its oxidative effects harmful to the retina, the reduction of choroidal blood flow, the promotion of ischemia, hypoxia, retinal microinfarcts and stimulation of neovascularization. Alcohol also increases oxidative stress. The regular performance of physical activity is also very important;
- **ocular factors:** include a possible association between hypermetropia and AMD;
- **factors related to systemic diseases:** *diabetes* and *arterial hypertension* contribute to increasing the risk of onset of retinal pathology;
- **genetic factors:** it could be hypothesized to associate AMD with a complex genetic disorder in which one or more genes concur to determine the individual susceptibility for the development of the disease.

In addition to the senile one, other forms of maculopathy are:

- myopia maculopathy;
- diabetic maculopathy;
- exudative maculopathy after venous thrombosis of the retina;
- macular Pucker.

Among the numerous pathologies, this study focuses precisely on maculopathy as the functional alterations of the macular region can represent the pathological aspect that involves the increase in latency and the reduction in the amplitude of the VEP wave, whose collection and analysis are the purpose of this thesis. In fact, 90% of the photoreceptors responsible for the generation of VEP are part of the macula and consequently a localized pathology in this area, through the VEP analysis, could be easily identified [19]. However, for a correct interpretation of the alterations in the response of the VEP, observed in clinical practice, it is always recommended, and often necessary, to associate electrophysiological tests that specifically explore retinal and macular function, such as the *electroretinographic test* (ERG) [3]. As part of the ERG we remind:

- focal ERG (**F-ERG**);
- multifocal ERG (**mf-ERG**);
- pattern ERG (**P-ERG**).

Modifications of these single bioelectrical responses are indicative of a dysfunction of the various retinal elements that generated the specific recorded electroretinographic signal.

## 1.4 VEPs: Visual Evoked Potentials

*Visual evoked potentials* are defined as variations of the bio-electric potentials of the occipital cortex evoked by visual stimuli. They are therefore the manifestation of complex neurosensory events related to transduction phenomena and transmission of the nervous impulse along the visual pathways, from the retinal photoreceptors up to the visual cortex [20]. VEPs express in fact the electrical correlation of the activity of the visual pathways up to the *calcareous cortex* and allow to obtain information about the functionality of the human visual system in a non-invasive way [3]. For this reason they have been used in neurophthalmological diagnostics as a complement to ophthalmological and neurological semiotics for over five decades.

VEPs have a *good temporal resolution* (in the order of ms), useful in order to study the dynamic change that takes place in the central nervous system not only in different pathological conditions, but also in response to different types of stimulus.

Because of the nature of these events related potentials, the extraction of VEPs from the electroencephalographic recording requires specific techniques such as the averaging technique [1]. In fact, the aforementioned technique consists in the medium operation of all the acquired epochs, where an epoch is the interval of time interposed between two successive stimuli.

There are two main types of VEP, which are characterized by different types of stimulus [21]:

- **flash VEP**, in which the administered stimulus consists of a *luminance variation*;
- **pattern VEP**, in which the administered stimulus consists of a *contrast variation*. Among the pattern VEPs it is still possible to recognize the *patternreversal VEPs*, *pr-VEPs*, and the *pattern onset/offset VEPs*.

### 1.4.1 Flash VEPs

They have a rather limited field of application in the field of neurological diseases that affect the visual pathways as they offer highly variable responses in the control population and are less sensitive than the pattern VEPs [3]. The flash VEPs are visual evoked potentials recorded after stimuli constituted by a stroboscopic flash, with the possibility to change the intensity of the light and the frequency of the flashes. The flash VEPs reflect the overall macular function of the photopic system and the conditions of its signal along the macular visual pathways, up to the primary visual areas [22]. These potentials consist of a series of six positive and negative waves, which can be displayed in the time interval between 30 and 300 ms after the stimulus.

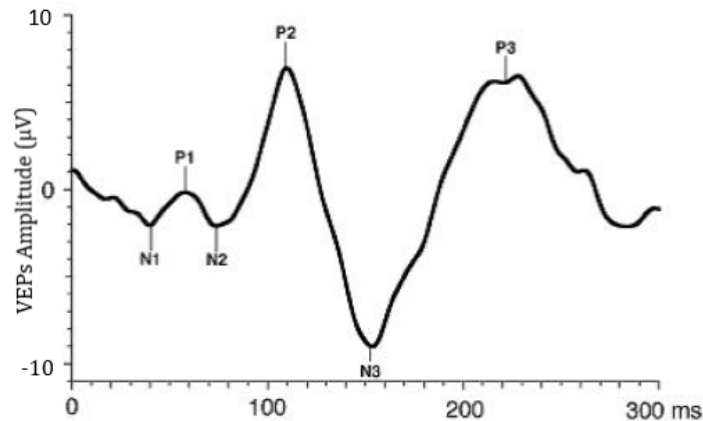


Figure 1.8: Typical morphology of a flash VEP of a healthy subject where it is possible to distinguish peaks that are defined with the letter indicating the polarity [23].

The VEP flash is useful in cases where poor optical quality, poor collaboration or poor vision make the use of pattern stimulation ineffective [24].

However, flash VEPs have two substantial disadvantages in clinical application:

1. large physiological variability of the response;
2. relative insensitivity in the presence of visual function disturbances [1].

Despite these limitations, the VEP flash proved to be a useful method in the study of physiological and pathological brain ageing processes. In particular, it has recently been proposed for the early diagnosis of Alzheimer’s type dementia [25].

In 1959 Barlow suggested that cortical neurons required specific visual patterns to produce maximum response [26]. Based on these considerations, the contrast stimuli that characterize the pattern VEPs have been realized.

## 1.4.2 Pattern VEPs

This type of stimulation adapts optimally to the physiological demands of the high-resolution retinal areas (fovea), also favoring the functional exploration of the optic nerve fibers [1]. Pattern VEP stimulation consists of periodic images with a geometrically oriented structure, whose contrast is modulated while maintaining the overall brightness constant [26]. Usually the image proposed to the patient consists of a *checkerboard* with black and white elements, whose periodic inversion represents the visual stimulus. During inversions, the patient must turn his attention

to a fixed point in the center of the checkerboard. It is possible to select the most suitable features for the clinical analysis of the various components of the visual system, which can be activated differently from the *spatial*, *temporal*, *chromatic* and *contrast* properties of the image [25].

The *spatial frequency* (FS) of a pattern stimulus, expressed in minutes of arc, measures how many times the contrast of an image passes from the minimum to the maximum value in a degree of visual angle. A reversal corresponds to complete alternation from a light to a dark element in a degree of visual angle. The different FS allow to explore the different sectors of the visual field by physiologically stimulating the different neuronal systems of the visual pathway.

The electrophysiological response obtained with a pattern VEP also depends on the *temporal frequency* (FT), ie the speed with which the pattern appears or disappears (in the case of the pattern onset/offset) or with which the elements of the model reverse their position (in the case of the pattern reversal) [3]. The FT is measured in reversals per second (rps).

In the *pattern on/off* the repetitive stimulus involves the replacement of structured elements with a neutral background, without variations in total brightness. This stimulation technique may be useful for the treatment of patients with nystagmus. The response to pattern on / off stimulation physiologically consists of three main peaks in adults, which are in the time interval between 75 and 150 ms after the stimulus.

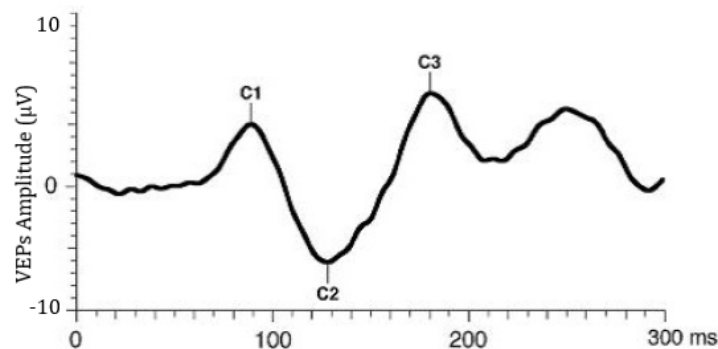


Figure 1.9: Typical morphology of a on/off pattern VEP of an healthy subject [24].

In most clinical studies, however, the most commonly used pattern is the *reversal* one, which involves the complete alternation of a light element with a dark chessboard element, with a specific number of inversions per second. The variation of the temporal frequency with which the elements are inverted between them determines at the low frequencies (<4 Hz) a *transient* response and at high frequencies (>4

Hz) a *steady state* response [3]. In the reversal pattern commonly used in clinical practice, low stimulation FTs (between 1 Hz and 4 Hz) are used, which allow the recording of a transient electrophysiological response from the occipital cortex.

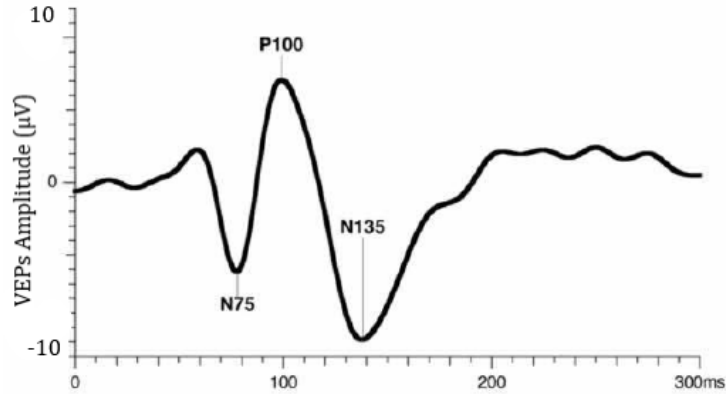


Figure 1.10: Typical morphology of a pattern reversal VEP of an healthy subject [24].

The transient potential of the pattern reversal consists of a typical series of three deflections with alternating polarity, reproducible latency and morphology, in which it is possible to recognize:

1. **N75**: negative peak visible after 75 ms from the stimulus;
2. **P100**: positive peak visible after 100 ms from the stimulus;
3. **N135**: negative peak visible after 135 ms from the stimulus [21].

The positive wave P100 represents the most stable, repeatable and maximum amplitude component. Many studies state that the P100 wave originates at the primary visual cortex. In particular, a historical study reported that, in a patient with severe lesions of the visual areas that however spared the primary visual area, it was still possible to record an almost intact P100. It is thought instead that the other two negative components of the potential, N75 and N135, originate at the level of the striatal and extra-striatal cortex, respectively [3]. However, these responses are variable and therefore not very significant in clinical practice.

Other studies match the origin of these waves to different areas of the visual system and this disagreement could be due to the different technical characteristics of the stimulation systems used. Furthermore, post processing could also be conducted in different ways, leading to slightly different results.

The types of stimulation presented so far are standardized by *International Society for Clinical Electrophysiology of Vision* (ISCEV) protocol. In particular, the

VEP reversal pattern is the type of stimulation used for the purposes of this work and its technical stimulation characteristics will be discussed in more detail in the "Materials and Methods" chapter.

## 1.5 Pattern Reversal VEP Physiological Interpretation

The evaluation of morphology, amplitude and above all latency (retino-cortical conduction time) of the potential P100 represents the fundamental element for the electrophysiological study of the integrity of the optical pathways, especially at the pre-chiasmatic level. Although the anomalies of VEPs are not specific and may concern a wide variety of ophthalmologic and neurological pathologies, the alterations of this potential are all reflected in a decrease in amplitude and/or in an extension of the latency time of the different components that constitute the potential itself [3]. The topographical position, the size and the degree of the visual deficit strictly condition the possible anomalies detected in the analysis of pr-VEPs.

In order to proceed with a first visual interpretation of the VEP anomalies it is appropriate to compare the case of the potential relative to a healthy subject with that of a pathological one. *Figure 1.11* shows a good comparison between healthy and pathologic signals acquired in our laboratory.

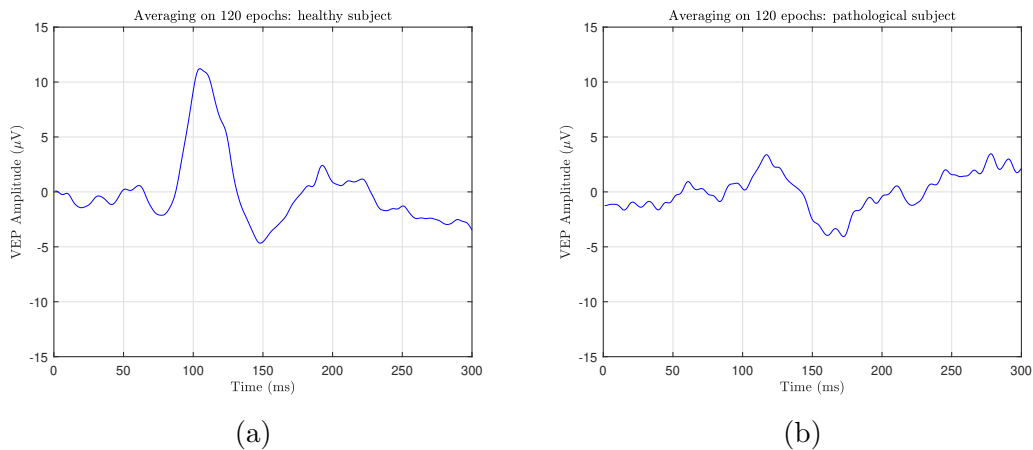


Figure 1.11: Comparison between an healthy (a) and a pathological (b) subject. In the pathological VEP, it is observed both a decrease in amplitude of the P100 wave and its time delay.

The main parameters that must be taken into consideration, to determine whether the answer is physiological or pathological, are the following:

- P100 peak latency;
- P100 wave width (measured from N75 peak);
- latency difference between the P100 waves of the right and left eye;
- time interval between N75 and N135 waves;

For example, if the amplitude of the VEP waves falls within the range of expected values while the latency marks appear altered, then the test could have highlighted a conduction anomaly typical of demyelinating pathologies, such as *multiple sclerosis*. Otherwise, in the case of *retinitis pigmentosa*, the VEP may not be identified as the expected waveform is absent. Finally, in the case of *retinal detachment*, the amplitude values of the waves decrease in relation to the extent of detachment.

## 1.6 Clinical Applications and State of Art

In addition to the diagnostic capabilities of the pr-VEP to detect maculopathy, presented in *paragraph 1.3*, pr-VEPs represent also an accurate indicator of anomalies of the whole visual system. For instance, they are used to investigate pathologies related to demyelinating or axonal issues. [3]. The phenomena of demyelination, for example, involve changes in latency, in fact the cortical retinal conduction time is greater. The presence of axonal damage, on the other hand, is evidenced by alterations in amplitude and morphology of the acquired waveform.

The VEP test can therefore also be used to investigate the following diseases:

- multiple sclerosis;
- demyelination of the optic nerve;
- ischemic neuropathy of the optic nerve;
- compression pathologies of the optical pathways;
- pseudotumor cerebri;
- degenerative diseases (Parkinson's, Alzheimer's);
- migraine;
- primitive alterations of retinal ganglion cells.

In this thesis work, *Retimax CSO*, a commercial device for pr-VEP is used to validate the prototype here proposed. Retimax CSO is an ocular electrophysiology system suitable both for clinical practice, as a *medical device*, and for scientific

investigations. Retimax CSO performs the recording, analysis of amplitude and latency of the bio-potential of action of the retina in response to light stimuli. The diagnostic methods of the Retimax system, which will be extensively described in the "*Materials and Methods*" chapter, comply with the ISCEV standardization.

# Chapter 2

## Materials and Method

### 2.1 Retimax CSO

As anticipated, one of the systems currently in use for ocular electrophysiology is the Retimax CSO. In the experimental study that supports this work of thesis, this medical device was used for pr-VEP tests. In this way it was possible to compare the results obtained with Retimax with those obtained using the device proposed by us. The purpose of the comparison is the validation of our device, which, together with the results and performances, will be discussed later.

Retimax CSO is classified according to EN60601-1:

- type of protection against direct and indirect contacts: *class I*;
- applied parts: *type BF*.

Among the possible configurations of the Retimax system, the *advanced version* is the one used here. The system consists of:

1. *230V-230V isolation transformer*: for supplying the entire system, in compliance with EN61558-2-15 and directives 73/23 / CEE and 93/68 / CEE;
2. *flash stimulator*: for the presentation of flashes of light with variable intensity or bright light that alternate on a precise visual angle subtended in the spectrum of visible light;
3. *two-channel pre-amplifier*: able to detect electrical biopotentials generated by the retina and the occipital visual cortex; presents patient galvanic isolation, 10 dB CMRR and 10 M $\Omega$  input impedance;
4. *pattern stimulator*: for the presentation of structured images on a 19" TV screen, contrast ranging from 1 to 99%; stimulated visual angle selectable

according to the distance of the subject from the stimulator with automatic conversion of the spatial frequency in cycles per degree or in minutes of arc;

5. *signal analysis system*: consisting of a computer with "Retimax software" application software capable of processing the signal and measuring its amplitude and latency components;
6. *computer monitor*: for displaying the signals obtained.

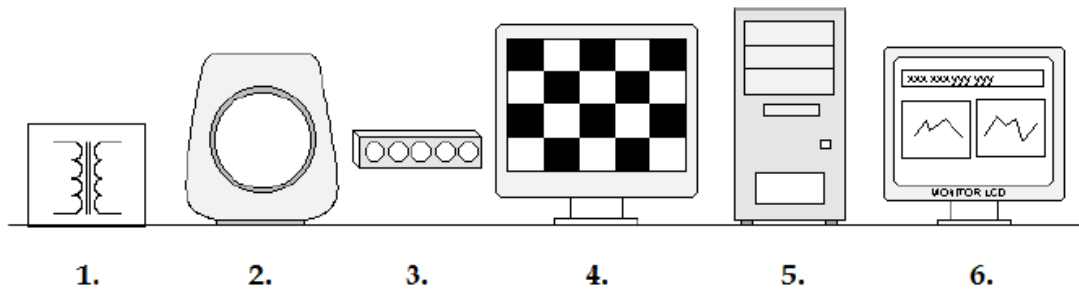


Figure 2.1: Components of the Retimax CSO system.

Other accessory tools used in combination with Retimax CSO during the examination are:

- *Nuprep Skin Gel*, for effectively lowers impedance: abrasive gel for improving conductivity and helping achieve efficiency with the equipment;



Figure 2.2: Nuprep Skin Gel.

- *Ag/AgCl EEG Gold Skin Passive Electrodes "SKIN CUP"*, with connecting cables;



Figure 2.3: Skin cup.

- *KONIX EEG Paste*: it allows the correct application of the electrodes on the skin, limiting the electrode-skin impedance.



Figure 2.4: KONIX EEG Paste.

In addition to the VEP tests, the Retimax CSO system can be used for the following diagnostic tests:

- **ERG**, electroretinogram;
- **PERG**, pattern electroretinogram;
- **EOG**, electrooculogram;
- **ENG**, electronistagmogram;

The reason why we want to present a new VEP stimulation, detection and calculation system, despite the results obtained so far through the Retimax system are repeatable and reliable, it consists mainly in the non-portability of the system. In fact, its imposing size makes it difficult to transport, thus giving rise to the need of

a portable and equally accurate system, such as the one representing the purpose of this thesis.

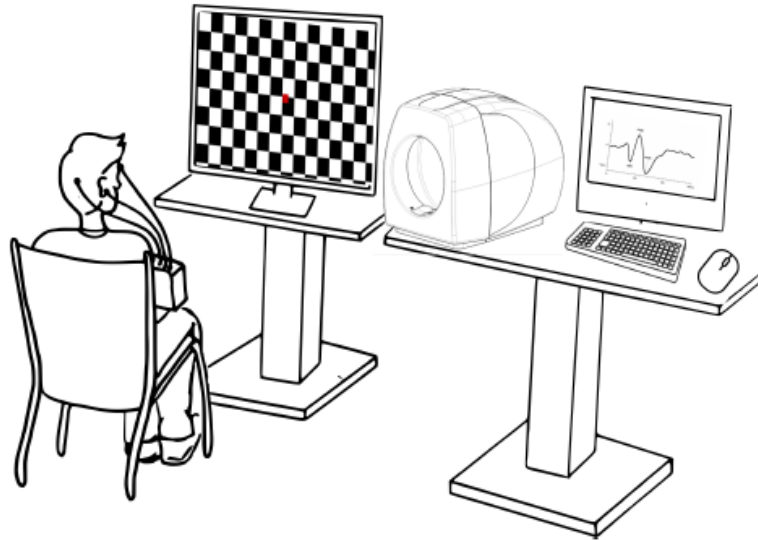


Figure 2.5: A representation of the entire Retimax system while it is working.

At the end of the test, the following screen appears on the computer monitor:

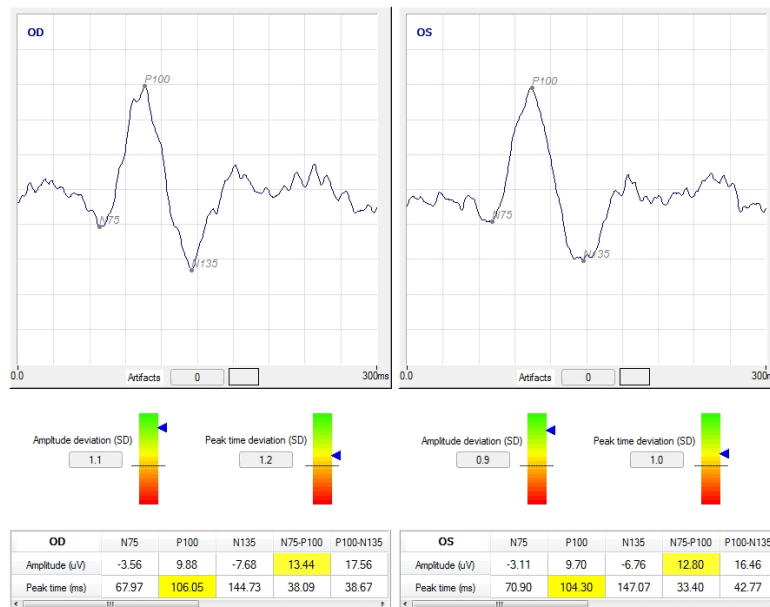


Figure 2.6: Retimax system screen.

## 2.2 Epson Moverio BT-200

With the aim of making the stimulation and analysis system for VEP tests portable, the device proposed in this thesis consists of a pair of smart glasses equipped with a a pocket unit with trackpad touch for managing the actions, based on *Android operating system*.



Figure 2.7: Smart glasses Epson Moverio BT-200 and external touchpad [27].

The same pattern of visual stimulation that the patient saw on the TV screen of the Retimax CSO system is now provided to the patient through the glasses, clearly smaller than a television screen and therefore easily transportable. The Moverio BT-200 are equipped with LCD monitors integrated in the lenses, one for lenses, which overlap the field of view of the person wearing them. The monitors are equivalent to about a 40-inch TV watched from 2 m away and the field of vision covers about 23 degrees. [27]. On these monitors, 960x540 pixel resolution images are projected, which in this specific case will be geometrically structured images, aimed at visual stimulation of the patient, as will be discussed in detail in the following paragraphs. Moverio BT-200 has an 8GB internal memory, expandable with micro-SD up to 32, a 1.2GHz dual core processor, 1GB of RAM and a refresh rate of 60 Hz [28].

The smart glasses are equipped with a camera, gyroscope, GPS and other integrated sensors that allow the software to perceive the movements of the wearer. Moreover, regarding the connectivity, these glasses have a Wi-Fi, Bluetooth and USB connection. They too come with Android and are available on the market for around \$700.

Moverio BT-200 is born as a device that allows *augmented reality* [27] but in this

case they are used as a stimulator of visual evoked potentials, through the development of an Android application loaded on the external controller. The application lets to set the stimulation parameters (temporal frequency, spatial frequency) before performing the test [21].

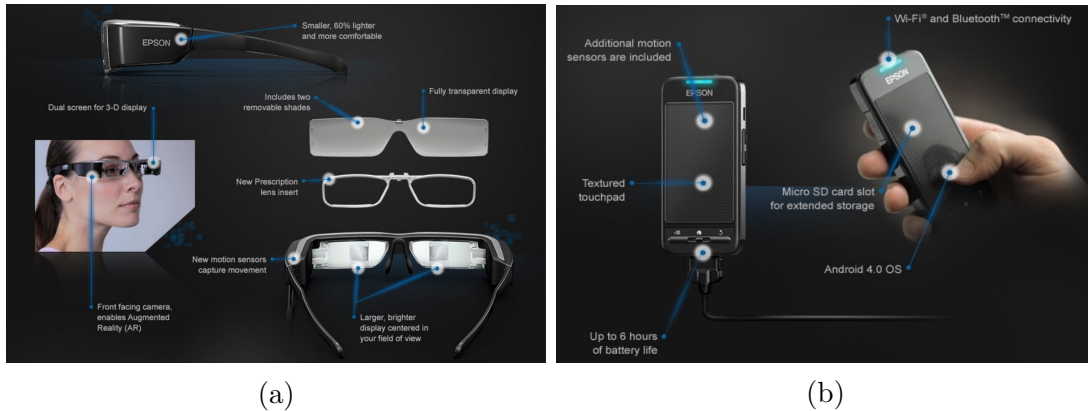


Figure 2.8: Features of the system: (a) Smart glasses; (b) External controller [28]

## 2.3 g.HIamp-Research

g.HIamp-Research is a multi-channel biosignal amplifier with USB technology from *g.tec*, a growing enterprise founded in 1999, with branches in Austria, Spain and the United States and distribution partners all over the world. g.HIamp is used for invasive and non-invasive measurements of brain functions and is intended only for applications of research and scientific investigation. In fact, it is not a medical device, so it cannot be used for diagnosis, treatment of diseases or other medical applications. g.HIamp provides 80, 144 or 256 channels per unit. The amplifier can be connected directly to a PC via a USB connector without the need for other data acquisition devices. Each channel is equipped with a synchronized analog to digital converter to perform the simultaneous sampling. Each 24-bit converter can operate up to 614.4 KHz and performs a 16 times oversampling, to obtain a high signal-to-noise ratio and a perfect signal resolution. This leads to a sampling frequency of up to 38400 Hz for each channel. Furthermore, the device is equipped with an internal unit for *impedance control*, as will be explained in detail in the "*Hardware and Software*" section. The electrodes used for picking up the signals, the same used with the Retimax CSO system, can be connected to the g.HIamp via the special 64-channel driver box supplied.



Figure 2.9: (a) g.HIamp-Research multi-channel biosignal amplifier; (b) 64-channel passive electrode driver box for g.HIampB [29].

In this thesis work, the 144-channel g.HIamp model was used as a measurement and processing device for EEG signals taken from the subject's scalp following visual stimulation with the Epson Moverio BT-200, in order to calculate the VEPs. g.HIamp is able to measure, without any saturation, also:

- *ECoG*, electrocortioculogram;
- *EOG*, electrooculogram;
- *ECG*, electrocardiogram;
- *EMG*, electromyogram.

### 2.3.1 g.HIamp-Research basic component

g.HIamp-Research consists of the following items:

- g.HIamp-Research USB biosignal amplifier;
- GlobTek GTM21097-3005 - power supply unit;
- Power line cord;
- USB cable;
- Parallel port cable;
- 64-channel electrode connector box;
- Connection cable from 64 channel electrode connector box to g.HIamp-Research;
- Instruction for use.

### 2.3.2 Technical specifications

|                                |                                |
|--------------------------------|--------------------------------|
| <b>Model</b>                   | g.HIamp-Research               |
| <b>Type</b>                    | 144-Channel Research Amplifier |
| <b>Rated power consumption</b> | 20 VA                          |
| <b>Rated DC voltage</b>        | 5 V                            |
| <b>Rated current of fuse</b>   | 4 A, type 20 mm                |
| <b>Rated voltage of fuse</b>   | 250 V                          |
| <b>Produced</b>                | HR-2018.02.04                  |
| <b>Producer</b>                | g.tec medical engineering GmbH |

Table 2.1: g.HIamp-Research.

|                     |        |
|---------------------|--------|
| <b>USB</b>          | 5 V DC |
| <b>HOLD</b>         | 5 V DC |
| <b>DIGITAL IN</b>   | 5 V DC |
| <b>POWER SUPPLY</b> | 5 V DC |

Table 2.2: Maximum voltages at the previous sockets.

|                        |                   |
|------------------------|-------------------|
| <b>Sensitivity</b>     | $\pm 250$ mV      |
| <b>Highpass</b>        | 0 Hz              |
| <b>Lowpass</b>         | 19.2 kHz          |
| <b>Input Impedance</b> | $>100$ M $\Omega$ |

Table 2.3: Amplifier Settings for all channels.

|                           |                      |
|---------------------------|----------------------|
| <b>ADC resolution</b>     | 24 bit               |
| <b>Sampling frequency</b> | 38400 Hz per channel |
| <b>Number of ADCs</b>     | 144                  |

Table 2.4: Analog-digital converter (ADC).

|  |           |
|--|-----------|
| <b>Isolated power supply</b>                     |           |
| <b>Rated power consumption</b>                   | 30 VA     |
| <b>Rated AC voltage (input)</b>                  | 100-240 V |
| <b>Rated frequency</b>                           | 50-60 Hz  |
| <b>Rated DC voltage (output)</b>                 | 5 V       |
| <b>Rated DC current</b>                          | 6 A       |
| <b>Maximum voltage on Power Supply connector</b> | 5 V DC    |

Table 2.5: Power supply.

## 2.4 Data Acquisition: Hardware and Software

### Premise

As anticipated, the pattern of visual stimulation that is provided to the patient consists in the complete inversion of the squares of a checkerboard from white to black and vice versa. This inversion occurs once every 500 ms: since it is this inversion that represents the stimulation pulse, it is necessary to synchronize the VEP calculation at each stimulation instant. This requires a *trigger signal*. Stimulation parameters will be discussed in detail in section “2.5 Acquisition Protocol for the Experimental Tests”.

#### 2.4.1 First prototype system for trigger generation

The sequence of images representing the stimulation pattern was overlaid by an *impulsive audio signal*, produced through Matlab, starting at the same time as the images sequence. The audio signal can be seen as a voltage signal that has peaks every 500 ms and that is output via audio jack [21].

The objective is to send this audio signal, which is an analog signal, to the *Arduino Uno* and, using its ATmega 328 microcontroller, output a digital trigger signal.

This digital trigger signal is then sent to the parallel port of the g.HIamp-Research which is connected via USB to the PC, where upon arrival of the trigger, using the appropriate software, the VEP calculation starts.

The sound signal, however, has very low amplitude voltage peaks, around 170 mV: then, before sending this signal to Arduino, an amplification circuit is required.

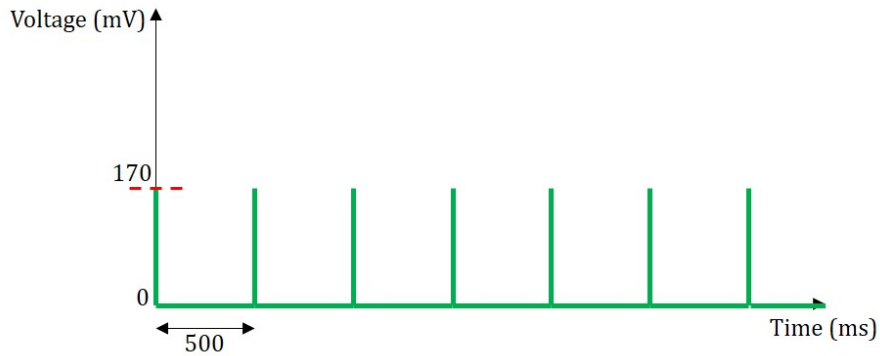


Figure 2.10: Audio signal before amplification.

The amplification circuit has been mounted on a breadboard and consists of:

- an LM324N non-inverting operational amplifier;
- a 22 k $\Omega$  feedback resistance;
- a 2.2 k $\Omega$  resistance;
- various connectors.

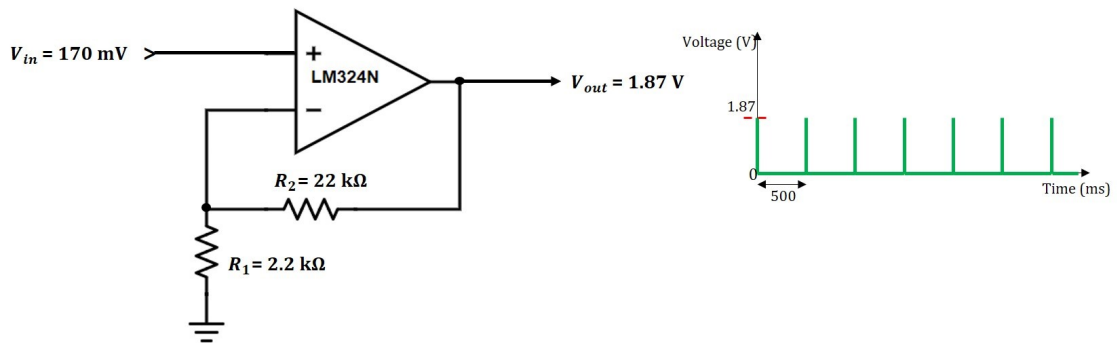


Figure 2.11: Electric scheme of the amplification circuit and audio output signal.

Now the amplified audio signal can be input to Arduino, whose microcontroller has been programmed as follows:

```

int analogPin = A0;    // pin to which the amplified analog signal arrives
int outputTrigger = 13; // output pin of the square wave to be taken to the parallel port of g.HIamp
int threshold = 1.5;  // threshold (expressed in V) beyond which the square wave must be put out

void setup()
{
  // initialization pin 13 as output for the trigger
  pinMode(outputTrigger, OUTPUT);
  // initialize serial communications:
  Serial.begin(9600);
}
void loop()
{
  // reading of the analogue input voltage value
  int analogValue = analogRead(analogPin);

  // if the analogue input is higher than the preset threshold, the square output wave starts
  if (analogValue >= threshold)
  {
    digitalWrite(outputTrigger, HIGH);
    delay(250); // time expressed in ms
    digitalWrite(outputTrigger, LOW);
    delay(250);
  }
}

```

Figure 2.12: Arduino code for generating the square wave.

The analog input pins and the digital output ones are initialized. If the microcontroller receives an input voltage value higher than the set threshold, it then outputs a square wave in the 0-5 V range (Arduino voltage range) with 50% duty cycle: 250 ms on and 250 ms off. In this way, the parallel port, set by software to read only the rising edges, gets a high logic level every 500 ms and therefore every 500 ms the VEP calculation starts.

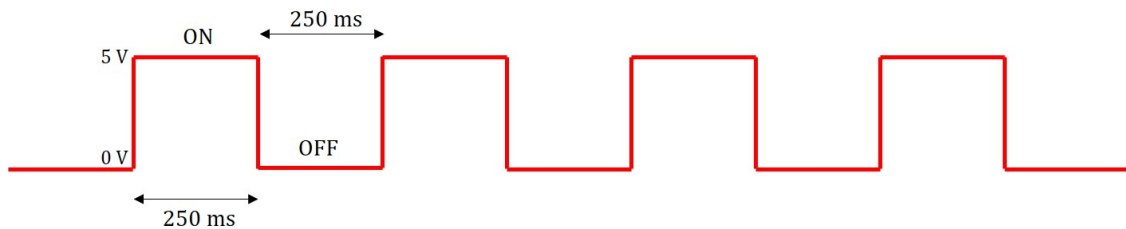


Figure 2.13: First square wave model generated by Arduino.

Since the technical specifications report the value of 5 V as the maximum input voltage to the parallel port, to stay in safe conditions it was preferred to send this input square wave to a voltage divider composed of 2 equal resistances. In this way the value of the input voltage to the parallel port has been halved, now equal to 2.5 V. This value is acceptable since the minimum voltage value recognized by the parallel port as a high logic level is 1.8 V.

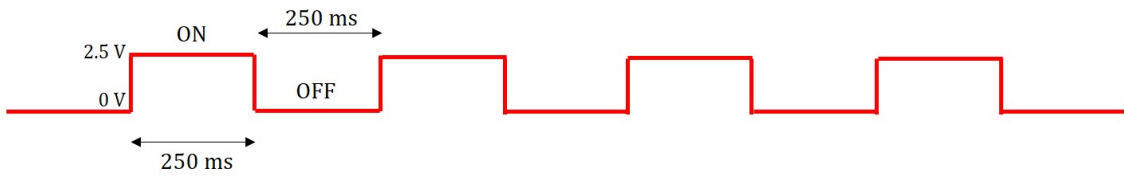


Figure 2.14: Trigger signal.

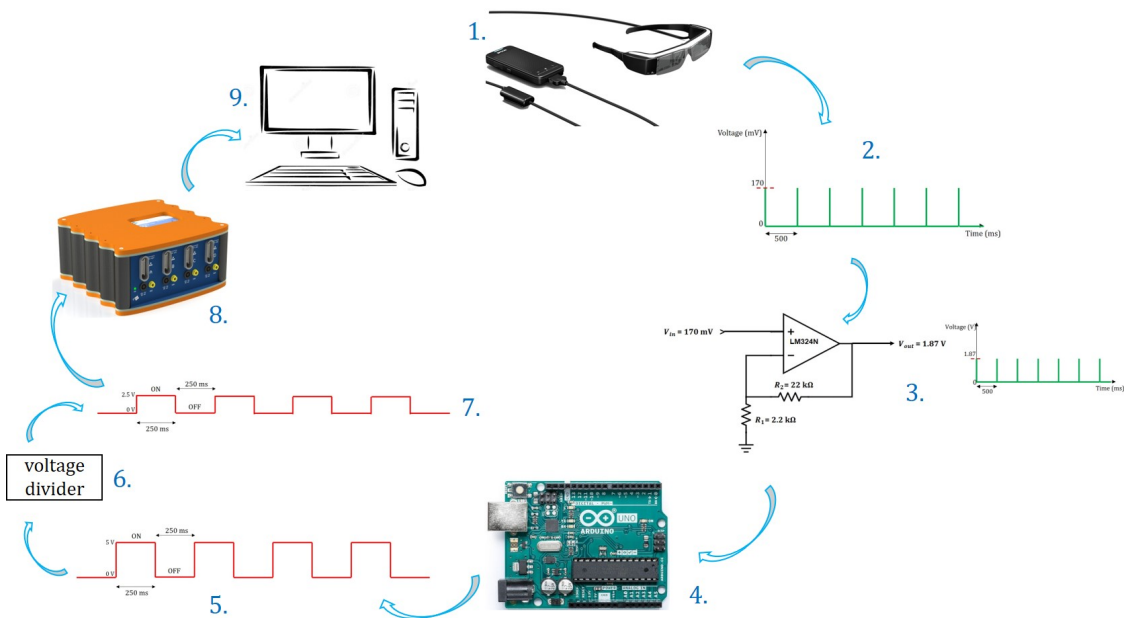


Figure 2.15: First prototype: 1.Smart glasses with jack output; 2.Original audio signal; 3.Amplification circuit and amplified audio signal; 4.Arduino Uno; 5.Square wave 0-5 V; 6.Voltage divider; 7.Square wave 0-2.5 V: trigger signal; 8.g.HIamp-Research; 9. PC with software for VEP calculation.

It was noted, however, that using this trigger generation system, an average delay of about 275 ms was introduced in the VEP calculation.

|            |           |
|------------|-----------|
| <b>DX1</b> | 372.50 ms |
| <b>DX2</b> | 378.33 ms |
| <b>DX3</b> | 371.67 ms |
| <b>DX4</b> | 375.83 ms |
| <b>DX5</b> | 374.17 ms |
| <b>SX1</b> | 382.50 ms |
| <b>SX2</b> | 375.9 ms  |
| <b>SX3</b> | 365.83 ms |
| <b>SX4</b> | 375.83 ms |
| <b>SX5</b> | 372.5 ms  |

Table 2.6: 5 acquisitions on the right eye and 5 acquisitions on the left eye of a healthy subject: the time of P100 wave manifestation is reported. Note how, due to the delay of about 275 ms, the P100 peaks appear on average after 375 ms from the stimulus.

Probably this delay is due to the time required by Arduino for the conversion from analog to digital and its magnitude is not acceptable because it is greater than half of an epoch, equal to 500 ms. Because of this delay the VEP wave appears shifted to the right, as shown in the *figure 2.15*:

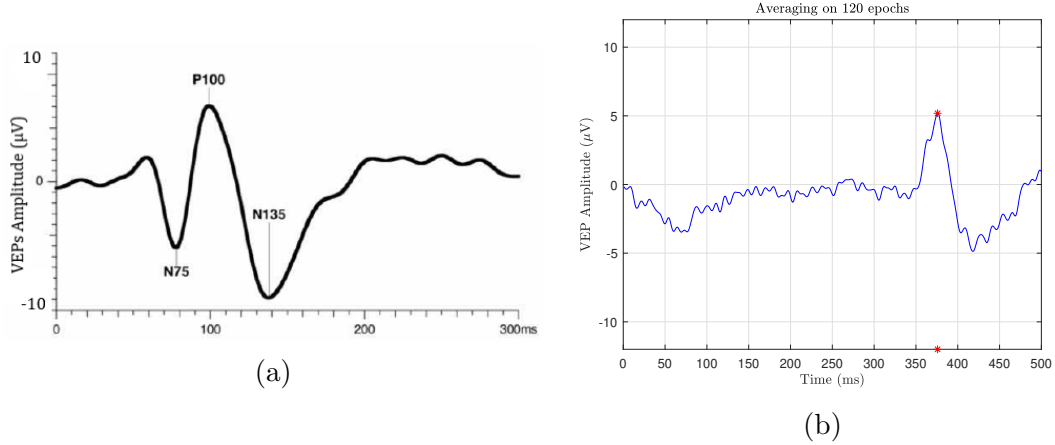


Figure 2.16: (a) Theoretical result [24]; (b) Result obtained through this first prototype system for trigger generation.

Since this delay was constant, a first idea was to take it into account in post-processing and to shift 275 ms to the left the acquired signals. Later it was preferred to think of a new trigger generation strategy, avoiding the use of Arduino. Hence, the development of the second prototype discussed in the next paragraph.

## 2.4.2 Second and definitive prototype system for trigger generation

This prototype consists of the following blocks:

1. **amplifier block;**
2. **rectifier block;**
3. **threshold comparator block.**

The preliminary step was the modification of the impulsive audio signal superimposed on the stimulation pattern. Through an Matlab algorithm an ON/OFF sound signal was generated, having the following parameters:

- duration: 60 s;
- sampling frequency: 20000 Hz;
- voltage amplitude: 170 mV;
- 250 ms ON and 250 ms OFF.

Each interval of 250 ms of ON consists of a sinusoid at a frequency of 800 Hz.

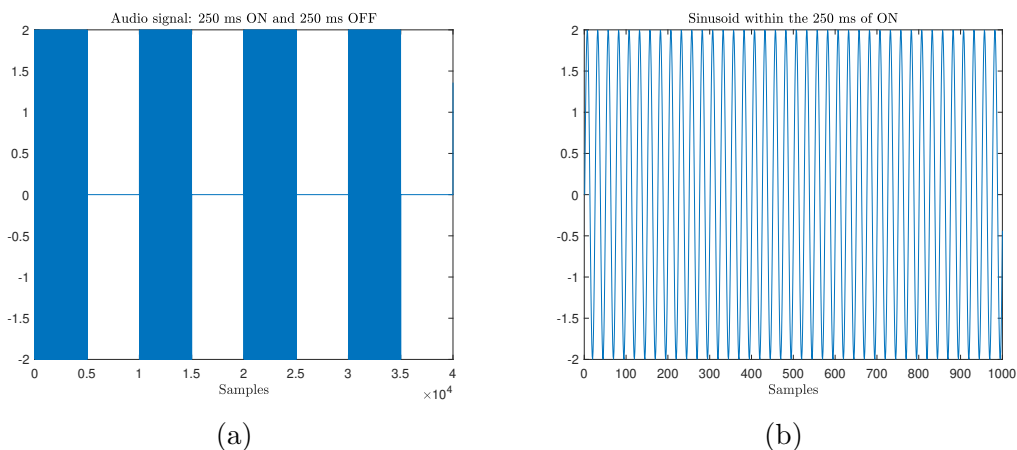


Figure 2.17: (a) On/off audio signal; (b) Sinusoid at high frequency which shapes the ON range.

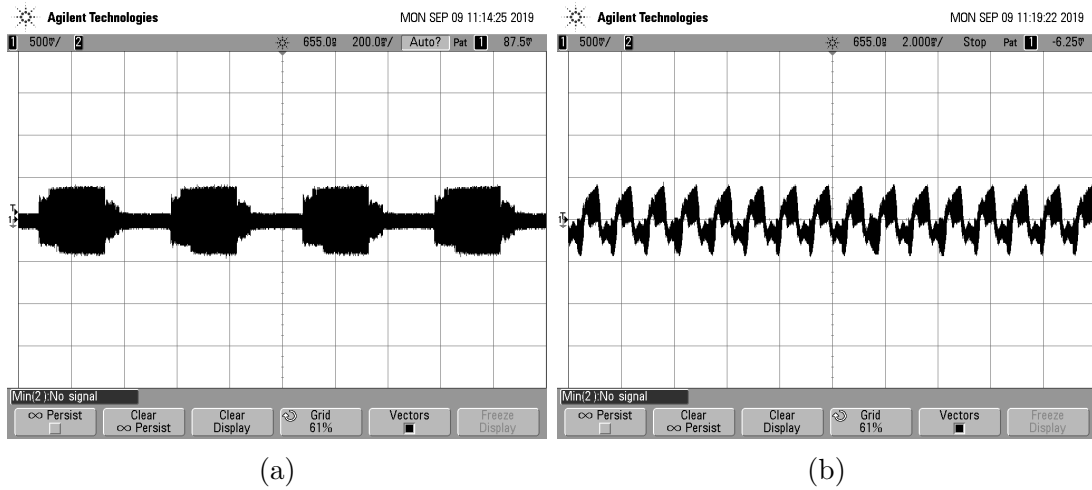


Figure 2.18: (a)On/off audio signal: oscilloscope; (b)Sinusoid at high frequency which shapes the ON range: oscilloscope.

It's useful to keep only the positive half-waves of this audio signal with the aim of bringing out a square wave that can act as a trigger signal.

### Step 1: audio signal amplification

It is necessary to amplify the new audio signal in view of the following steps: to obtain the final square wave to be used as a trigger signal, the audio signal must pass through a rectifier circuit, as will be explained in detail in *Step 2*. This circuit foresees the presence of a silicon diode with a voltage drop of approximately 0.6 V. Since the original audio signal has an amplitude of 0.170 V it needs its initial amplification.

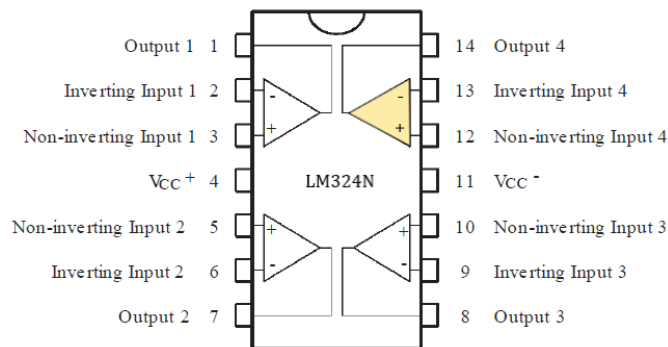


Figure 2.19: It is highlighted the op amp used to amplify the original audio signal.

It was decided to use the LM324N integrated circuit, which has 4 op amps: one of these was used for signal amplification. LM324N was powered by a single power supply, so the amplified output signal only has positive semiwaves. The integrated circuit is supplied at a voltage of 3.6 V through the series of three 1.2 V batteries each.



Figure 2.20: Circuit power supply: batteries in series.

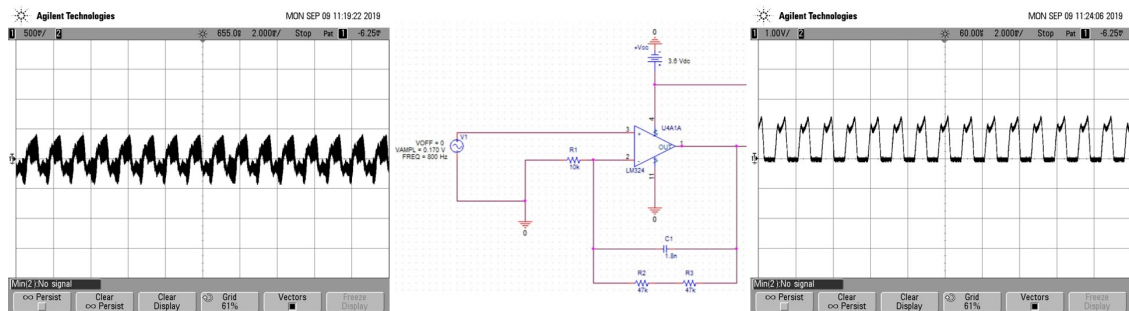


Figure 2.21: Sequentially, original audio signal, amplification circuit, amplified audio signal.

This amplifier block consists of:

- one of the LM324N operational amplifiers;
- a  $10\text{k}\Omega$  resistor;
- the series of two  $47\text{k}\Omega$  feedback resistors;
- a  $1.8\text{ nF}$  capacitor.

The capacitor acts as a *low-pass filter* to eliminate frequencies that are too high compared to the carrier frequency of 800 Hz. The choice of this capacitor allows frequencies up to 900 Hz.

Now the amplified audio signal has an amplitude of 0 - 1.7 V.

## Step 2: audio signal rectification

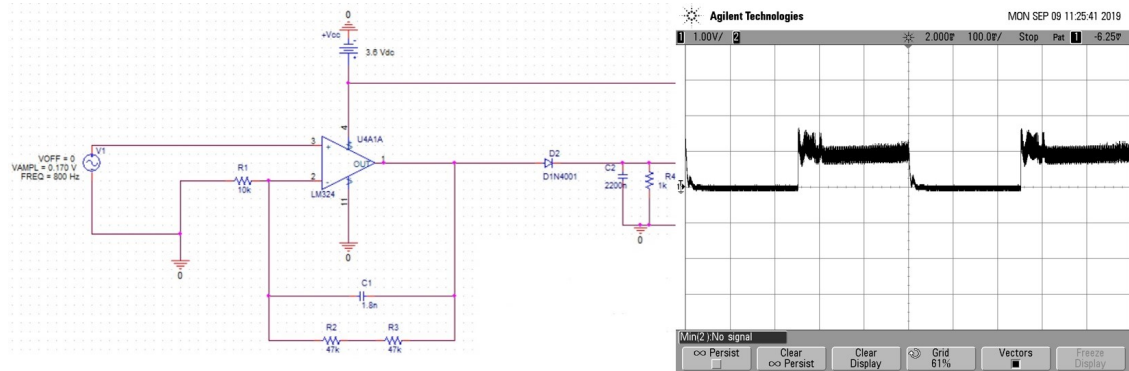


Figure 2.22: Amplifier block followed by rectifier block. The rectified signal is shown.

The rectifier block consists of:

- a silicon diode of the 1N4001 series;
- a 2.2  $\mu\text{F}$  capacitor acting as a capacitive filter;
- a 1k $\Omega$  resistor.

The waveform output from the rectifier block belongs to the range 0 - 1.1V, as the audio signal undergoes the voltage drop on the silicon diode.

## Step 3: threshold comparator and trigger signal generation

The output signal from the rectifier finally becomes the input of a threshold comparator, which is another LM324N op amp.

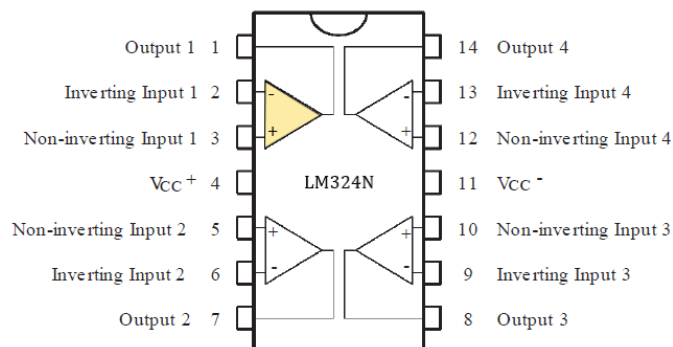


Figure 2.23: It is highlighted the op amp used as threshold comparator.

The *threshold voltage* has been obtained by means of a voltage divider (a 10kohm resistor and the series of two 1kohm resistors) which receives the input supply voltage and brings a voltage output value of about 0.5 V. This value was wanted because it was greater than that due to the circuit noise, about 0.3 V.

The threshold comparator is a module that performs a step function: it converts an analog input (the rectified audio signal) into a logical output value. In this way, as threshold comparator output, the desired square wave is obtained to be used as a synchronization signal to be sent to g.HIamp.

This square wave falls within the 0 - 2 V range, the maximum output voltage value by feeding the LM324N at 3.6 V and has the same timing as the square wave obtained through the first prototype.

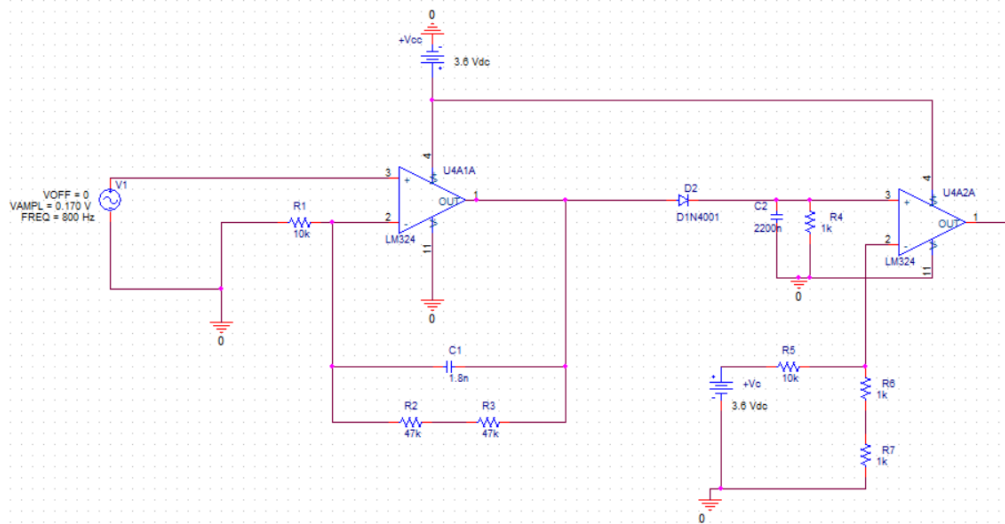


Figure 2.24: Final prototype for trigger generation.

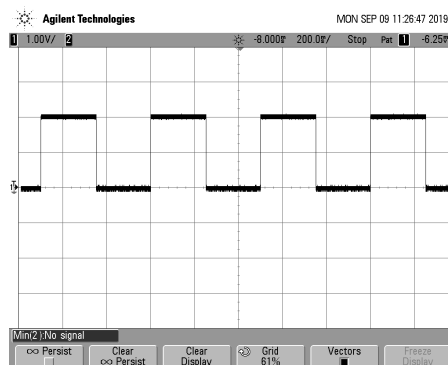


Figure 2.25: Trigger signal to send to the parallel port of g.HIamp.

## Hardware Improvement: supply voltage control

It has been said that the entire circuit is supplied with a voltage of 3.6 V via the series of three batteries.

Since the circuit requires a minimum supply of 3 V to function properly, it was decided to carry out a control of the supply voltage, so as to replace the batteries just before the power supply drops below the minimum threshold required.

The supply control circuit consists of:

- a third LM324N op amp used as a threshold comparator;
- a 220  $\Omega$  resistor;
- a 5.6 k $\Omega$  resistor;
- a zener diode 3.3 V as voltage stabilizer;
- a 100  $\Omega$  resistor;
- one red LED.

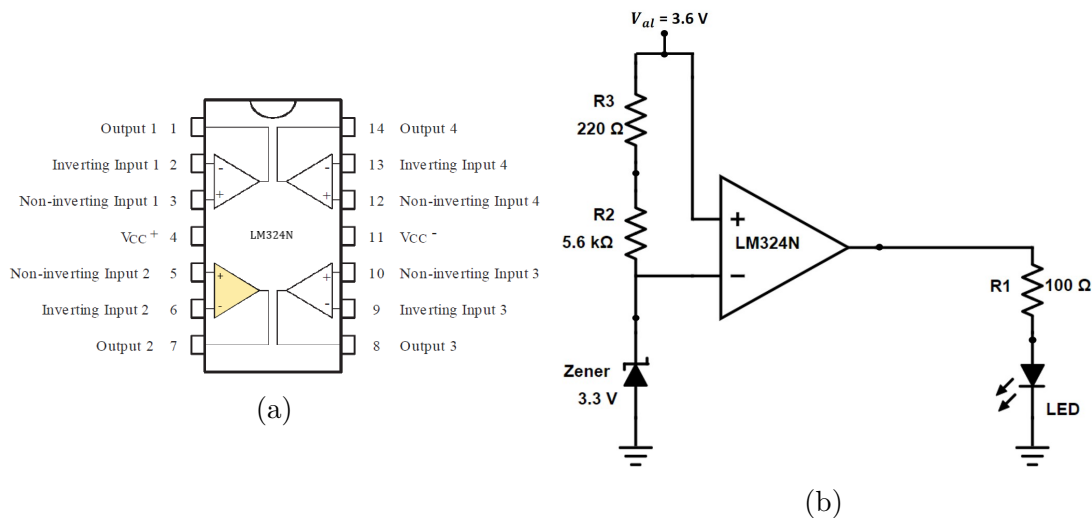


Figure 2.26: (a) It is highlighted the op amp used as threshold comparator; (b) Electric scheme of the supply voltage control circuit.

After its inverse polarization, the zener diode maintains the threshold voltage at 3.3 V independently of the variation of the supply voltage. As long as the power supply voltage is higher than the threshold then the red LED remains on, otherwise it turns off: in this case it is time to replace the batteries.

Finally, the entire trigger generation circuit, including the power control one, has been made easily portable thanks to welding on the matrix board, as shown in the *figure 2.25*:

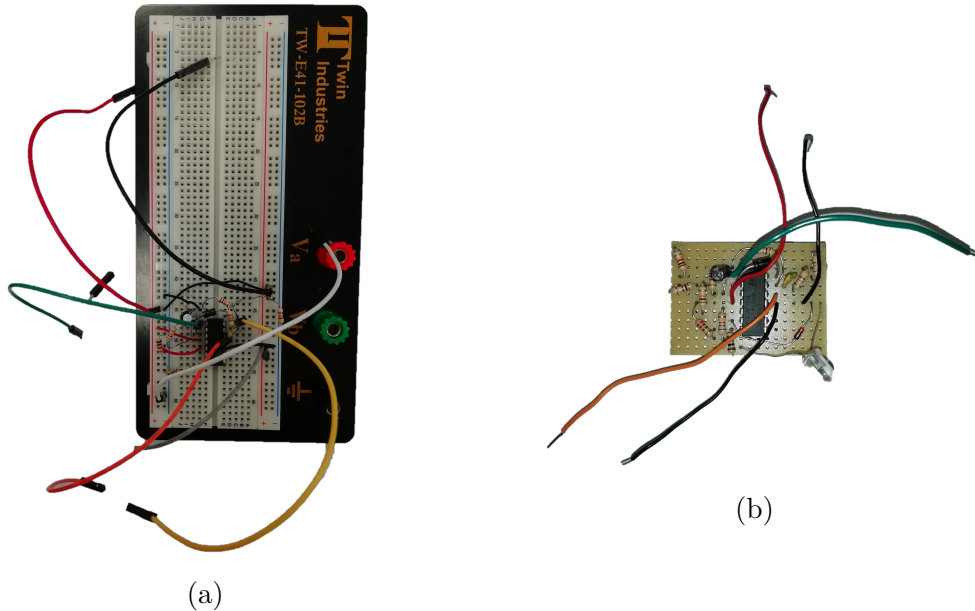


Figure 2.27: (a)Circuit on breadboard; (b)Circuit on matrix board: small and portable.

### 2.4.3 g.Recorder Software

The g.tec support software (under Windows) is *g.Recorder*, which allows the recording, display and storage of biosignals, ensuring a comfortable hardware configuration. The data is stored in *hdf5 format*.

Particular software extensions allow the extraction and online visualization of some signal parameters useful for clinical research:

- Compressed Spectral Array (**CSA**);
- Heart Rate (**HR**);
- Heart Rate Variability (**HRV**).

Signal and parameters can also be checked in display mode, stored in disk and re-displayed later in offline/replay mode.

For the purposes of this thesis work, g.Recorder was used for the acquisition of the EEG signal and for the calculation of VEPs. After setting the channels that will be used for the acquisition, the software receives the trigger signal generated by

the prototype shown in the previous paragraph via parallel port and synchronizes the start of the VEP calculation with the rising edges of this signal.



Figure 2.28: (a)List of triggers that can be selected: the trigger 7 was chosen arbitrarily. The trigger reading is enabled only on the rising edge; (b)Reading of trigger 7 every 500 ms.

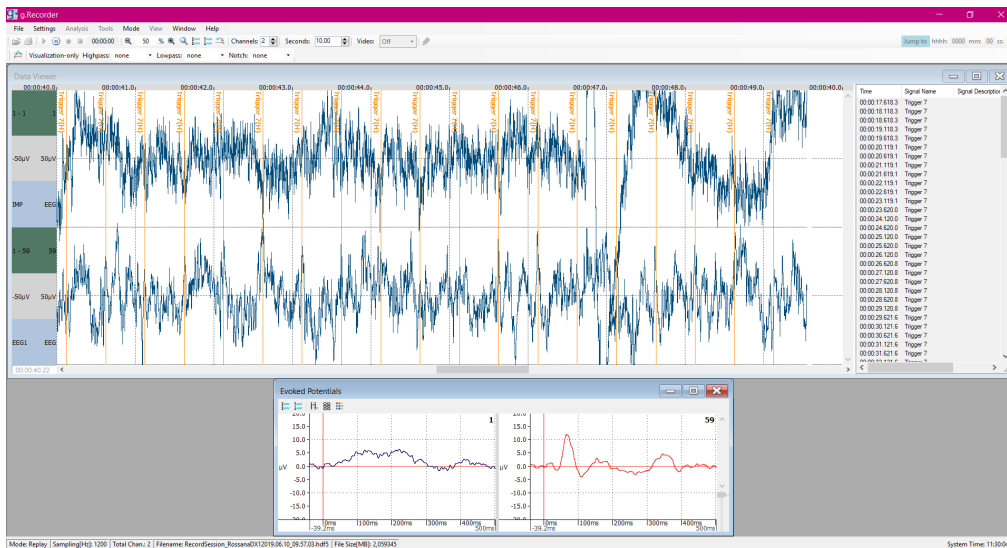


Figure 2.29: Main screen of the software during an acquisition.

Furthermore, in the "*Evoked Potentials*" section, the following settings have been set:

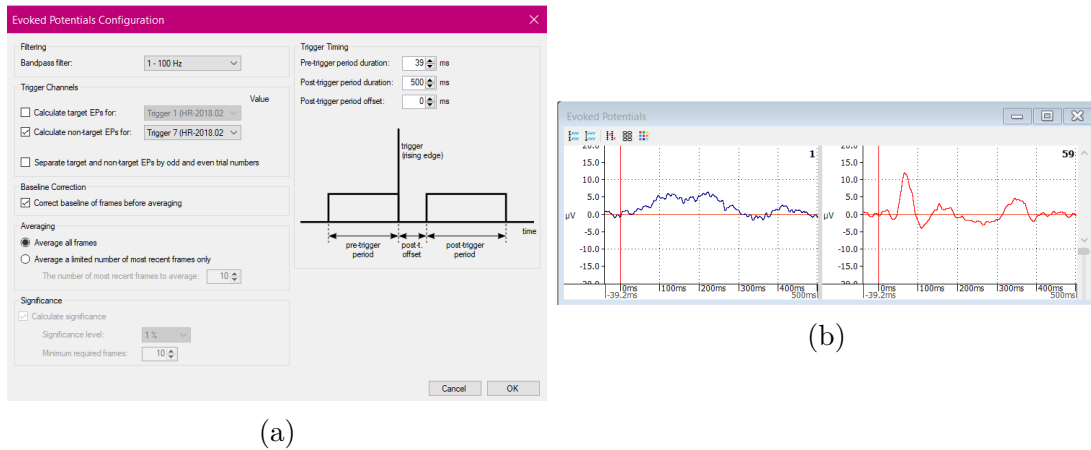


Figure 2.30: (a) Filtering, epochs to mediate and trigger settings; (b) VEP at the end of an acquisition.

From the settings it's possible to see how the pre-trigger value has been set to  $39\text{ ms}$ . It was noticed, in fact, that the overlapping audio signal - sequence of stimulation images was not perfect and that the audio signal was  $39\text{ ms}$  late with respect to the stimulation video.

The resulting VEP is given by the average of all the epochs acquired.

## 2.5 Acquisition Protocol for the Experimental Tests

As anticipated, the purpose of this thesis work is the comparison between the visual stimulation system, VEPs acquisition and calculation proposed by us and the Retimax CSO currently in use, for a possible validation of our prototype.

Consequently, for the comparison to be valid, the stimulation and parameters conditions must be the same for both systems.

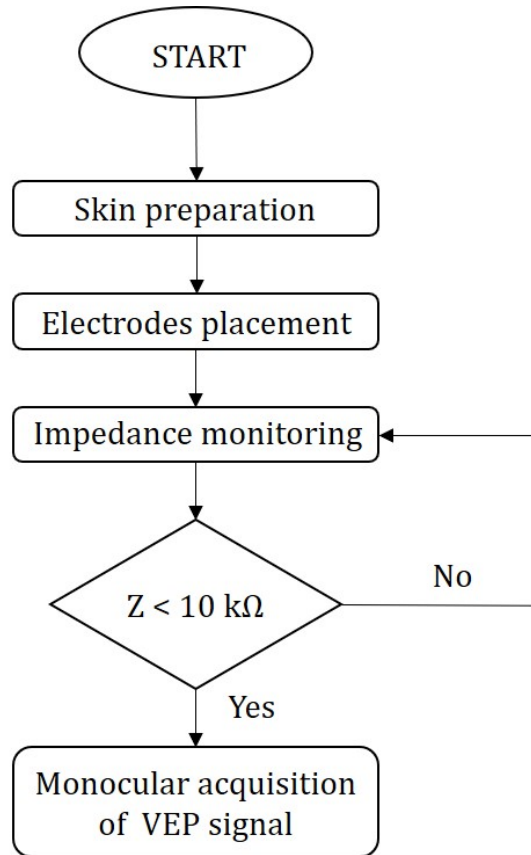


Figure 2.31: Clinical acquisition protocol.

## Skin preparation

The first step consists in preparing those areas of the patient's skin where the sampling electrodes will be placed. This preparation involves the use of *Nuprep Skin Gel*, necessary to degrease the patient's skin, eliminating any dead cells that would hinder the good contact between skin and electrodes.

## Electrodes placement: International Standard 10/20

For electrode placement the *international standard 10/20* has been followed, as required by the ISCEV standard. Four electrodes have been used for our purposes:

- active electrode in  $O_z$ ;
- reference electrode for  $O_z$  in  $F_{pz}$ ;
- ground electrode at the left mastoid;

- electrode for measuring impedance in  $F_{p1}$  (only for our prototype).

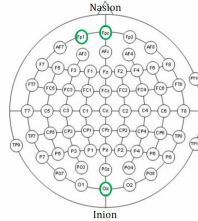


Figure 2.32: Extended 10/20-System with 30 channels [30].

The electrodes are positioned using *KONIX EEG* conductive paste to reduce contact impedance.

## Impedance monitoring

Once the electrodes are positioned, to ensure good signal quality it is advisable to check the impedance. An impedance value greater than 10 k $\Omega$  could make the picked signal unreliable.

The g.Recorder software presents a tool for calculating the impedance, as shown in the *figure 2.31*.

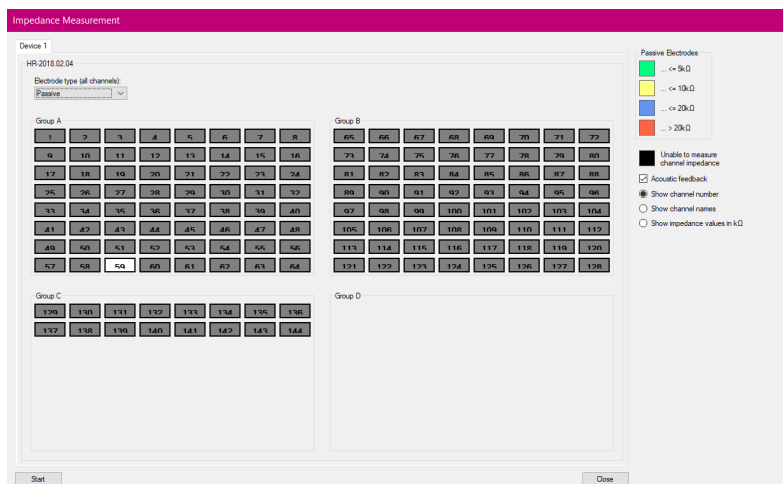


Figure 2.33: Impedance assessment tool.

Impedance evaluation is allowed through channel 1 of the g.HIamp driver box, also called *channel Z*. The test can start when the impedance value is within the *yellow-green range*.

## Monocular acquisition of VEP signal: parameters of stimulation

After covering one of the patient's eyes and after darkening the room where the exam will take place, the test can begin. In the case in which our prototype is used, the patient is made to wear Smart Glasses, while if it's used the Retimax CSO system the patient is asked to observe the television screen where the stimulation pattern will appear.

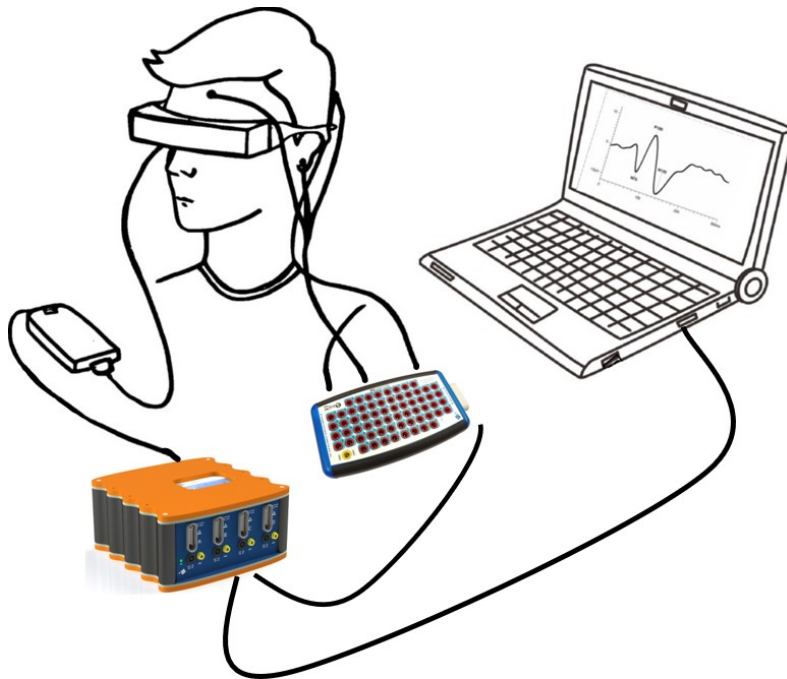


Figure 2.34: A representation of our prototype while it's working.

In both cases, as anticipated, the stimulation pattern consists of the total inversion of the elements of a checkerboard, during which the patient is required to observe a red dot in the center of the same, called *fixation point*.

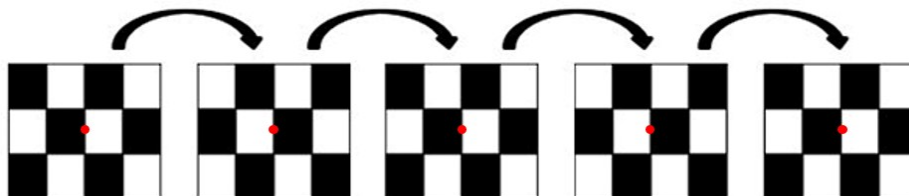


Figure 2.35: Stimulation pattern for pr-VEP tests [31].

The stimulation pattern has the following features:

| <i>Parameters</i>                             | <i>Value</i>                      |
|---|-----------------------------------|
| <i>Duration</i>                               | 60 s                              |
| <i>Temporal frequency</i>                     | 2 reversal per second (rps)(2 Hz) |
| <i>Spatial frequency</i>                      | 60 minutes of arc                 |
| <i>Duration of an epoch</i>                   | 500 ms                            |
| <i>Number of epochs acquired and averaged</i> | 120                               |
| <i>Sweeps time</i>                            | 300 ms                            |
| <i>Contrast</i>                               | 81%                               |
| <i>Field size</i>                             | 23°                               |
| <i>Bandpass filter</i>                        | 1 - 100 Hz                        |

Table 2.7: Stimulation parameters set for both systems.

The time frequency is kept so low mainly for two reasons:

1. to fatigue the patient's tested eye as little as possible, thus giving the possibility to repeat the test several times. This aspect is particularly important in the context of this thesis work, as the patient is tested twice through the two different devices;
2. to avoid inducing seizures.

The choice to set the contrast to 81% was dictated by the Smart Glasses LCD screen.

During the acquisition of the various epochs, the average of the selected periods is gradually calculated and displayed on the PC screen. The VEP signal obtained at the end of the test is the average of all the epochs acquired: it is therefore the result of the averaging technique.

## 2.6 Advice for the successful execution of an exam

The artifacts in the electrophysiological examination are represented by any electrical disturbance generated by the muscular movements or electroencephalogram of the subject examined, or electromagnetic disturbances generated by the recording instruments themselves, or commonly present in the surrounding environment. All electrical devices generate electromagnetic disturbances and these devices should therefore be at an appropriate distance from the recording instrument and the patient examined. Cell phones should be kept off during the examination. Artifacts can alter the bioelectric response generated by the patient subjected to the examination so as to make the examination itself unreliable.

In the VEP exam registration the main artifact is constituted by the patient's electroencephalographic activity: however, it is recalled that it can be eliminated with the averaging technique.

Muscle tension can generate highly significant electrical activity. During an examination, it is therefore strongly advised to inform the patient not to stretch the neck muscles, to not chew and not to blink too frequently. In fact, eye movements can produce artifacts in the electro-functional test. In particular, eye movement artifacts and patient's fixation problems produce baseline variations. Under ideal conditions the baseline should look like a horizontal line with minimal oscillations. In the event of excessive fluctuations of the baseline, the patient should be reminded to observe carefully the fixation point or the structured stimulus.

The environmental characteristics must be such as to produce the total *darkness* in the examination room in order to obtain adequate retinal adaptation, avoiding light reflections on the stimulator screen.

The VEP exam is generally performed in *monocular vision*: the unexamined eye must be occluded during the examination. It is also necessary to pay attention to the distance between the patient and the pattern stimulator, in order to guarantee the correct visual angle and the relative spatial frequency subtended by the stimulus.

The impedance of electrical contact between the subject and the electrodes used for recording the biopotential should be less than 10 k $\Omega$ . The lower the value, the better the signal-to-noise ratio.

It is necessary to use original accessories, such as electrodes, conductive paste and other complying with the EU directive 93/42/EEC. The electrodes must always be disinfected and sterilized before their use. Carefully degrease the patient's skin where the electrode will be applied. The electrodes in contact with the skin must be used together with an adequate quantity of gel or conductive paste specific for these electrodes, in order to favor their contact with the skin.

If after applying the suggestions listed above the artifacts generated by muscle movements were still excessive, it will be possible to resort to further solutions, such as increasing the number of mediated samples during recording. A further solution is to reduce the amplifier bandwidth by selecting a narrower filter capable of reducing the amplitude of such disturbances. Digital filtering through *Fast Fourier Transform* is also a remedy for the elimination of disturbances. By decomposing the sampled signal in all its harmonic components it will be possible to select only

those of interest, eliminating the others. It will then be possible to reassemble the signal without the eliminated components and thus obtain a cleaner signal.

## 2.7 Data Post-processing

As listed in *Table 2.7*, the VEP acquisition is done by setting a 1-100 Hz bandpass filter for both devices, without any notch filters as ISCEV standards require [21].

The sampling frequency is originally different:

- 1200 Hz for g.HIamp-Research;
- 1700 Hz for Retimaz CSO.

Then the signals obtained from both devices are imported to *Matlab* and each of them is stripped of the *average value*. Subsequently, signals obtained through Retimax were *sub-sampled* at 1200 Hz, to make the sampling frequencies of the signals obtained from the two different devices equal. This gives the same number of samples for all signals.

At this point the same acquisitions, made through the two different acquisition systems, are plotted superimposed, so as to be able to make a first visual comparison.

It was also thought to perform a *frequency analysis* of the acquired signals. In this regard it has been asked which approach, between the *Power Spectral Density (PSD)* and the *Fast Fourier Transform (FFT)*, was the most useful to extrapolate the information of interest. The PSD describes how the signal power is distributed along the frequencies, while the FFT shows the spectral content of the signal, the amplitude and the phase of the signal harmonics.

Being interested in identifying the range of frequencies in which it is found the greater information of the signals, it is chosen to calculate the PSD. The calculation was made using the *periodogram method*, in which the PSD is the FFT signal framework module. It is emphasized that the simple periodogram, or *Schuster's periodogram*, introduces an excessive variability of the estimate. Then, as proposed by the literature, the method is integrated with the mathematical tool that reduces random variability: the media operation. The *Daniell's*, *Barlett's* and *Welch's methods* are all designed to mitigate the variability of the estimate.

For our analysis the **Welch's method** has been used, as it represents a middle way between attenuation of the variability and maintenance of the resolution. The method involves the fragmentation of the signal in contiguous segments that can

be overlapped up to 50% and this leads to have a greater number of segments to mediate. For this reason, compared to the other methods, Welch’s provides a better spectral resolution. The fragmentation of the signal happens through the choice of a suitable window, that in our case is the *Hamming window*.

From the frequency representation a particularly interesting aspect has been evidenced: the greater information of the signals appears in band 1-30 Hz, as shown in *Figure 2.34* and *2.35*.

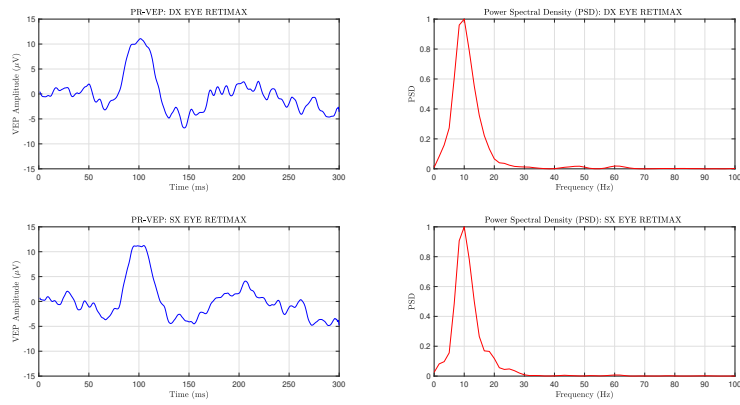


Figure 2.36: Right and left eye signals obtained via Retimax and their PSD.

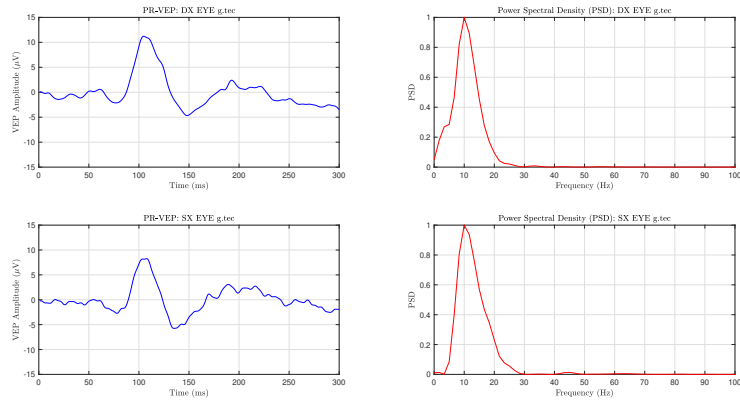


Figure 2.37: Right and left eye signals obtained via g.HIamp and their PSD.

The complete results will be reported in Chapter “*Results*”.

From these observations it was thought to further filter the signals, using a **1-30 Hz band-pass filter**. In doing so, as will be shown in the next chapter, we obtain cleaner signals, not altered either in amplitude or latency and easier to interpret.

To determine whether or not the 1-30 Hz filtering removes an important information content of the signals it was decided to:

1. extract the power quantity of each 1-100 Hz filtered signal;
2. mediate all these numerical values of all 1-100 Hz filtered signals;
3. extract the power quantity of each 1-30 Hz filtered signal;
4. mediate all these numerical values of all 1-30 Hz filtered signals;
5. repeat these operations for both Retimax and Smart glasses signals.

If, as we want to demonstrate, the 1-30 Hz band filtering does not eliminate any important information of the acquired signals, the averages relative to the power content of the 1-100 Hz and 1-30 Hz signals must be very similar. The obtained results are shown in the next chapter.

## 2.8 An alternative visual stimulator: the Cardboard

Cost reduction represents the most current technological challenge: the primary objective is to achieve good performance by limiting economic investments as much as possible.

In light of these intentions, in this thesis work it was thought to try a new system for visual stimulation, much cheaper than both the Retimax system and the Smart Glasses.

For the price of a few euros, there are commercially available folding cardboard glasses called "**Google Cardboard**".

Created by David Coz and Damien Henry, this platform is designed just like a low-cost system to encourage interest and development in virtual reality applications. To use Cardboards, just be equipped on your smartphone with specific applications for your own purposes. The phone is placed on the back of the viewer and the applications are used by looking through the lenses.



Figure 2.38: Cardboard as cheap visual stimulator.

In order to use the Cardboards as a visual stimulation system, a simple application for Android has been developed. This application allows the cardboard wearer to initiate the visual stimulation pattern as soon as he feels ready to begin the test. In fact the first screen of the application presents the "play" button on which the user can click through the Cardboard conductive lever which activates a touch event on the phone screen. Clicking on "play" starts the visual stimulation video already described in the previous paragraphs. The test is carried out also in this case in monocular mode.

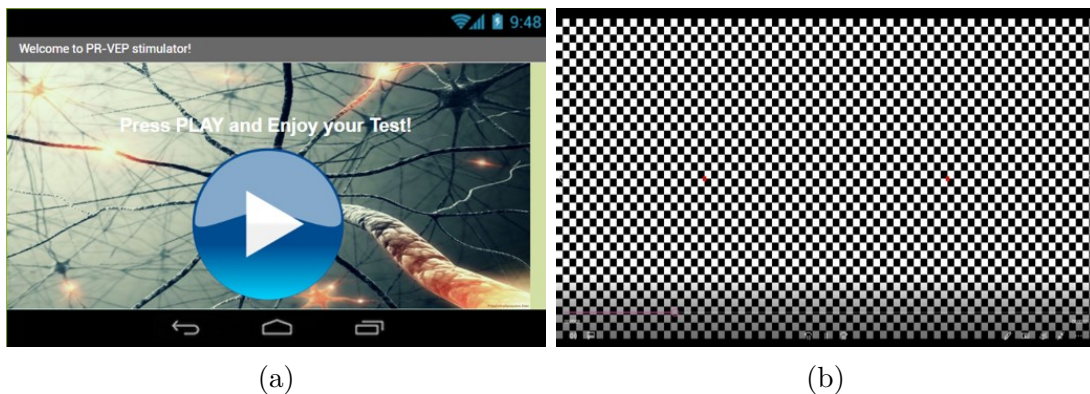


Figure 2.39: (a)Screen 1 of the application; (b)Screen 2 of the application. The red fixation points are two because in monocular mode they are seen individually.

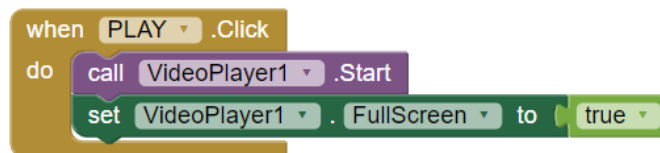


Figure 2.40: Functional blocks of the application.

The obtained results are reported:

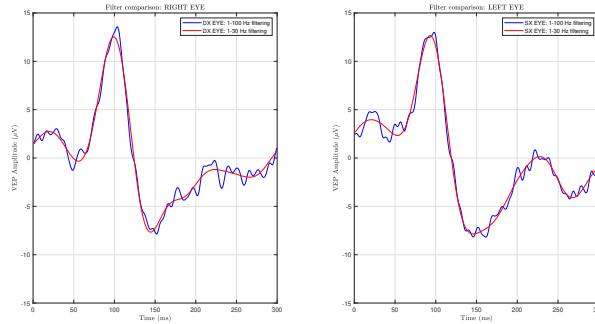


Figure 2.41: Cardboard: subject MC. Acquisitions on the right eye and left eye; 1-100 Hz and 1-30 Hz filtering.

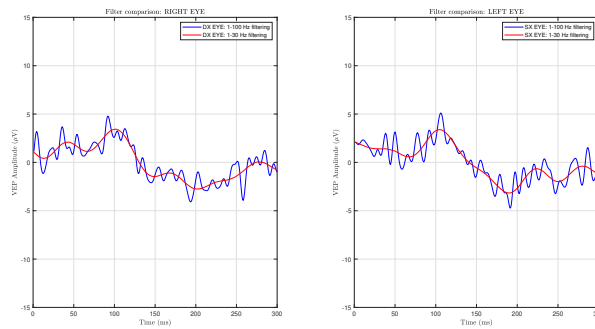


Figure 2.42: Cardboard: subject PC. Acquisitions on the right eye and left eye; 1-100 Hz and 1-30 Hz filtering.

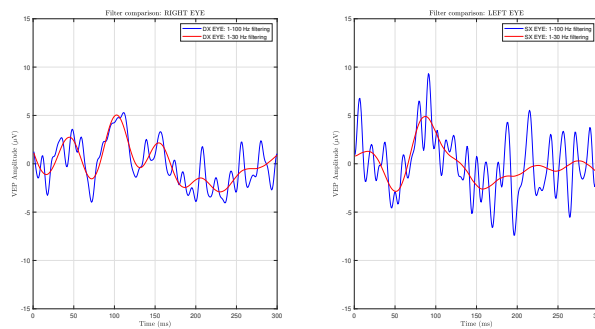


Figure 2.43: Cardboard: subject MU. Acquisitions on the right eye and left eye; 1-100 Hz and 1-30 Hz filtering.

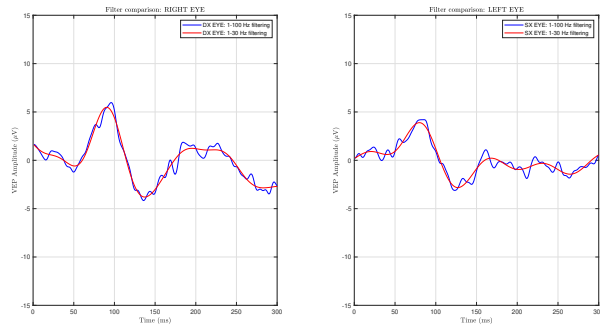


Figure 2.44: Cardboard: subject TR. Acquisitions on the right eye and left eye; 1-100 Hz and 1-30 Hz filtering.

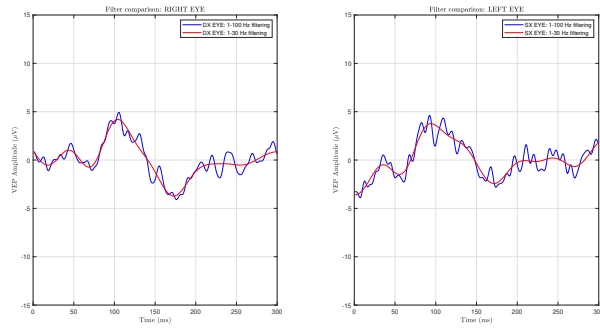


Figure 2.45: Cardboard: subject VA. Acquisitions on the right eye and left eye; 1-100 Hz and 1-30 Hz filtering.

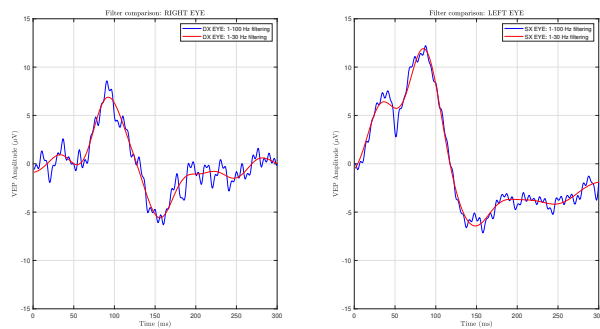


Figure 2.46: Cardboard: subject SP. Acquisitions on the right eye and left eye; 1-100 Hz and 1-30 Hz filtering.

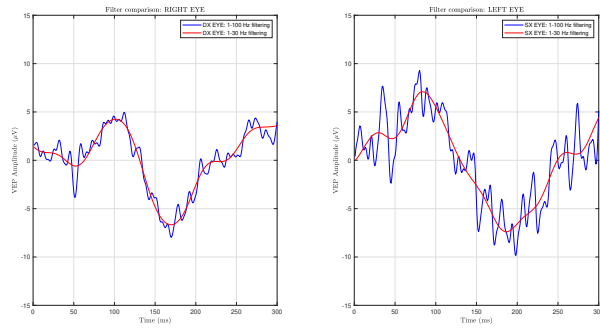


Figure 2.47: Cardboard: subject SS. Acquisitions on the right eye and left eye; 1-100 Hz and 1-30 Hz filtering.

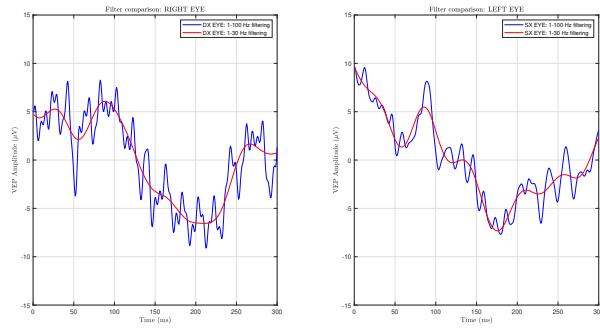


Figure 2.48: Cardboard: subject MG. Acquisitions on the right eye and left eye; 1-100 Hz and 1-30 Hz filtering.

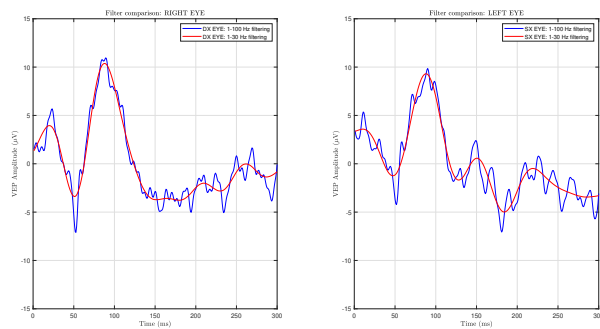


Figure 2.49: Cardboard: subject BA. Acquisitions on the right eye and left eye; 1-100 Hz and 1-30 Hz filtering.

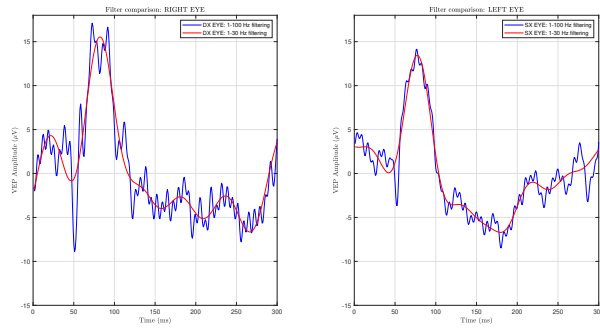


Figure 2.50: Cardboard: subject CG. Acquisitions on the right eye and left eye; 1-100 Hz and 1-30 Hz filtering.

For a qualitative comparison between the results obtained via Cardboard and via Smart glasses, *Figure 2.51* shows the average of the signals and the standard deviation.

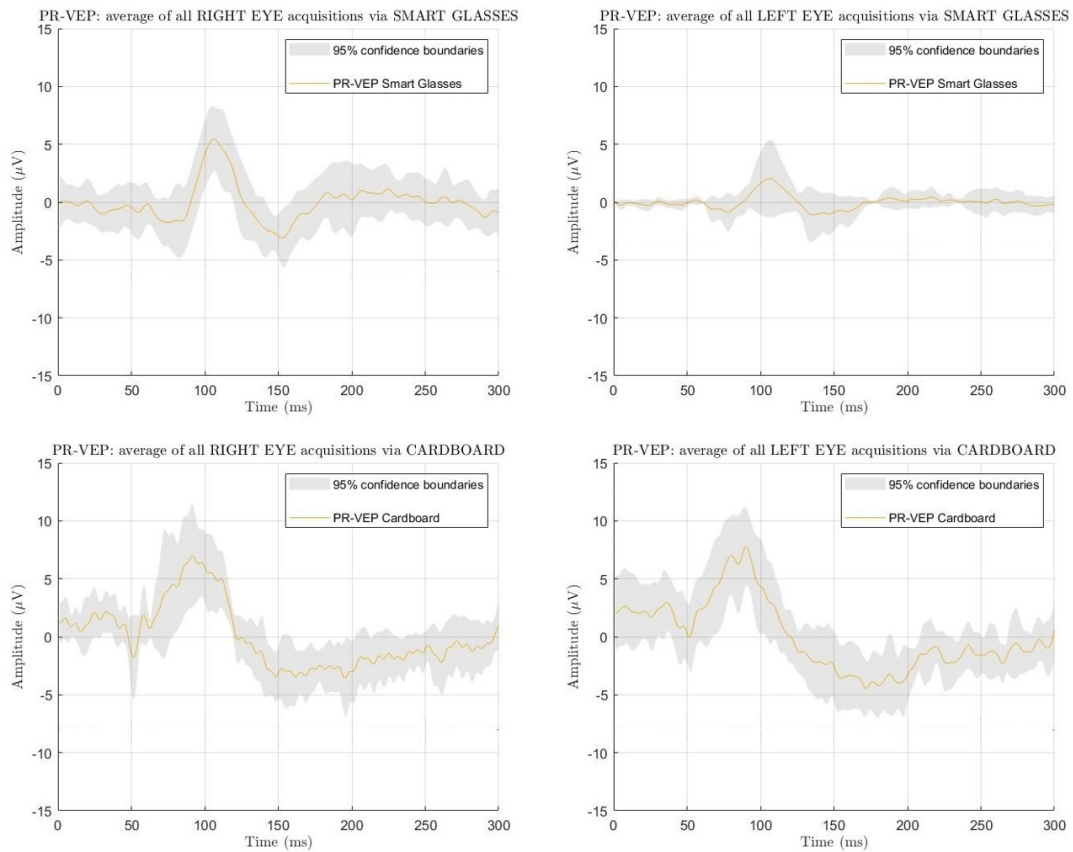


Figure 2.51: Comparison Cardboard-Smart Glasses: average and standard deviation.

From the average of the signals obtained via Cardboard it results that the three characteristic waves are recognizable, but with altered latencies. In particular, it is noted that the N75 wave is anticipated and it's detected around 50 ms. Instead, the N135 wave appears delayed, appearing around 150-160 ms. Finally, the main wave, the P100, presents more or less the latency provided by the literature.

All in all, with some precautions and improvements, the cardboard could become a good, innovative and economic idea for the future.

# Chapter 3

## Results

### 3.1 Calibration of our Prototype and Acquisitions on Healthy Subjects

With the aim of comparing the results obtained through the prototype we propose with those obtained through the Retimax CSO commercial system, the first necessary step is the calibration of our device.

10 healthy subjects, 6 females and 4 males, aged between 22 and 25 years were selected for this purpose. Informed consent was obtained from all individual participants included in the study. None of these subjects had ophthalmological diseases and, for those who needed it, the test was performed with glasses (see *Table 3.1*).

| <i>Subject code</i> | <i>Gender</i> | <i>Age</i> |
|---------------------|---------------|------------|
| LP                  | Female        | 24         |
| RT                  | Female        | 25         |
| FC                  | Female        | 24         |
| SS                  | Female        | 22         |
| AV                  | Male          | 24         |
| SS                  | Male          | 23         |
| FP                  | Male          | 24         |
| AT                  | Male          | 25         |
| MN                  | Female        | 23         |
| IT                  | Female        | 22         |

Table 3.1: Clinical details of the healthy subjects recruited: subject, gender and age.

The results obtained using the two devices compared are shown below.

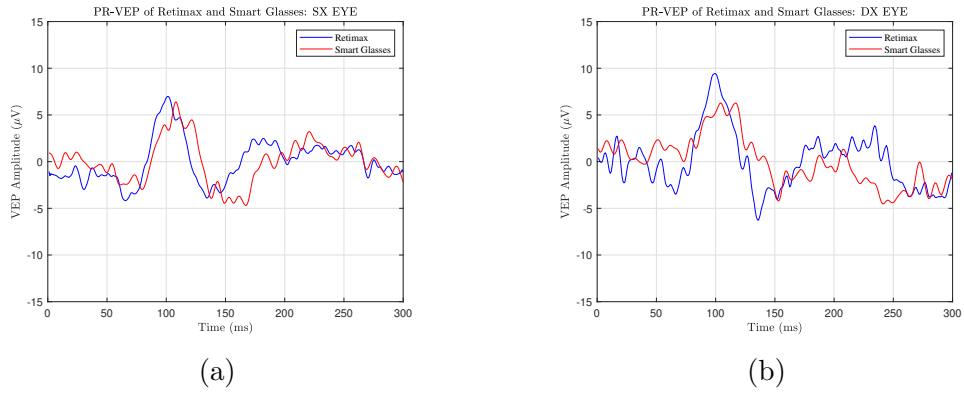


Figure 3.1: Subject LP:(a)tracks of the left eye; (b)tracks of the right eye.

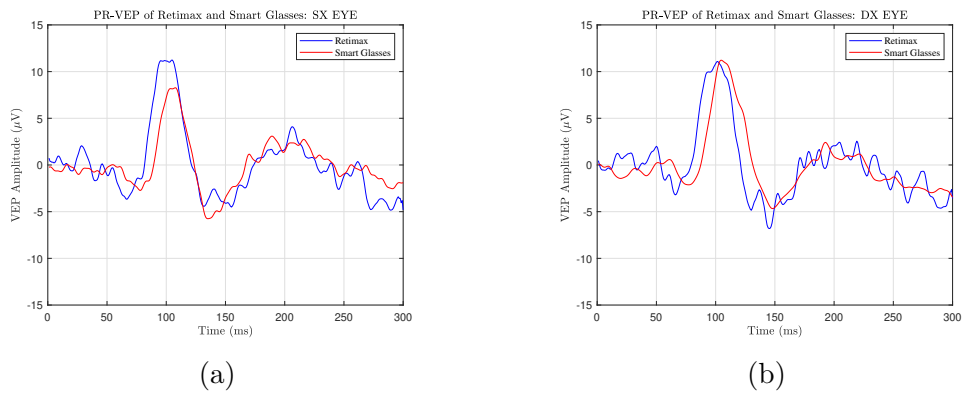


Figure 3.2: Subject RT:(a)tracks of the left eye; (b)tracks of the right eye.

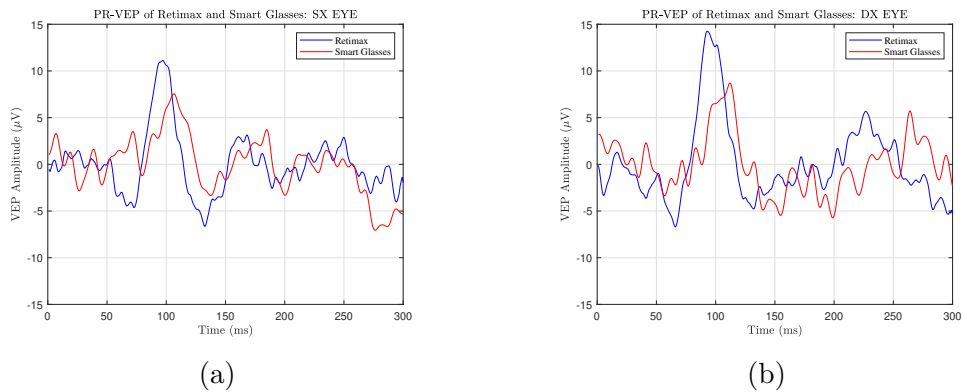
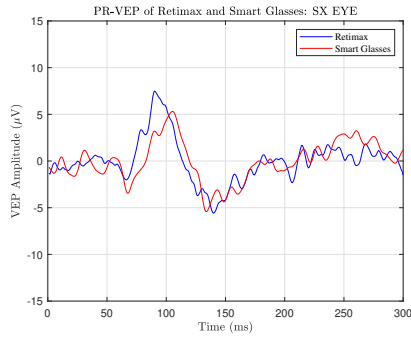
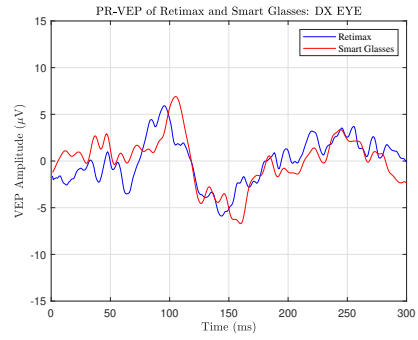


Figure 3.3: Subject FC:(a)tracks of the left eye; (b)tracks of the right eye.

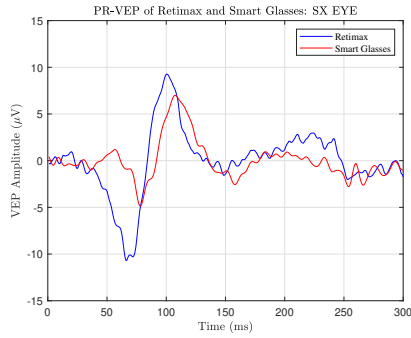


(a)

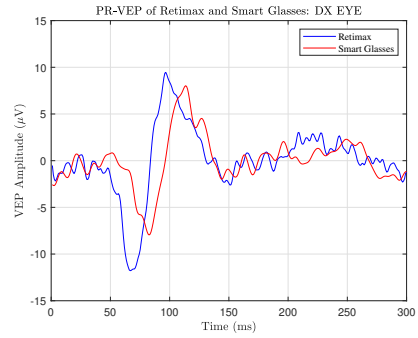


(b)

Figure 3.4: Subject SS:(a)tracks of the left eye; (b)tracks of the right eye.

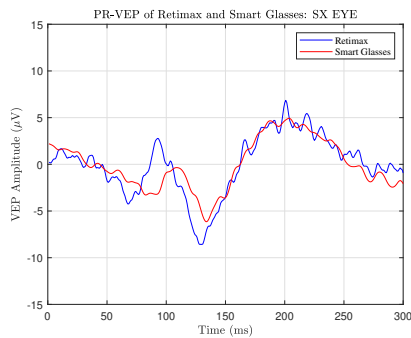


(a)

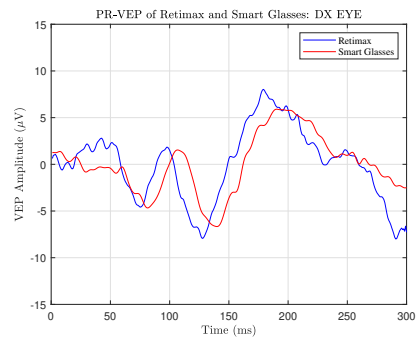


(b)

Figure 3.5: Subject AV:(a)tracks of the left eye; (b)tracks of the right eye.

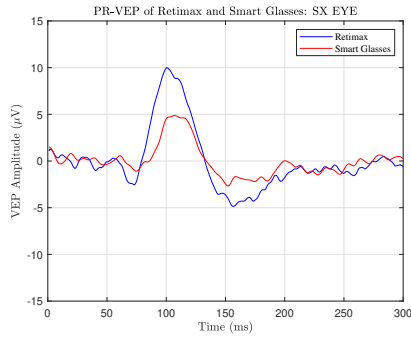


(a)

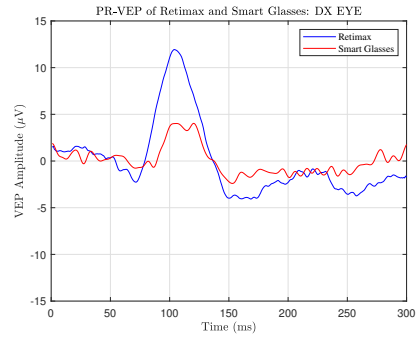


(b)

Figure 3.6: Subject SS:(a)tracks of the left eye; (b)tracks of the right eye.

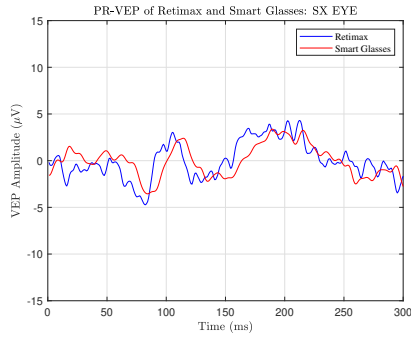


(a)

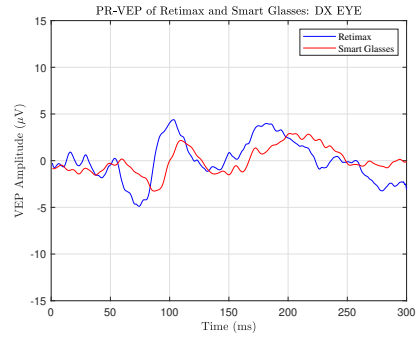


(b)

Figure 3.7: Subject FP:(a)tracks of the left eye; (b)tracks of the right eye.

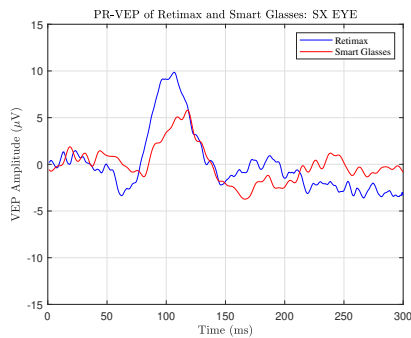


(a)

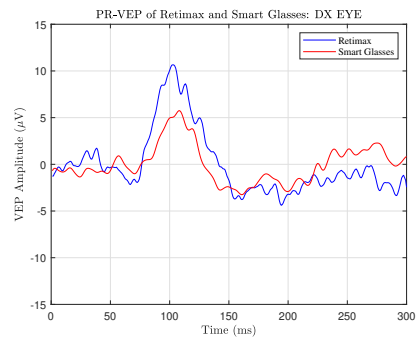


(b)

Figure 3.8: Subject AT:(a)tracks of the left eye; (b)tracks of the right eye.



(a)



(b)

Figure 3.9: Subject MN:(a)tracks of the left eye; (b)tracks of the right eye.

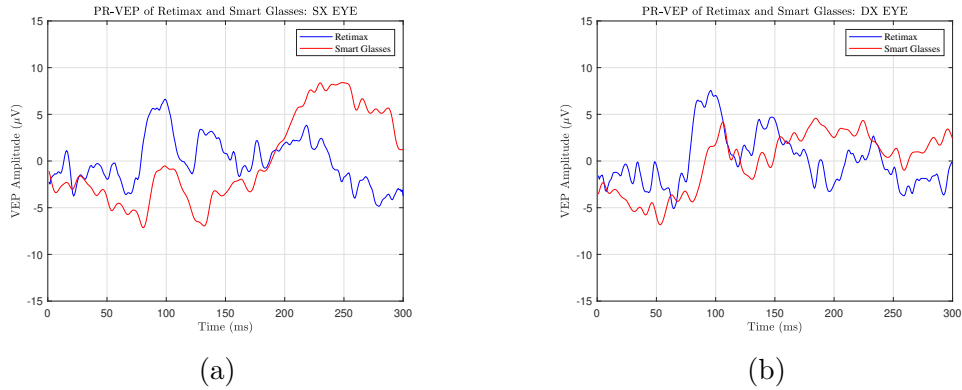


Figure 3.10: Subject IT:(a)tracks of the left eye; (b)tracks of the right eye.

The illustrated results have been analyzed during post-processing to determine the differences, in terms of latency and amplitude, between the signals obtained through the two different visual stimulation systems. In particular, the characteristics reported in *Table 3.2* and *Table 3.3* were investigated.

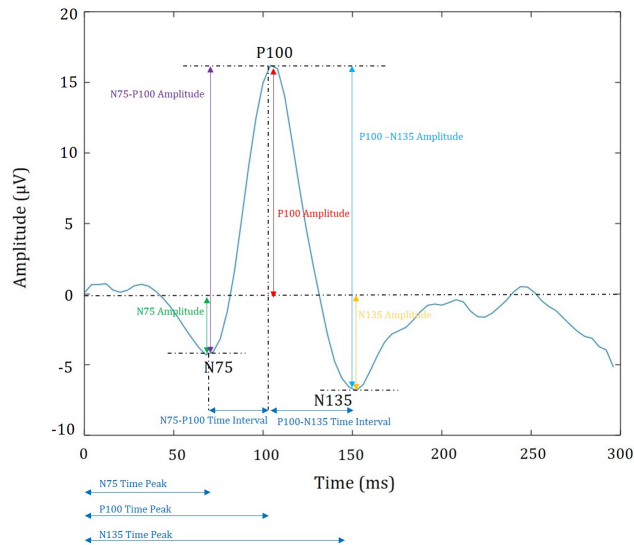


Figure 3.11: The characteristics of the pr-VEP investigated.

The values are reported as average of the 10 subjects  $\pm$  *standard deviation* and they show the differences between Retimax and Smart glasses stimulations in terms of PR-VEP amplitudes and latencies. The last column of the tables shows the *absolute mean difference (amd)*.

|                                      | <b>Left Eye</b>   |                      |            |
|--------------------------------------|-------------------|----------------------|------------|
|                                      | <i>Retimax</i>    | <i>Smart Glasses</i> | <i>amd</i> |
| <b>Amplitude(<math>\mu V</math>)</b> |                   |                      |            |
| N75 Amplitude                        | -4.08 $\pm$ 2.41  | -3.08 $\pm$ 1.96     | 1          |
| P100 Amplitude                       | 7.78 $\pm$ 3.01   | 4.77 $\pm$ 2.82      | 3.01       |
| N135 Amplitude                       | -3.88 $\pm$ 2.5   | -3.68 $\pm$ 2.33     | 0.2        |
| N75-P100 Amplitude                   | 11.86 $\pm$ 4     | 7.85 $\pm$ 2.6       | 4.01       |
| P100-N135 Amplitude                  | 11.66 $\pm$ 3.67  | 8.45 $\pm$ 2.99      | 3.21       |
| <b>Latency(ms)</b>                   |                   |                      |            |
| N75 Time Peak                        | 71.29 $\pm$ 5.65  | 79.62 $\pm$ 4.89     | 8.36       |
| P100 Time Peak                       | 98.87 $\pm$ 4.83  | 106.21 $\pm$ 3.77    | 7.34       |
| N135 Time Peak                       | 136.03 $\pm$ 7.43 | 136.6 $\pm$ 4.05     | 0.57       |
| N75-P100 Time Interval               | 27.58 $\pm$ 5.43  | 26.59 $\pm$ 6.17     | 0.99       |
| P100-N135 Time Interval              | 37.16 $\pm$ 8.64  | 30.39 $\pm$ 4.19     | 6.77       |

Table 3.2: Left eye: differences between Retimax and Smart glasses stimulations.

|                                      | <b>Right Eye</b>  |                      |            |
|--------------------------------------|-------------------|----------------------|------------|
|                                      | <i>Retimax</i>    | <i>Smart Glasses</i> | <i>amd</i> |
| <b>Amplitude(<math>\mu V</math>)</b> |                   |                      |            |
| N75 Amplitude                        | -4.46 $\pm$ 2.88  | -2.77 $\pm$ 2.38     | 1.69       |
| P100 Amplitude                       | 8.65 $\pm$ 3.75   | 5.82 $\pm$ 3         | 2.83       |
| N135 Amplitude                       | -4.20 $\pm$ 2.68  | -2.87 $\pm$ 2.2      | 1.33       |
| N75-P100 Time Interval               | 13.11 $\pm$ 4.85  | 8.59 $\pm$ 3.67      | 4.52       |
| P100-N135 Time Interval              | 12.85 $\pm$ 4.33  | 8.69 $\pm$ 3.97      | 4.16       |
| <b>Latency(ms)</b>                   |                   |                      |            |
| N75 Time Peak                        | 69.46 $\pm$ 4.23  | 77.96 $\pm$ 7.07     | 8.5        |
| P100 Time Peak                       | 99.01 $\pm$ 3.84  | 106.21 $\pm$ 3.95    | 7.2        |
| N135 Time Peak                       | 136.85 $\pm$ 9.63 | 137.51 $\pm$ 6.55    | 0.66       |
| N75-P100 Time Interval               | 29.55 $\pm$ 5.18  | 28.25 $\pm$ 7.29     | 1.3        |
| P100-N135 Time Interval              | 37.84 $\pm$ 8.67  | 31.30 $\pm$ 6.49     | 6.54       |

Table 3.3: Right eye: differences between Retimax and Smart glasses stimulations.

Data reported show that PR-VEP amplitudes from Retimax CSO are reasonably greater than those from Smart Glasses. Instead, the amplitudes relative to the N135 wave of the left eye signals are very similar. On the other hand, the latencies of the signal components appear to be greater for acquisitions made using Smart Glasses, of about 10 ms. Also in this case, the N135 wave is very similar, in latency, for both stimulators and for both eyes.

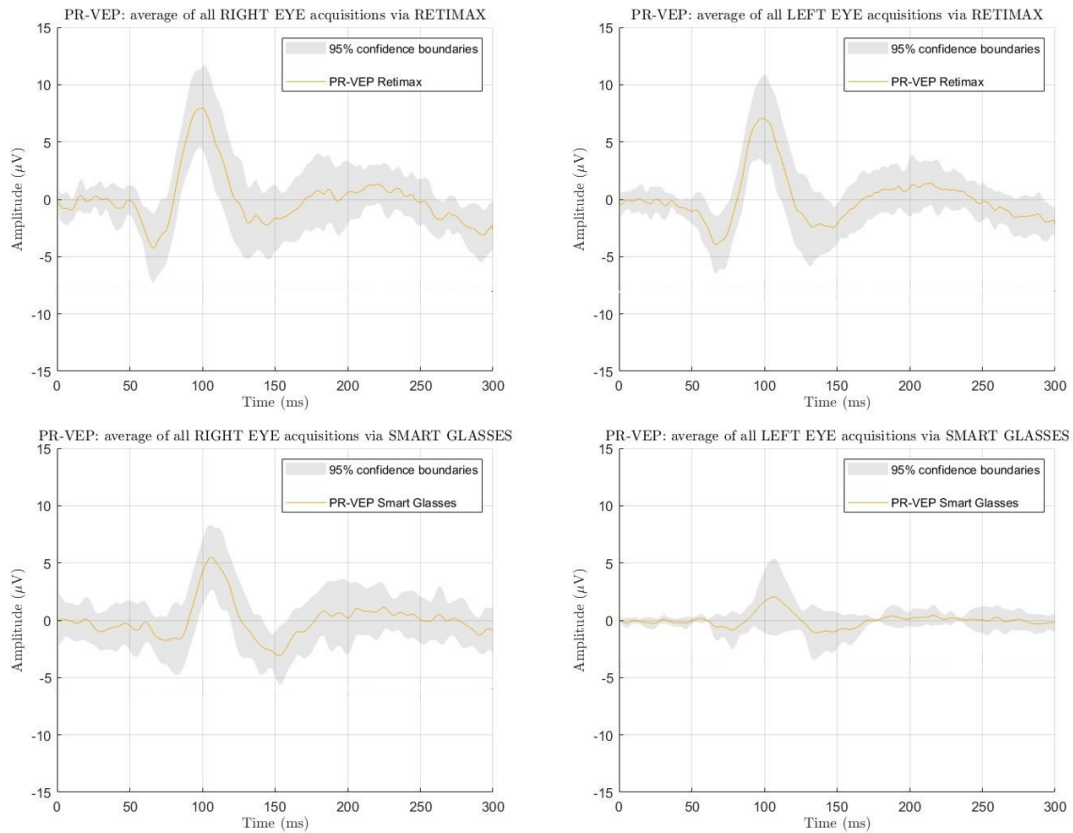


Figure 3.12: Average and standard deviation of all the PR-VEP waveforms obtained during the test using the Retimax stimulator and the Smart Glasses. Healthy subjects.

The PR-VEPs showed are well-defined in terms of N75, P100, and N135 components. The components relating to the acquisitions made via Smart Glasses on the left eye appear to be slightly pronounced, probably due to interference or artifacts.

## 3.2 Acquisitions on Pathologic subjects: Experimental Tests

As a support to this thesis work and to the prototype proposed by us, experimental tests were conducted at the Molinette hospital in Turin, ophthalmology department. With their consent, *30 pathological subjects* were recruited, 17 males and 13 females, aged between 49 and 86, each of whom presented at least one eye affected by some form of maculopathy. All procedures performed in studies involving human participants were in accordance with the ethical standards of the institutional and/or national research committee and with the 1964 Helsinki Declaration and its later amendments or comparable ethical standards. It is recalled that the study is aimed at the investigation of this pathology as it is particularly widespread especially among the elderly. Furthermore, the response to pr-VEPs of maculopathic subjects is much more standard than that of subjects suffering from other diseases and this facilitates the recognition of the waveform. *Tables 3.4* and *3.5* show the clinical details of all patients.

Pathology code:

- **EPR Dystrophy:** reticular dystrophy of retinal pigmented epithelium;
- **CNV:** choroidal neovascularization;
- **AVMD:** foveomacular calf dystrophy at adult onset;
- **CSC:** central serous chorioretinopathy.

Maculopathy classification:

- **Wet AMD:** wet age-related macular degeneration;
- **Dry AMD:** dry age-related macular degeneration.

## Left eye

| <i>Subject code</i> | <i>Gender</i> | <i>Age</i> | <i>Pathology</i> | <i>AMD</i> | <i>Visual Acuity</i> |
|---------------------|---------------|------------|------------------|------------|----------------------|
| AI                  | Female        | 77         | EPR Dystrophy    | Dry        | 3/10 SC              |
| BG                  | Male          | 67         | Drusen           | Dry        | 10/10 CL             |
| LR                  | Male          | 69         | Drusen           | Dry        | 4/10 SC              |
| MS                  | Male          | 65         | -                | -          | 9/10 SC              |
| CM                  | Female        | 56         | CNV              | Wet        | 3/10 CL              |
| DS                  | Male          | 78         | CNV              | Wet        | 3/10 CL              |
| LL                  | Female        | 68         | -                | -          | 2-3/10 CL            |
| PA                  | Male          | 49         | EPR Dystrophy    | Dry        | 2/10 CL              |
| BL                  | Female        | 78         | CNV              | Wet        | 6-7/10 CL            |
| BB                  | Male          | 58         | CNV              | Wet        | 3/10 SC              |
| MM                  | Female        | 51         | Drusen           | Dry        | 8/10 CC              |
| ZV                  | Female        | 52         | -                | -          | 8/10 CL              |
| FC                  | Male          | 79         | CNV              | Wet        | 2/10 CL              |
| IA                  | Male          | 79         | Drusen           | Dry        | 7-8/10 CL            |
| LS                  | Male          | 67         | AVMD             | Dry        | 4/10 CC              |
| CN                  | Male          | 65         | CNV              | Wet        | 6/10 SC              |
| CE                  | Male          | 86         | EPR Dystrophy    | Dry        | 1/10 CL              |
| LM                  | Male          | 52         | CNV              | Wet        | 1-2/10 CL            |
| PA                  | Male          | 79         | Drusen           | Dry        | 8/10 CL              |
| CG                  | Female        | 79         | -                | -          | 7-8/10 SC            |
| GG                  | Male          | 69         | CNV              | Wet        | 4/10 CL              |
| MG                  | Female        | 78         | -                | -          | 9/10 SC              |
| BA                  | Female        | 78         | Drusen           | Dry        | 2-3/10 CL            |
| SL                  | Female        | 71         | -                | -          | 4/10 CC              |
| BG                  | Male          | 79         | EPR Dystrophy    | Dry        | 3/10 SC              |
| CF                  | Female        | 73         | -                | -          | 8/10 CC              |
| GA                  | Female        | 76         | EPR Dystrophy    | Dry        | 2/10 SC              |
| SL                  | Female        | 74         | EPR Dystrophy    | Dry        | 8/10 SC              |
| GG                  | Male          | 77         | Drusen           | Dry        | 5-6/10 SC            |
| BL                  | Male          | 59         | CSC              | Wet        | 10/10 CL             |

Table 3.4: Clinical details of the pathologic subjects recruited: subject, gender, age, left eye pathology, maculopathy classification and left eye visual acuity. (CC=with correction; SC=without correction; CL=contact lens.)

## Right eye

| <i>Subject code</i> | <i>Gender</i> | <i>Age</i> | <i>Pathology</i> | <i>AMD</i> | <i>Visual Acuity</i> |
|---------------------|---------------|------------|------------------|------------|----------------------|
| AI                  | Female        | 77         | EPR Dystrophy    | Dry        | 8/10 SC              |
| BG                  | Male          | 67         | CNV              | Wet        | 3/10 CL              |
| LR                  | Male          | 69         | Drusen           | Dry        | 7-8/10 SC            |
| MS                  | Male          | 65         | CNV              | Wet        | 10/10 SC             |
| CM                  | Female        | 56         | -                | -          | 1/10 CL              |
| DS                  | Male          | 78         | EPR Dystrophy    | Dry        | 8/10 CL              |
| LL                  | Female        | 68         | CNV              | Wet        | 1/10 CL              |
| PA                  | Male          | 49         | EPR Dystrophy    | Dry        | 8/10 CL              |
| BL                  | Female        | 78         | Drusen           | Dry        | 10/10                |
| BB                  | Male          | 58         | EPR Dystrophy    | Dry        | 7-8/10 SC            |
| MM                  | Female        | 51         | Drusen           | Dry        | 6-7/10 CC            |
| ZV                  | Female        | 52         | CNV              | Wet        | 5-6/10 CL            |
| FC                  | Male          | 79         | AVMD             | Dry        | 3/10 CL              |
| IA                  | Male          | 79         | Drusen           | Dry        | 1-2/10 CL            |
| LS                  | Male          | 67         | AVMD             | Dry        | 2/10 CC              |
| CN                  | Male          | 65         | -                | -          | 6-7/10 SC            |
| CE                  | Male          | 86         | EPR Dystrophy    | Dry        | -                    |
| LM                  | Male          | 52         | CSC              | Wet        | 10/10 CL             |
| PA                  | Male          | 79         | Drusen           | Dry        | 6-7/10 CL            |
| CG                  | Female        | 79         | EPR Dystrophy    | Dry        | 3/10 SC              |
| GG                  | Male          | 69         | -                | -          | 2/10 CL              |
| MG                  | Female        | 78         | Drusen           | Dry        | 8/10 SC              |
| BA                  | Female        | 78         | EPR Dystrophy    | Dry        | 6-7/10 CL            |
| SL                  | Female        | 71         | EPR Dystrophy    | Dry        | 4-5/10 CC            |
| BG                  | Male          | 79         | -                | -          | 10/10 SC             |
| CF                  | Female        | 73         | CNV              | Wet        | 1/10 CC              |
| GA                  | Female        | 76         | EPR Dystrophy    | Dry        | 1/10 SC              |
| SL                  | Female        | 74         | EPR Dystrophy    | Dry        | 6-7/10 SC            |
| GG                  | Male          | 77         | Drusen           | Dry        | 3/10 SC              |
| BL                  | Male          | 59         | CNV              | Wet        | 1/10 SC              |

Table 3.5: Clinical details of the pathologic subjects recruited: subject, gender, age, right eye pathology, maculopathy classification and right eye visual acuity. (CC=with correction; SC=without correction; CL=contact lens.)

The results obtained using the two devices compared are shown below.

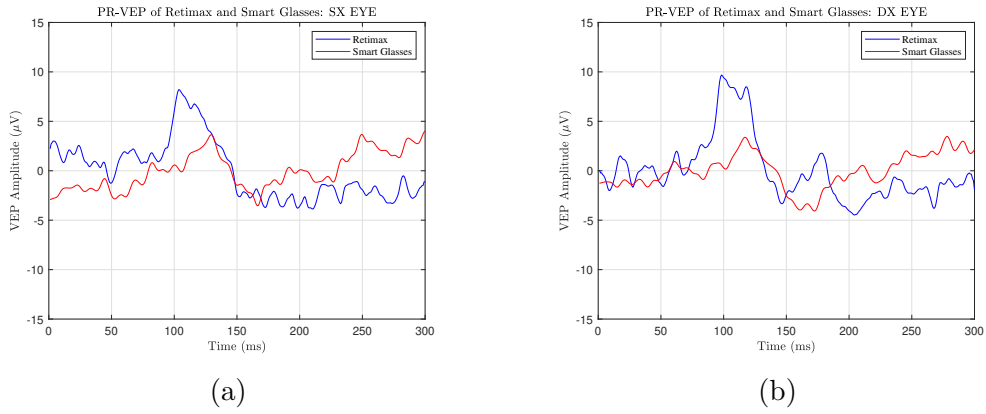


Figure 3.13: Patient AI:(a)tracks of the left eye; (b)tracks of the right eye.

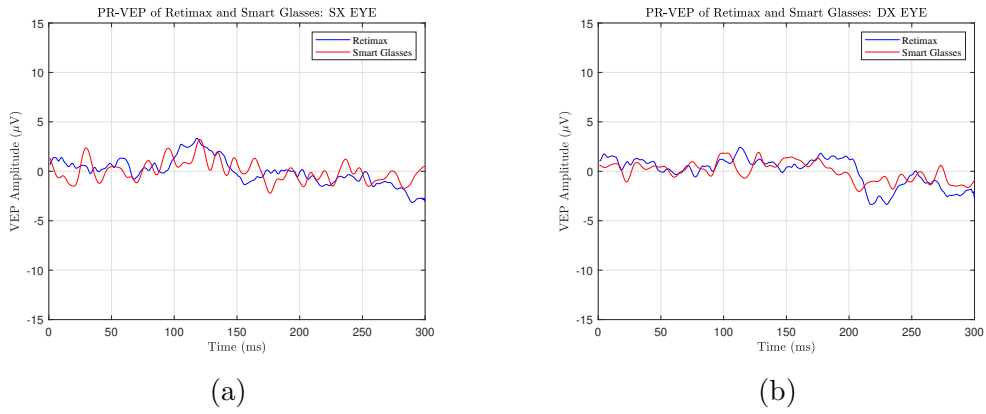


Figure 3.14: Patient BG:(a)tracks of the left eye; (b)tracks of the right eye.

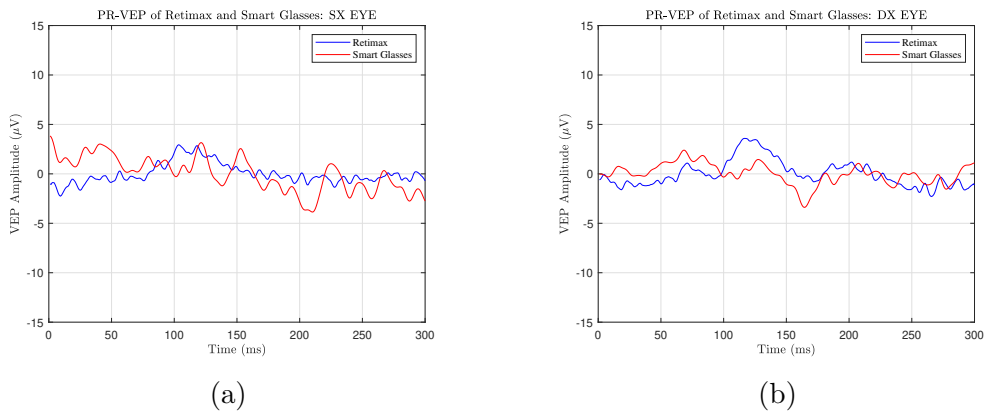


Figure 3.15: Patient LR:(a)tracks of the left eye; (b)tracks of the right eye.

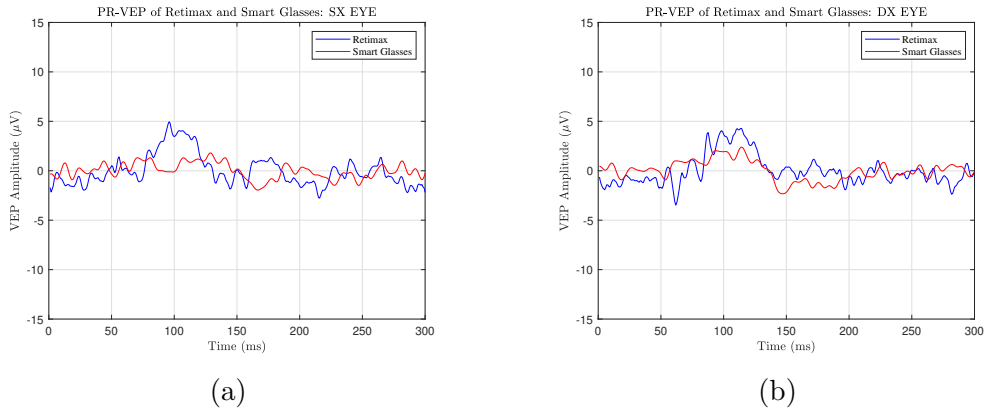


Figure 3.16: Patient MS:(a)tracks of the left eye; (b)tracks of the right eye.

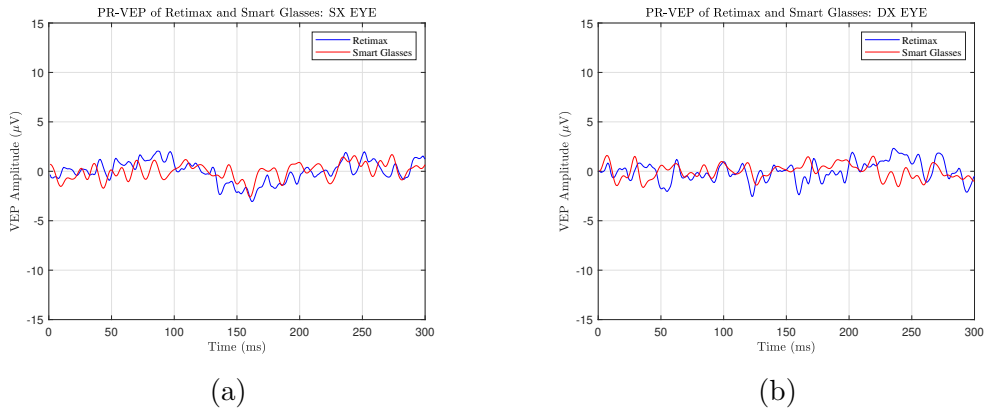


Figure 3.17: Patient CM:(a)tracks of the left eye; (b)tracks of the right eye.

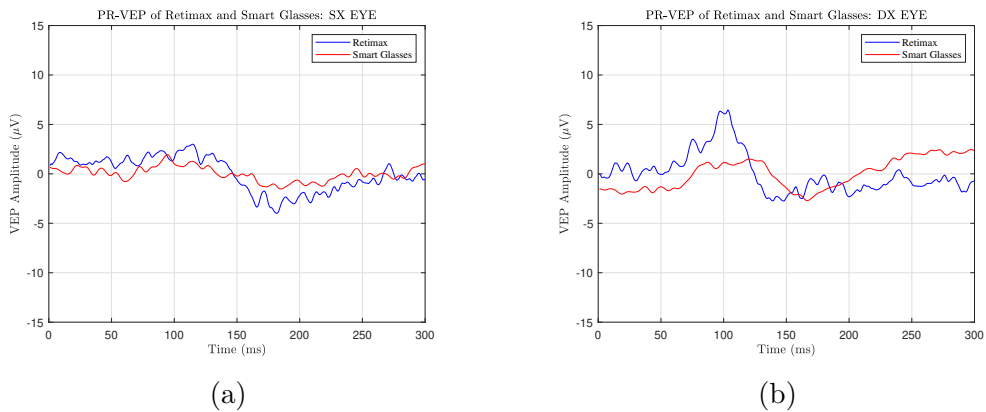


Figure 3.18: Patient DS:(a)tracks of the left eye; (b)tracks of the right eye.

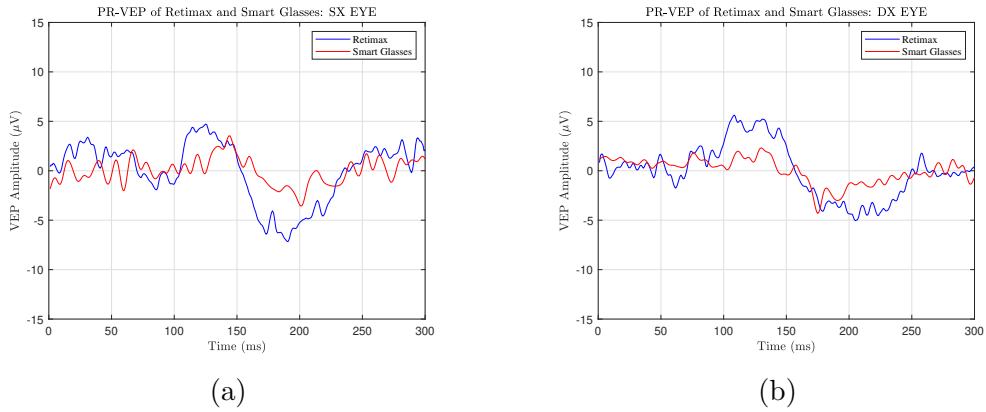


Figure 3.19: Patient LL:(a)tracks of the left eye; (b)tracks of the right eye.

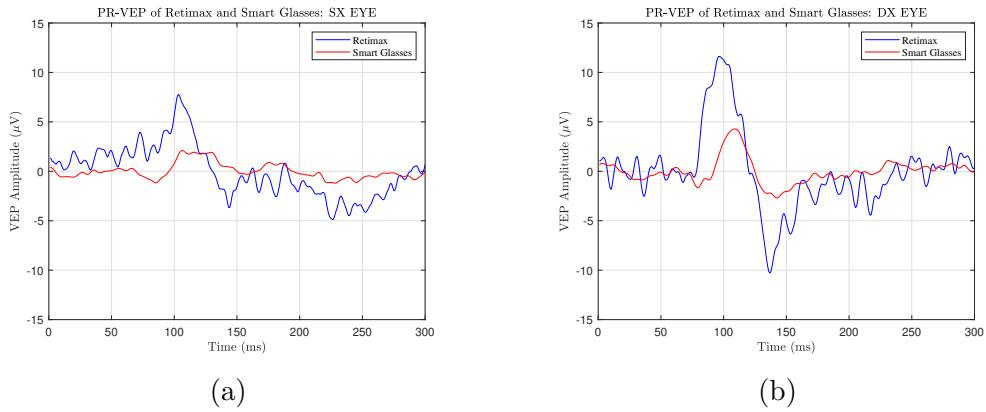


Figure 3.20: Patient PA:(a)tracks of the left eye; (b)tracks of the right eye.

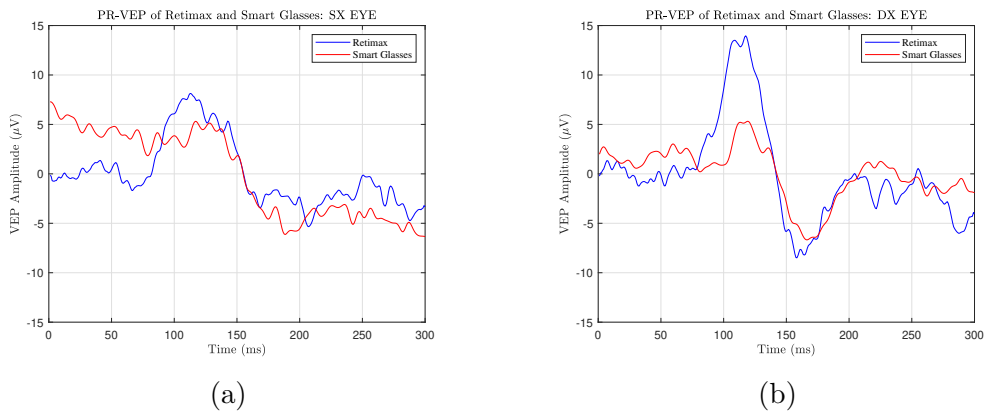


Figure 3.21: Patient BL:(a)tracks of the left eye; (b)tracks of the right eye.

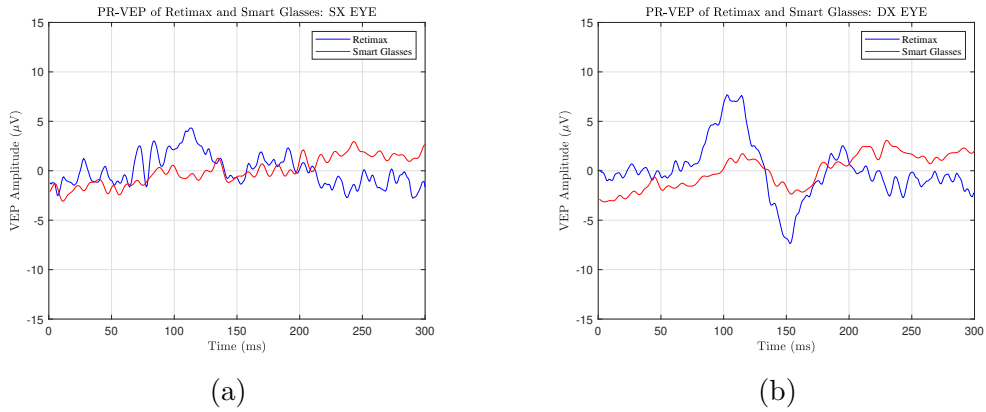


Figure 3.22: Patient BB:(a)tracks of the left eye; (b)tracks of the right eye.

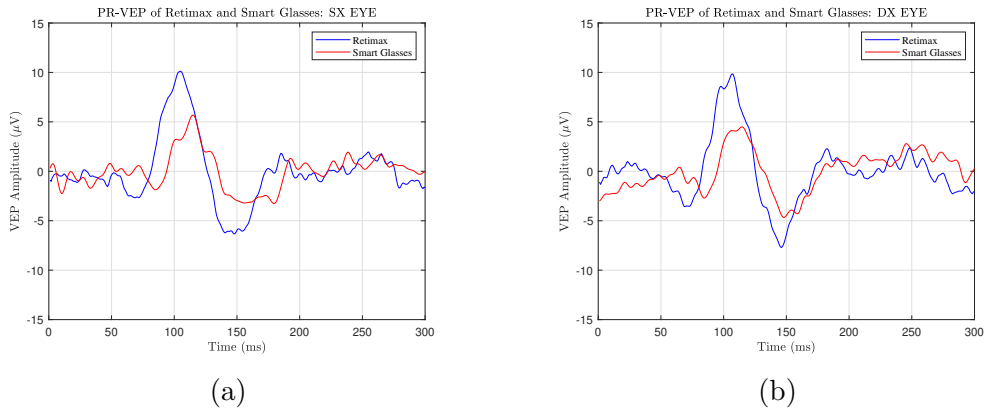


Figure 3.23: Patient MM:(a)tracks of the left eye; (b)tracks of the right eye.

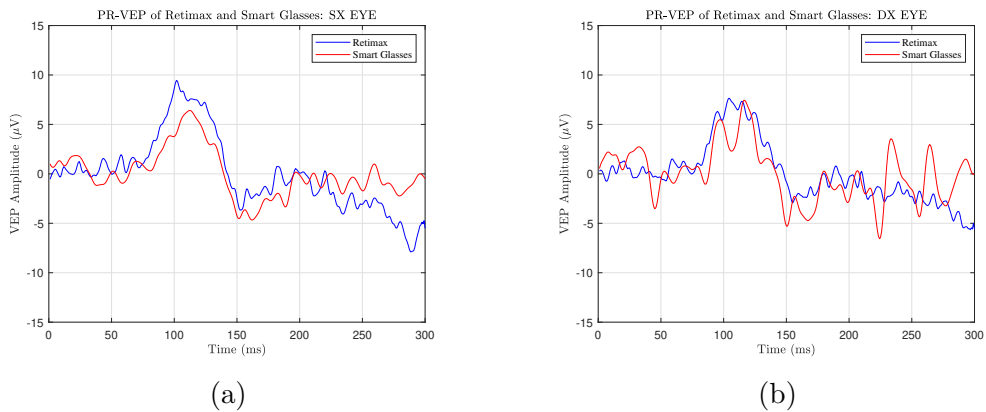


Figure 3.24: Patient ZV:(a)tracks of the left eye; (b)tracks of the right eye.

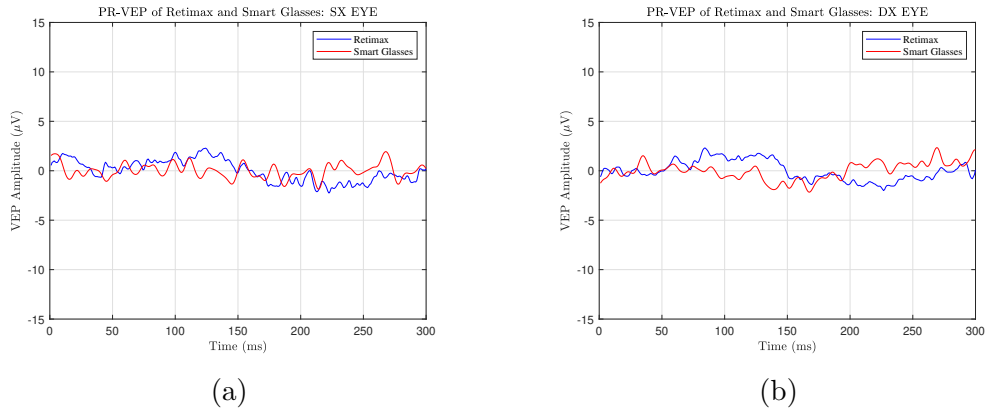


Figure 3.25: Patient FC:(a)tracks of the left eye; (b)tracks of the right eye.

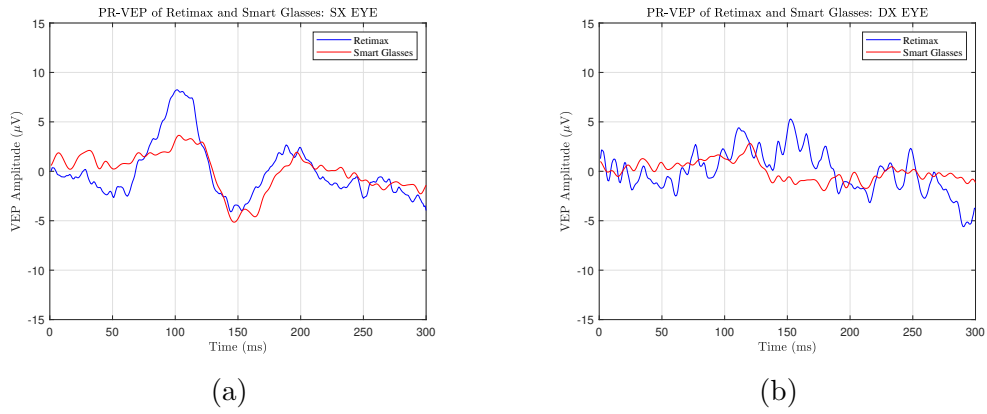


Figure 3.26: Patient IA:(a)tracks of the left eye; (b)tracks of the right eye.

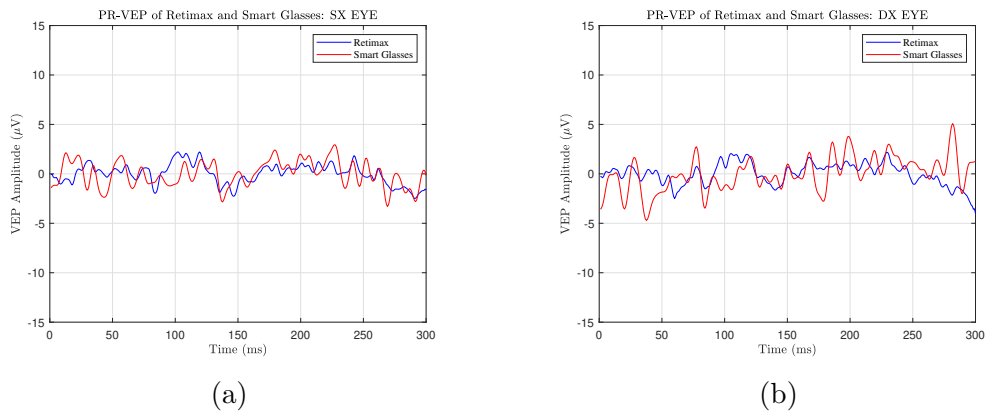


Figure 3.27: Patient LS:(a)tracks of the left eye; (b)tracks of the right eye.

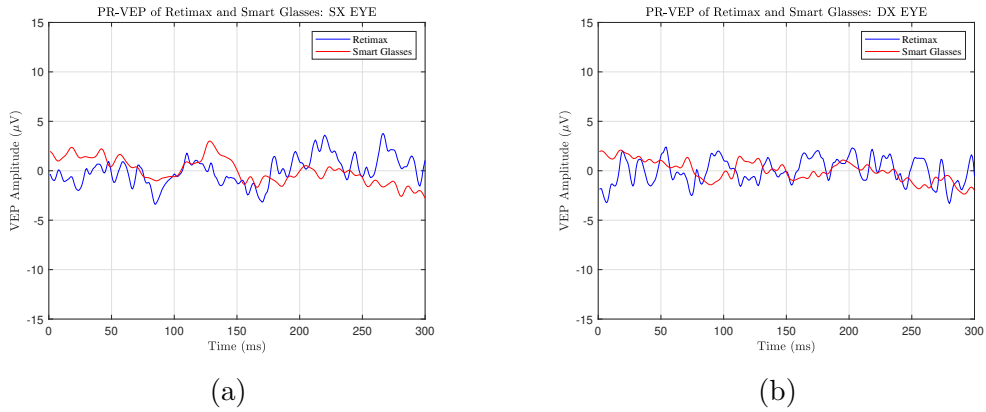


Figure 3.28: Patient CN:(a)tracks of the left eye; (b)tracks of the right eye.

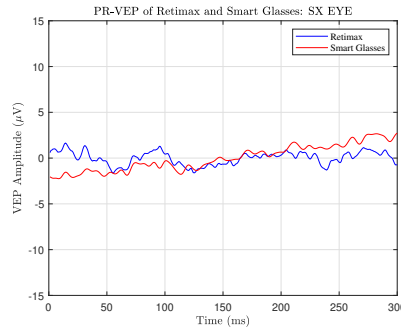


Figure 3.29: Patient CE: tracks of the left eye. The right eye sampling was not done because the patient had significant vision problems from this eye.

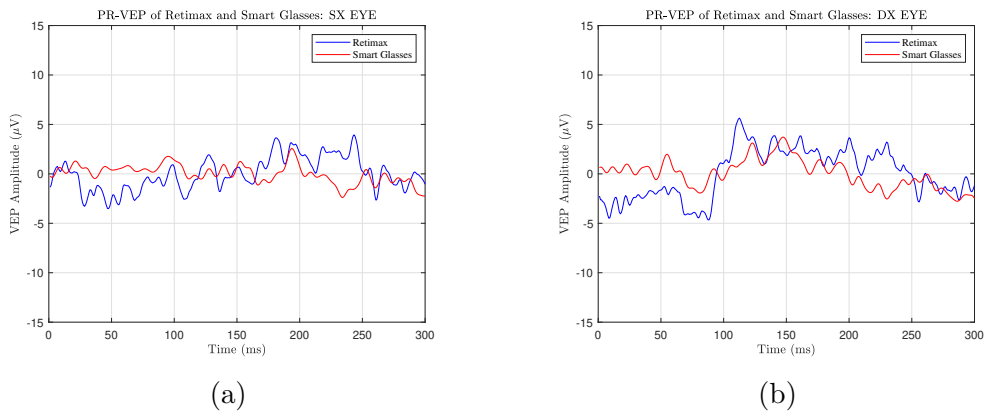


Figure 3.30: Patient LM:(a)tracks of the left eye; (b)tracks of the right eye.

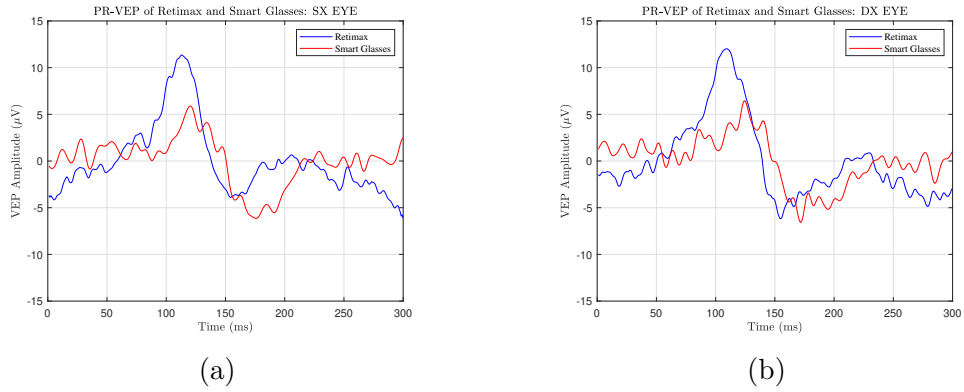


Figure 3.31: Patient PA:(a)tracks of the left eye; (b)tracks of the right eye.

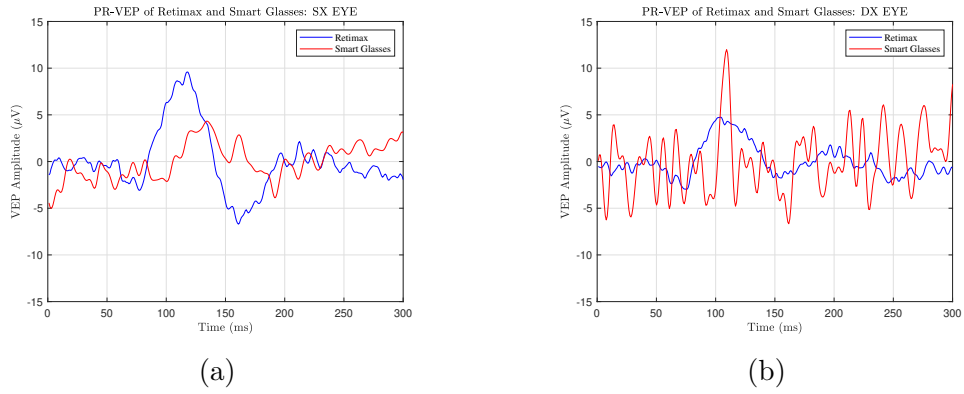


Figure 3.32: Patient CG:(a)tracks of the left eye; (b)tracks of the right eye. Acquisitions via our prototype are very corrupted by network interference.

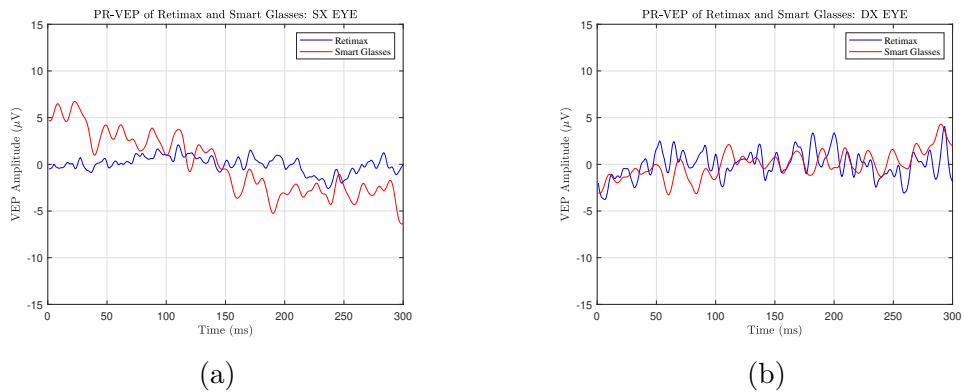


Figure 3.33: Patient GG:(a)tracks of the left eye; (b)tracks of the right eye.

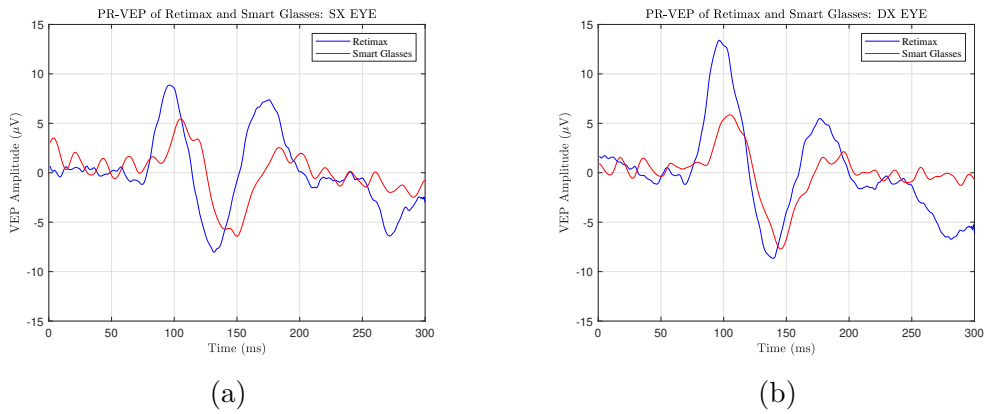


Figure 3.34: Patient MG:(a)tracks of the left eye; (b)tracks of the right eye.

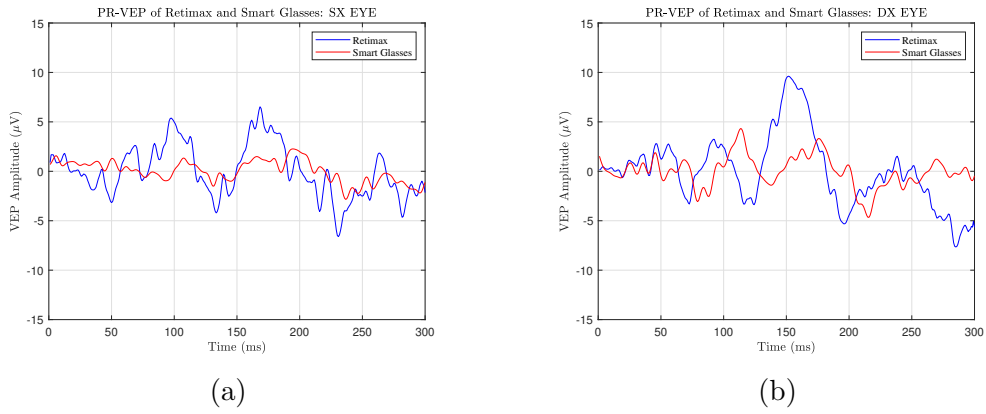


Figure 3.35: Patient BA:(a)tracks of the left eye; (b)tracks of the right eye.

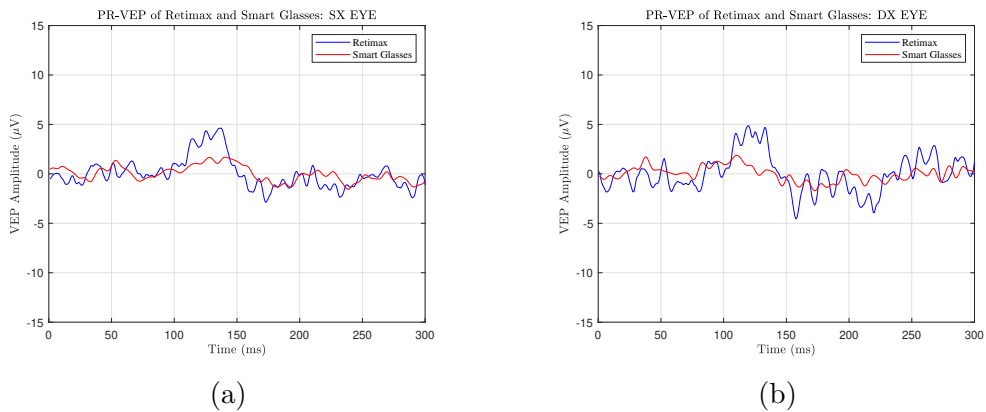


Figure 3.36: Patient SL:(a)tracks of the left eye; (b)tracks of the right eye.

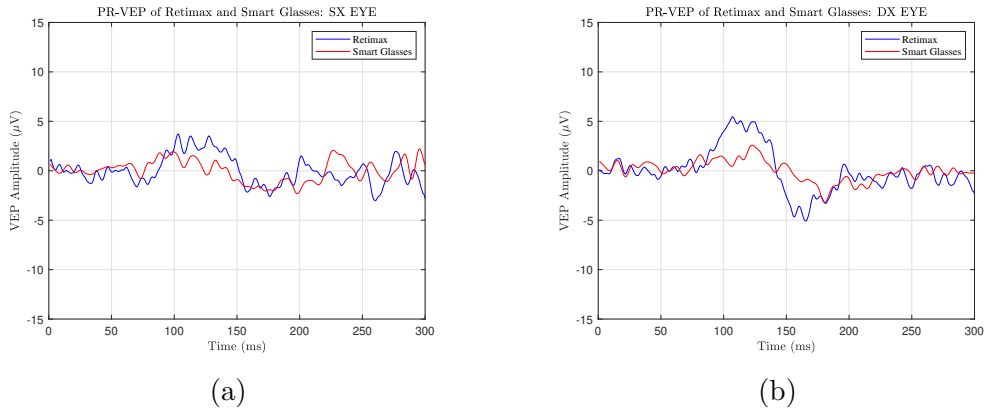


Figure 3.37: Patient BG:(a)tracks of the left eye; (b)tracks of the right eye.

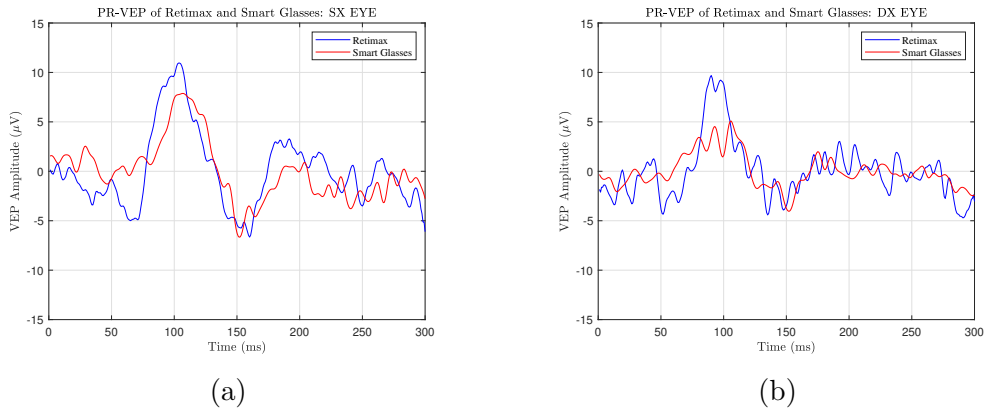


Figure 3.38: Patient CF:(a)tracks of the left eye; (b)tracks of the right eye.

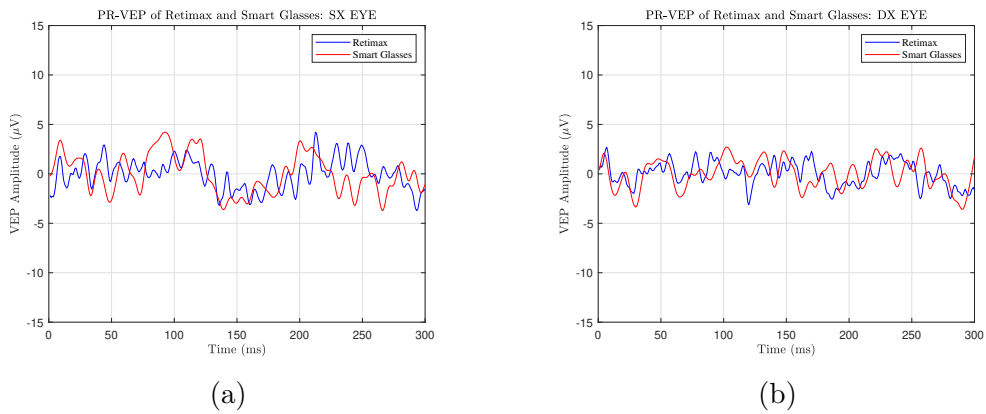


Figure 3.39: Patient GA:(a)tracks of the left eye; (b)tracks of the right eye.

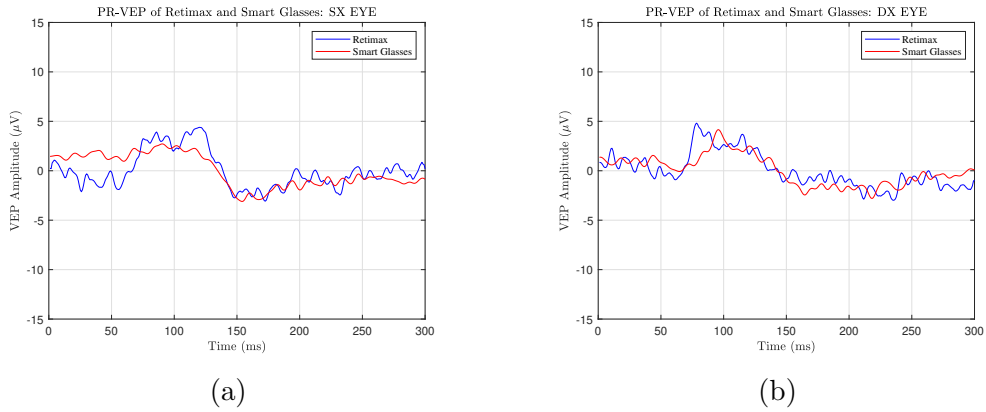


Figure 3.40: Patient SL:(a)tracks of the left eye; (b)tracks of the right eye.

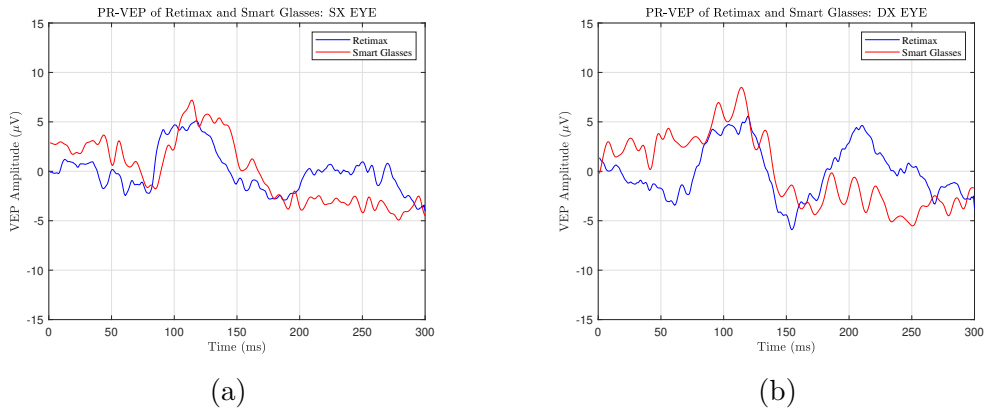


Figure 3.41: Patient GG:(a)tracks of the left eye; (b)tracks of the right eye.

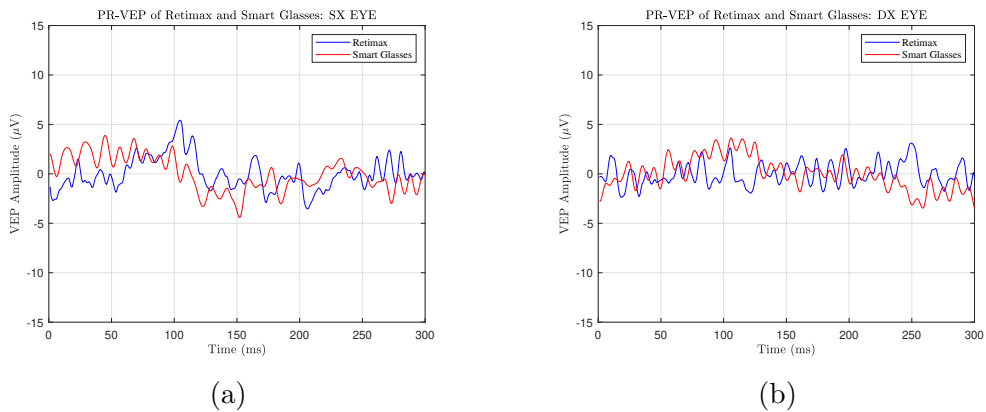


Figure 3.42: Patient BL:(a)tracks of the left eye; (b)tracks of the right eye.

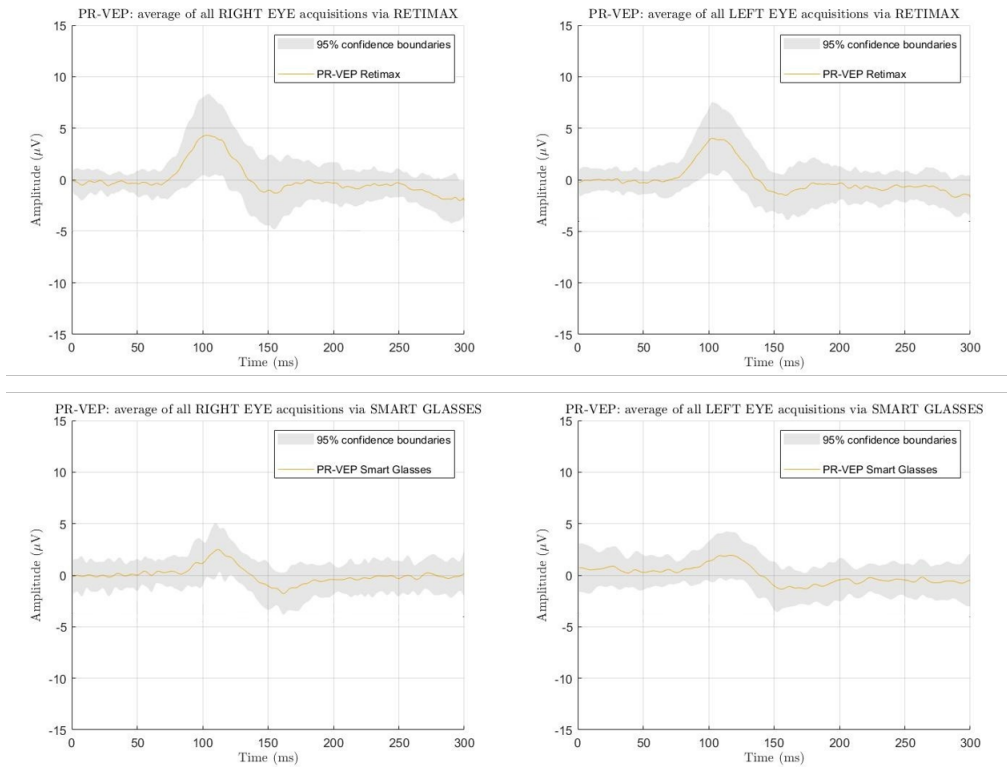


Figure 3.43: Average and standard deviation of all the PR-VEP waveforms obtained during the test using the Retimax stimulator and the Smart Glasses. Pathological subjects.

Finally, it was decided to compare the signals relating to patients suffering from **wet maculopathy** with those belonging to patients with **dry maculopathy**, as shown in *Figure 3.44* e *Figure 3.45*.

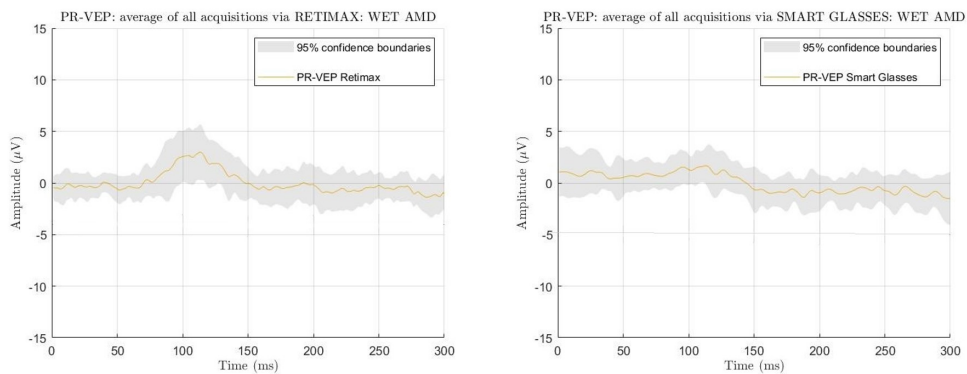


Figure 3.44: Wet Maculopathy: average and standard deviation of the signals obtained by Retimax CSO and via Smart Glasses.

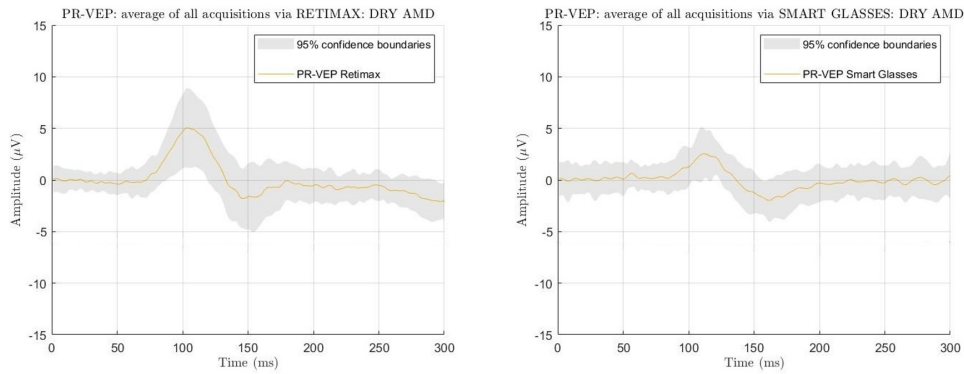


Figure 3.45: Dry Maculopathy: average and standard deviation of the signals obtained by Retimax CSO and via Smart Glasses.

This comparison has been made to verify what the literature suggests: it is expected that in the case of wet maculopathy the signals are more flat. In fact, between the wet maculopathy and the dry maculopathy, it is the wet one that causes the most serious damage, as it involves the rupture of the retinal pigmented epithelium. The results obtained confirm the expectations.

### 3.3 Power Spectral Density (PSD)

Of all the acquisitions made through both devices, a frequency domain analysis was made, using the PSD calculation. The objective has been, in fact, to identify the frequencies range that encloses the greater amount of information of each signal. This analysis has been carried out both on signals related to healthy subjects and on those belonging to pathological ones.

Numerical information is given in *subparegraph 3.4.2*.

## PSD of Healthy Subjects Signals

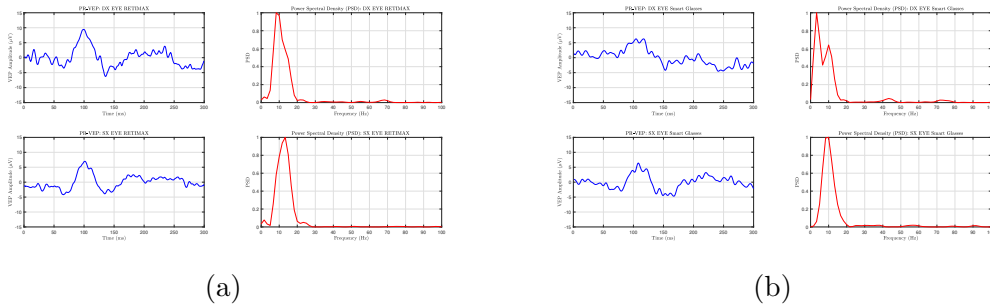


Figure 3.46: Subject LP: (a) PSD of left and right eye signals obtained with Reti-max;(b) PSD of left and right eye signals obtained with Smart Glasses.

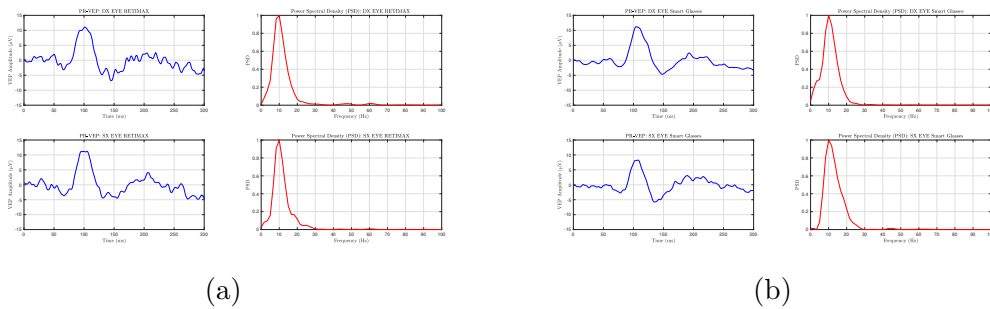


Figure 3.47: Subject RT: (a) PSD of left and right eye signals obtained with Reti-max;(b) PSD of left and right eye signals obtained with Smart Glasses.

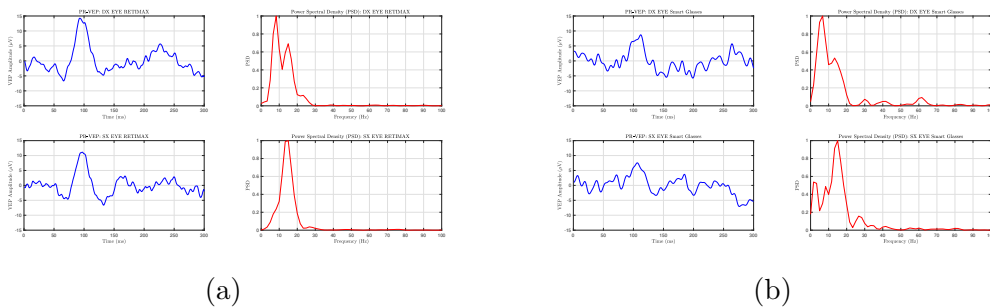


Figure 3.48: Subject FC: (a) PSD of left and right eye signals obtained with Reti-max;(b) PSD of left and right eye signals obtained with Smart Glasses.

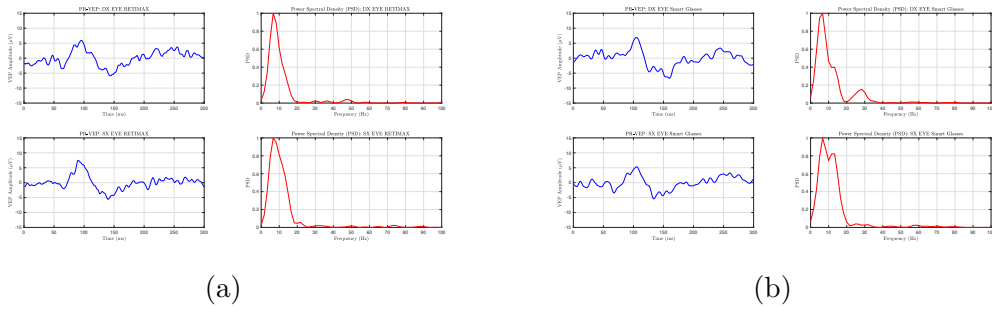


Figure 3.49: Subject SS: (a) PSD of left and right eye signals obtained with Reti-max; (b) PSD of left and right eye signals obtained with Smart Glasses.

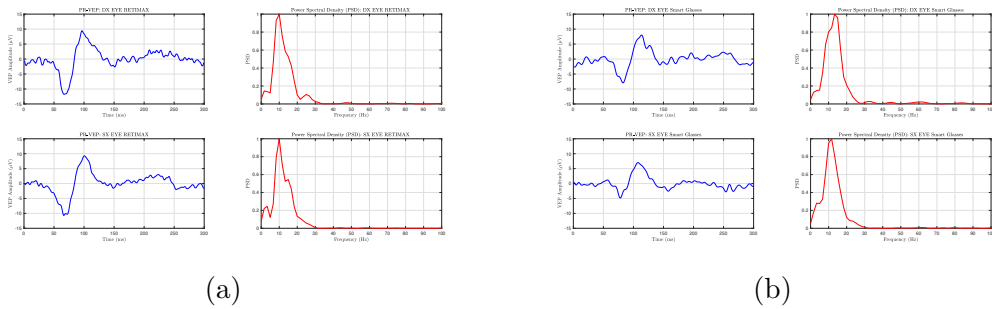


Figure 3.50: Subject AV: (a) PSD of left and right eye signals obtained with Reti-max; (b) PSD of left and right eye signals obtained with Smart Glasses.

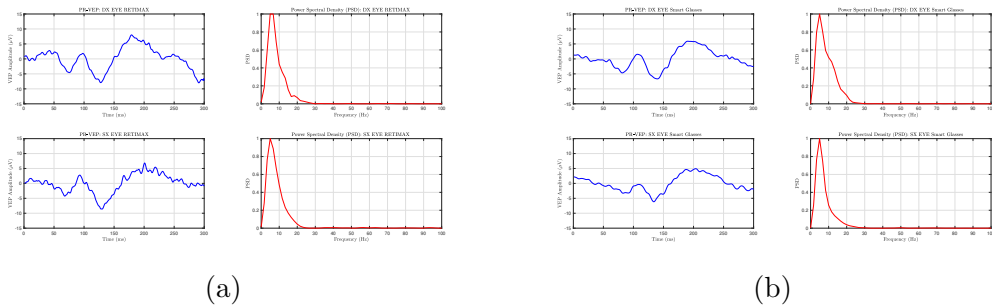


Figure 3.51: Subject SS: (a) PSD of left and right eye signals obtained with Reti-max; (b) PSD of left and right eye signals obtained with Smart Glasses.

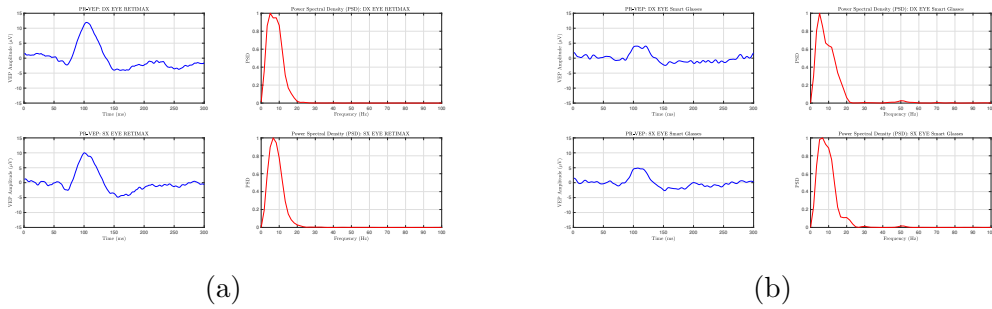


Figure 3.52: Subject FP: (a) PSD of left and right eye signals obtained with Retimax;(b) PSD of left and right eye signals obtained with Smart Glasses.

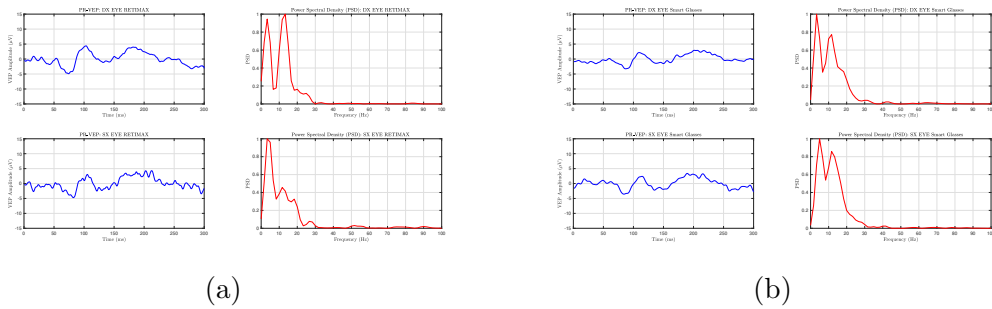


Figure 3.53: Subject AT: (a) PSD of left and right eye signals obtained with Retimax;(b) PSD of left and right eye signals obtained with Smart Glasses.

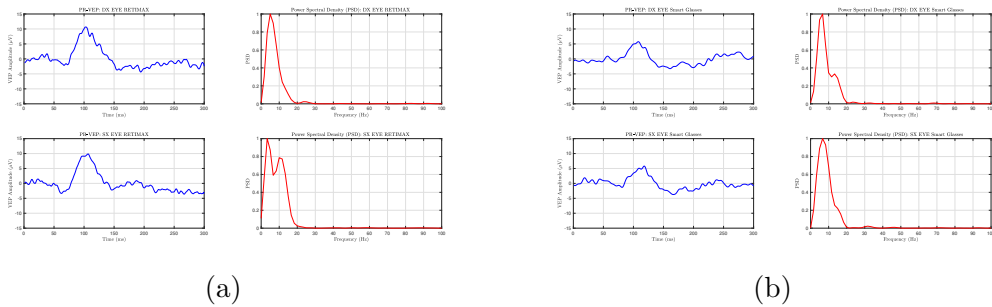


Figure 3.54: Subject MN: (a) PSD of left and right eye signals obtained with Retimax;(b) PSD of left and right eye signals obtained with Smart Glasses.

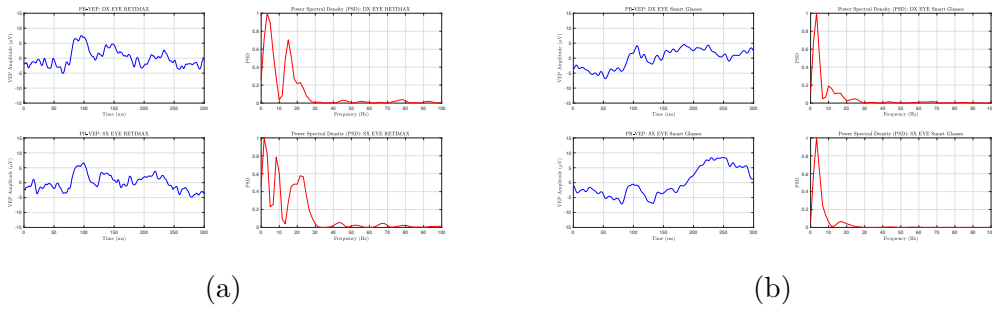


Figure 3.55: Subject IT: (a) PSD of left and right eye signals obtained with Reti-max; (b) PSD of left and right eye signals obtained with Smart Glasses.

### PSD of Pathological Subjects Signals

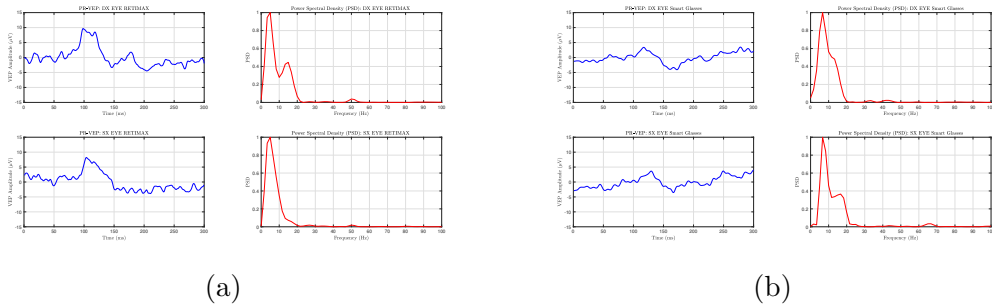


Figure 3.56: Patient AI: (a) PSD of left and right eye signals obtained with Reti-max; (b) PSD of left and right eye signals obtained with Smart Glasses.

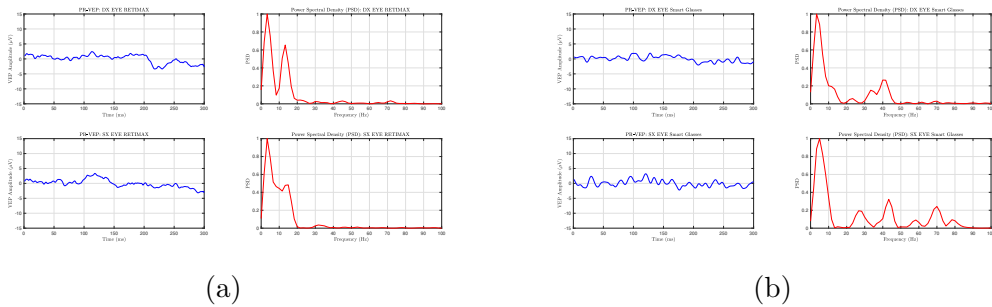


Figure 3.57: Patient BG: (a) PSD of left and right eye signals obtained with Reti-max; (b) PSD of left and right eye signals obtained with Smart Glasses.

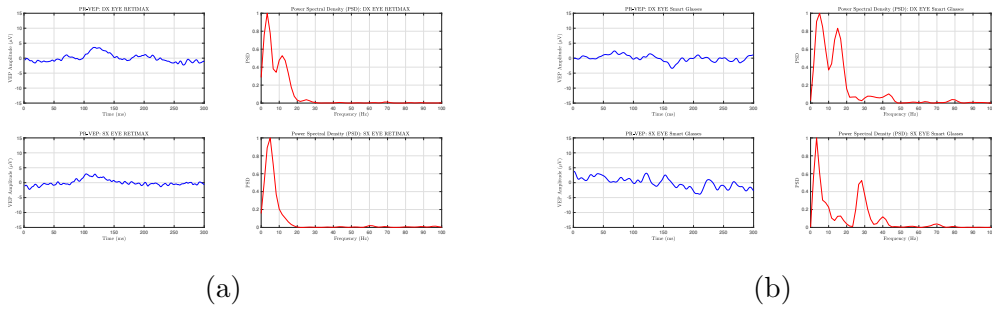


Figure 3.58: Patient LR: (a) PSD of left and right eye signals obtained with Retimax; (b) PSD of left and right eye signals obtained with Smart Glasses.

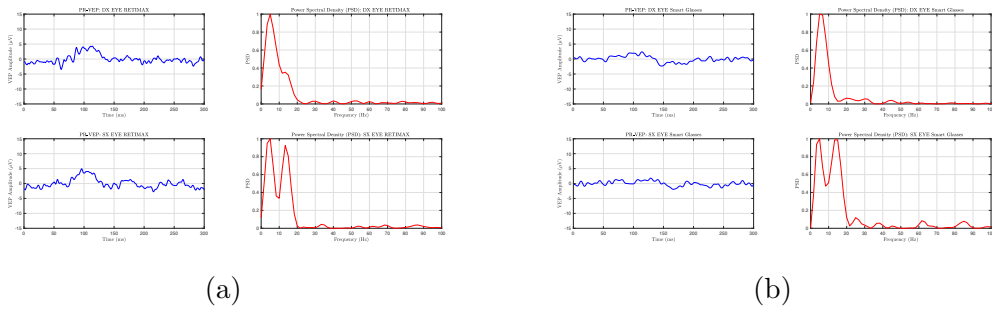


Figure 3.59: Patient MS: (a) PSD of left and right eye signals obtained with Retimax; (b) PSD of left and right eye signals obtained with Smart Glasses.

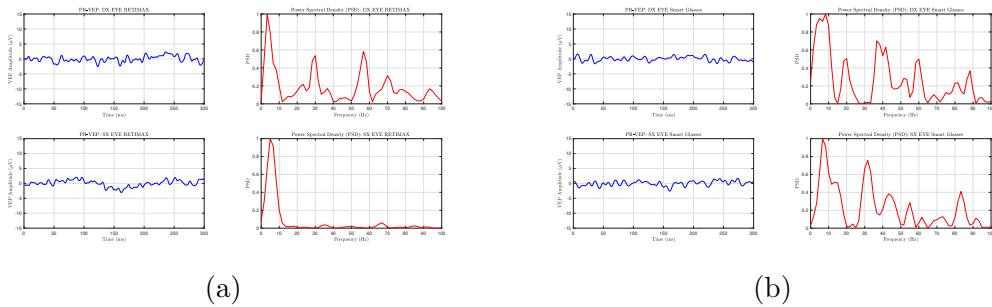


Figure 3.60: Patient CM: (a) PSD of left and right eye signals obtained with Retimax; (b) PSD of left and right eye signals obtained with Smart Glasses.

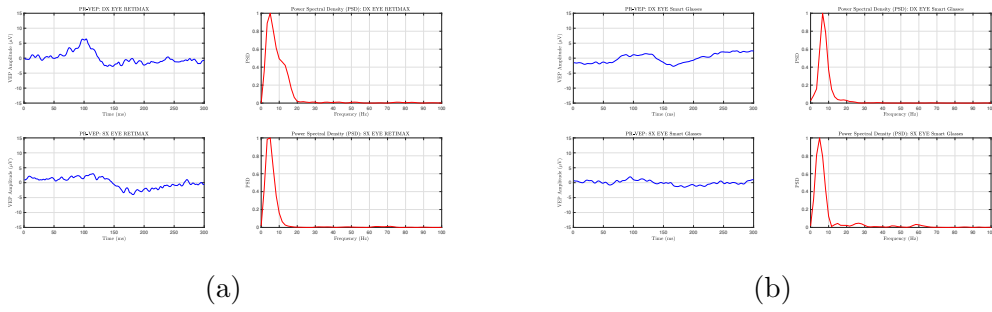


Figure 3.61: Patient DS: (a) PSD of left and right eye signals obtained with Reti-max; (b) PSD of left and right eye signals obtained with Smart Glasses.

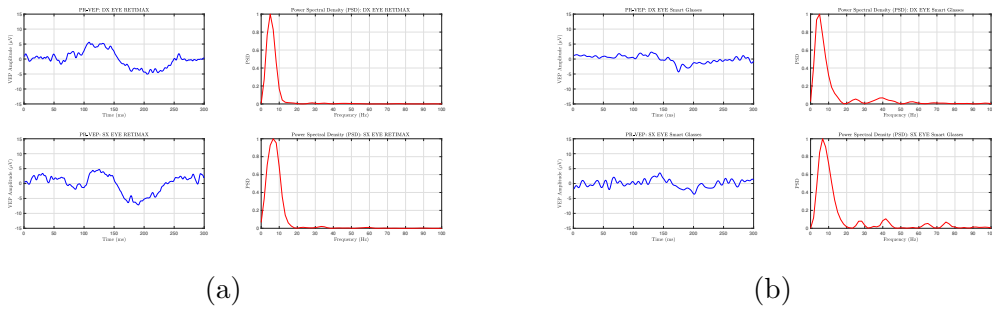


Figure 3.62: Patient LL: (a) PSD of left and right eye signals obtained with Reti-max; (b) PSD of left and right eye signals obtained with Smart Glasses.

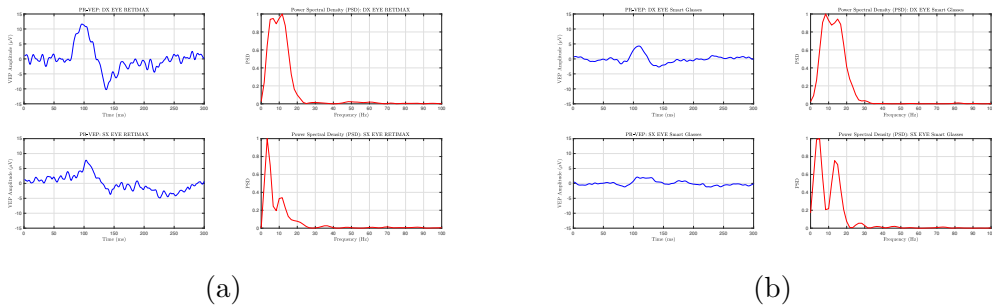


Figure 3.63: Patient PA: (a) PSD of left and right eye signals obtained with Reti-max; (b) PSD of left and right eye signals obtained with Smart Glasses.

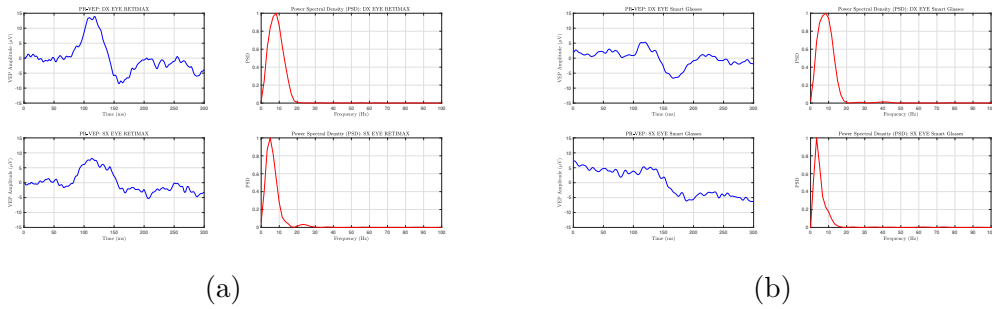


Figure 3.64: Patient BL: (a) PSD of left and right eye signals obtained with Retimax;(b) PSD of left and right eye signals obtained with Smart Glasses.

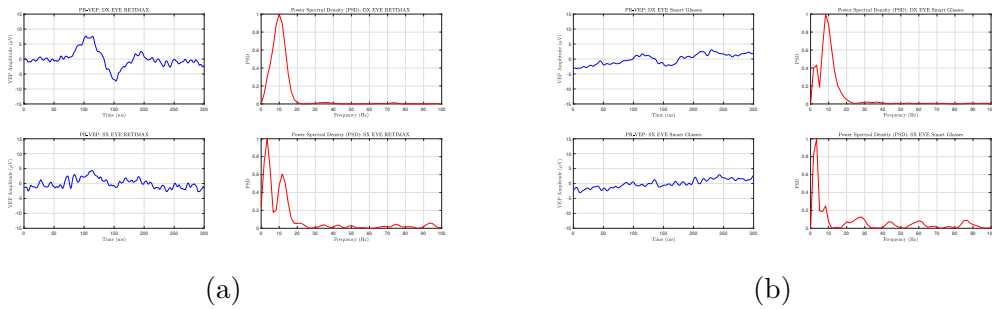


Figure 3.65: Patient BB: (a) PSD of left and right eye signals obtained with Retimax;(b) PSD of left and right eye signals obtained with Smart Glasses.

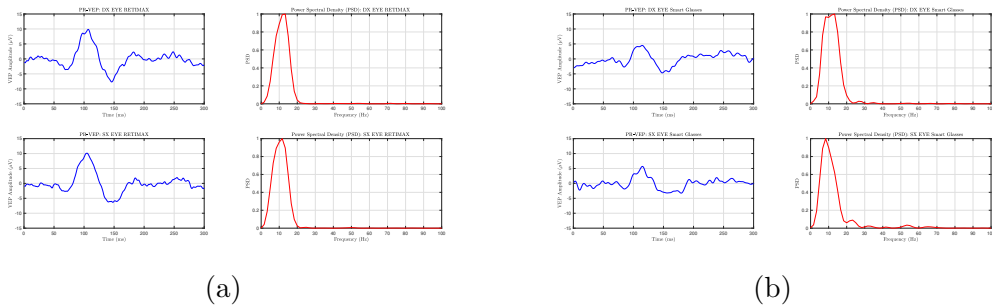


Figure 3.66: Patient MM: (a) PSD of left and right eye signals obtained with Retimax;(b) PSD of left and right eye signals obtained with Smart Glasses.

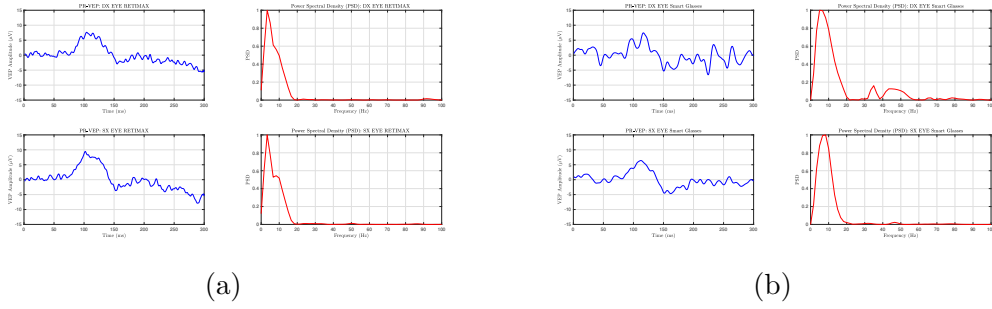


Figure 3.67: Patient ZV: (a) PSD of left and right eye signals obtained with Reti-max;(b) PSD of left and right eye signals obtained with Smart Glasses.

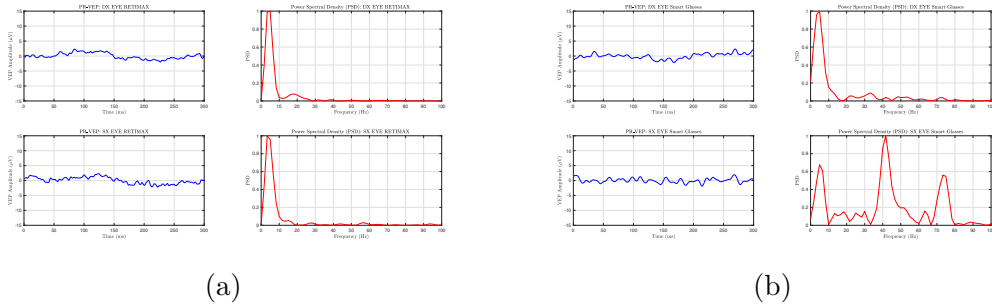


Figure 3.68: Patient FC: (a) PSD of left and right eye signals obtained with Reti-max;(b) PSD of left and right eye signals obtained with Smart Glasses.

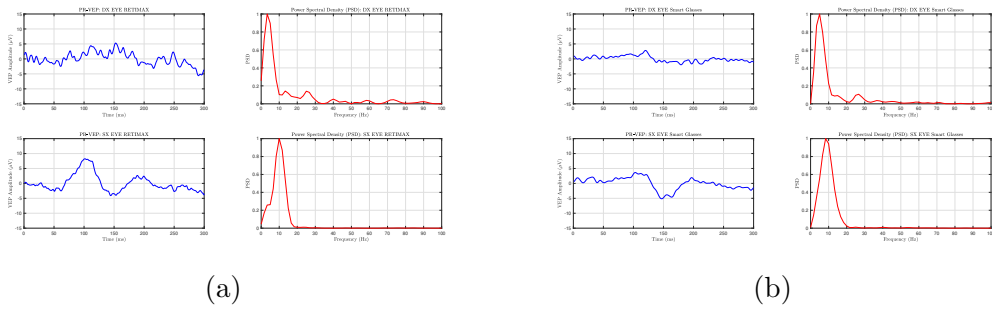


Figure 3.69: Patient IA: (a) PSD of left and right eye signals obtained with Reti-max;(b) PSD of left and right eye signals obtained with Smart Glasses.

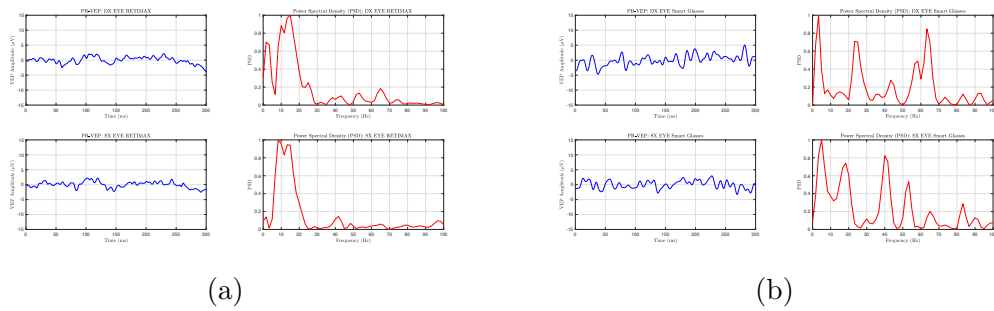


Figure 3.70: Patient LS: (a) PSD of left and right eye signals obtained with Retimax; (b) PSD of left and right eye signals obtained with Smart Glasses.

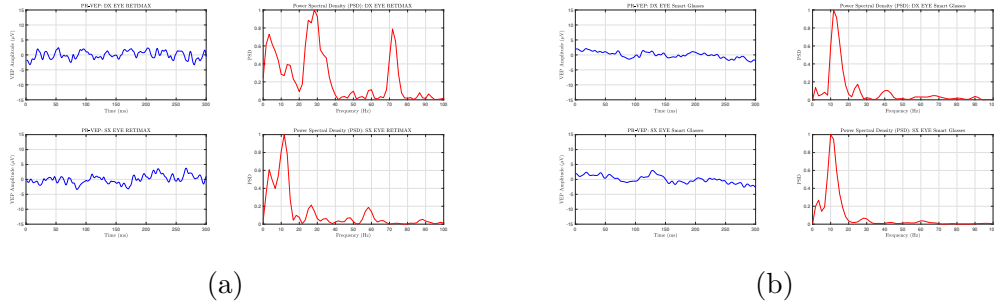


Figure 3.71: Patient CN: (a) PSD of left and right eye signals obtained with Retimax; (b) PSD of left and right eye signals obtained with Smart Glasses.

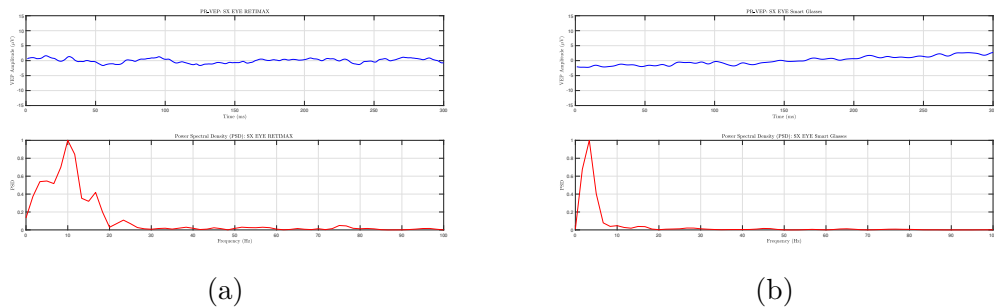


Figure 3.72: Patient CE: (a) PSD of left eye signal obtained with Retimax; (b) PSD of left eye signal obtained with Smart Glasses. The right eye sampling was not done because the patient had significant vision problems from this eye.

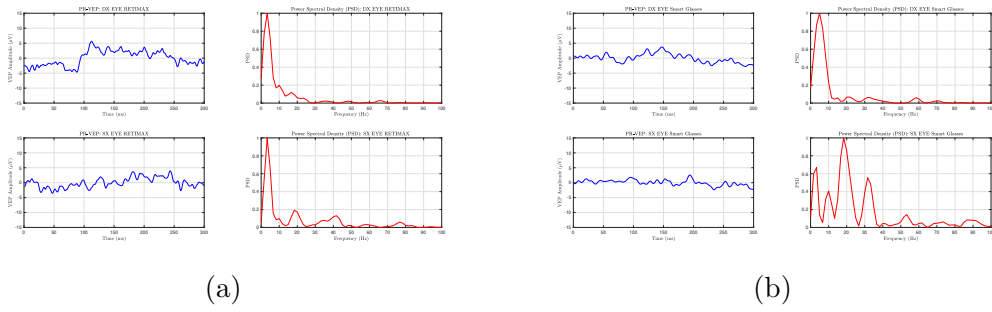


Figure 3.73: Patient LM: (a) PSD of left and right eye signals obtained with Reti-max;(b) PSD of left and right eye signals obtained with Smart Glasses.

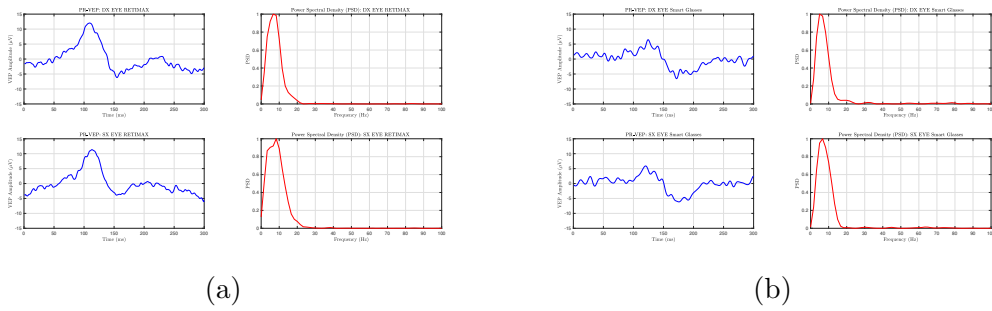


Figure 3.74: Patient PA: (a) PSD of left and right eye signals obtained with Reti-max;(b) PSD of left and right eye signals obtained with Smart Glasses.

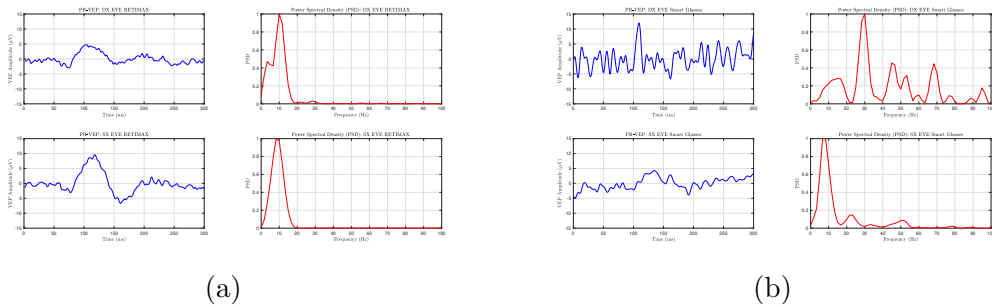


Figure 3.75: Patient CG: (a) PSD of left and right eye signals obtained with Reti-max;(b) PSD of left and right eye signals obtained with Smart Glasses.

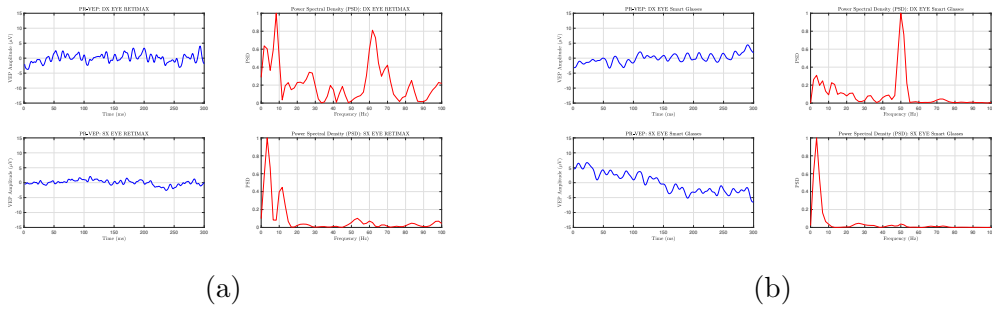


Figure 3.76: Patient GG: (a) PSD of left and right eye signals obtained with Retimax;(b) PSD of left and right eye signals obtained with Smart Glasses. The acquisitions made through our prototype appear corrupted by the network interference, as clearly shows the peak at 50 Hz in the PSD calculation.

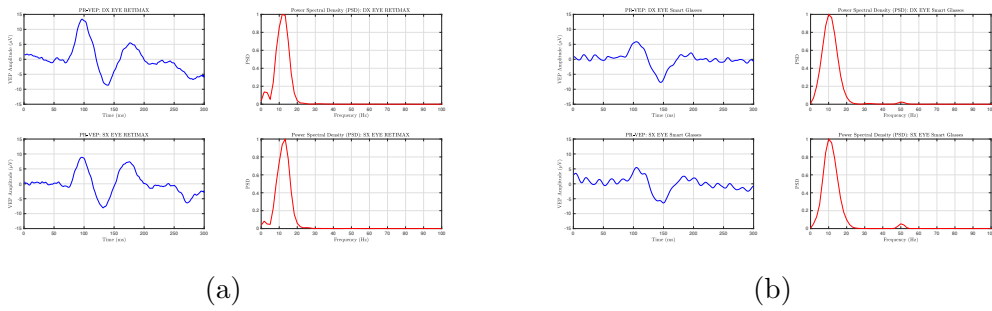


Figure 3.77: Patient MG: (a) PSD of left and right eye signals obtained with Retimax;(b) PSD of left and right eye signals obtained with Smart Glasses.

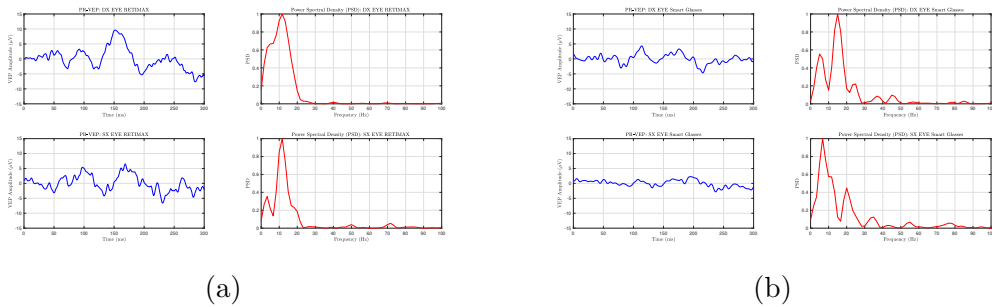


Figure 3.78: Patient BA: (a) PSD of left and right eye signals obtained with Retimax;(b) PSD of left and right eye signals obtained with Smart Glasses.

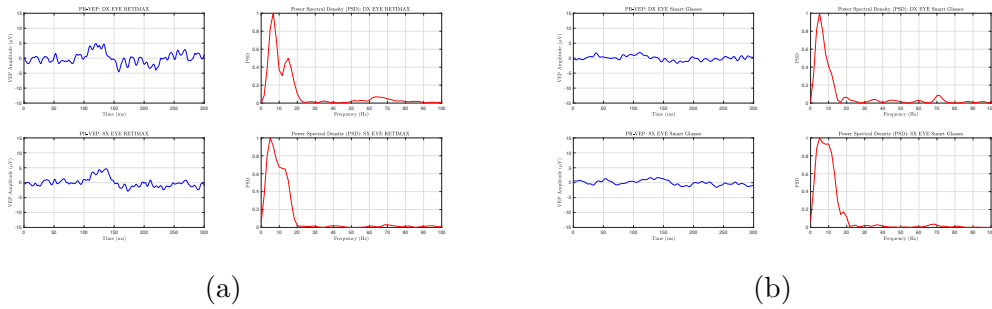


Figure 3.79: Patient SL: (a) PSD of left and right eye signals obtained with Reti-max; (b) PSD of left and right eye signals obtained with Smart Glasses.

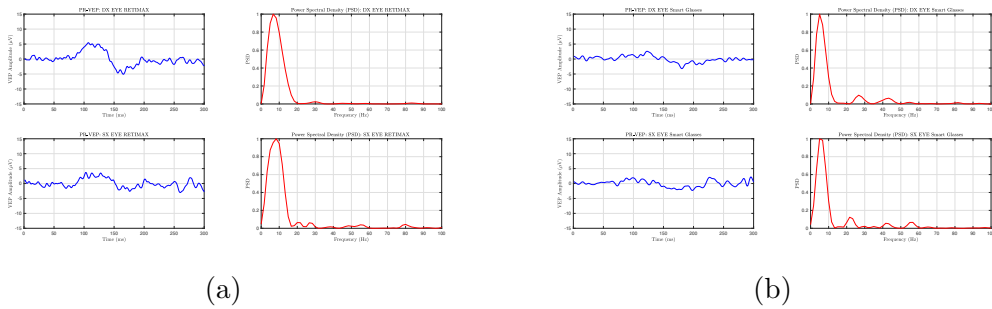


Figure 3.80: Patient BG: (a) PSD of left and right eye signals obtained with Reti-max; (b) PSD of left and right eye signals obtained with Smart Glasses.

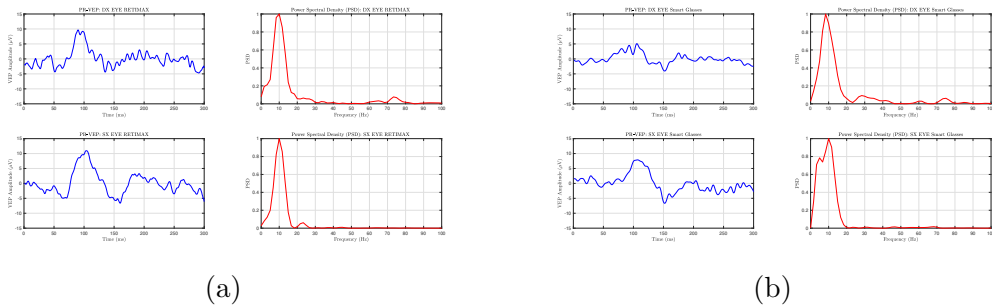


Figure 3.81: Patient CF: (a) PSD of left and right eye signals obtained with Reti-max; (b) PSD of left and right eye signals obtained with Smart Glasses.

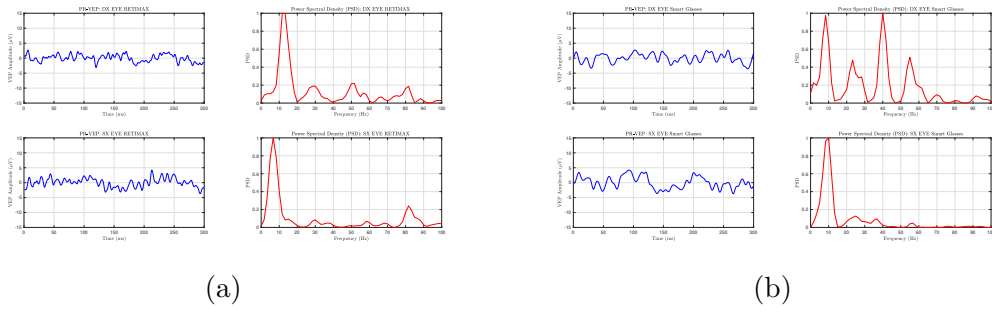


Figure 3.82: Patient GA: (a) PSD of left and right eye signals obtained with Reti-max; (b) PSD of left and right eye signals obtained with Smart Glasses.

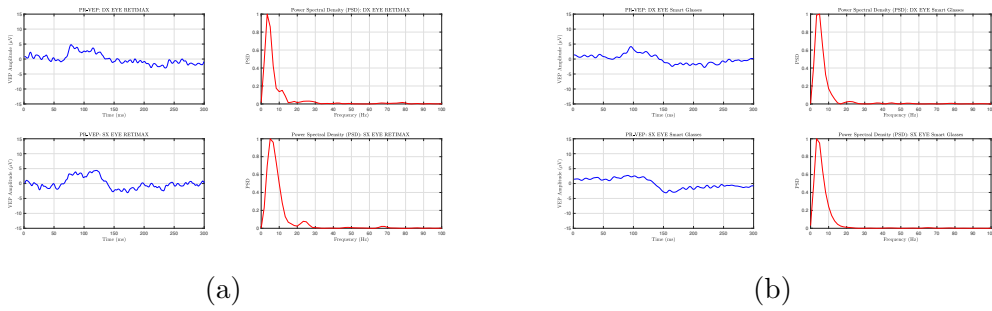


Figure 3.83: Patient SL: (a) PSD of left and right eye signals obtained with Reti-max; (b) PSD of left and right eye signals obtained with Smart Glasses.

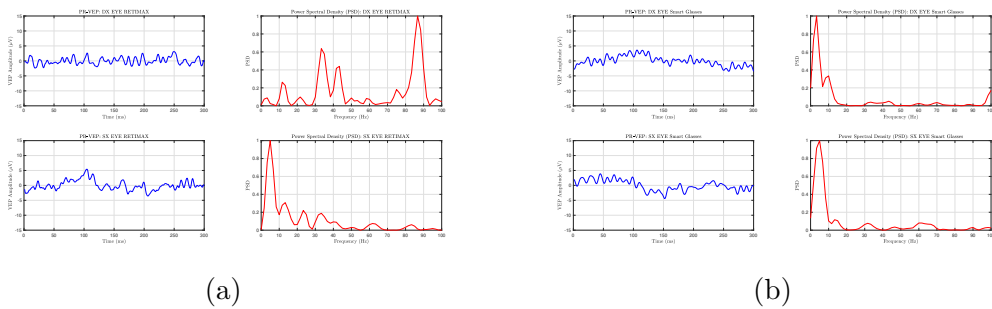


Figure 3.84: Patient BL: (a) PSD of left and right eye signals obtained with Reti-max; (b) PSD of left and right eye signals obtained with Smart Glasses.

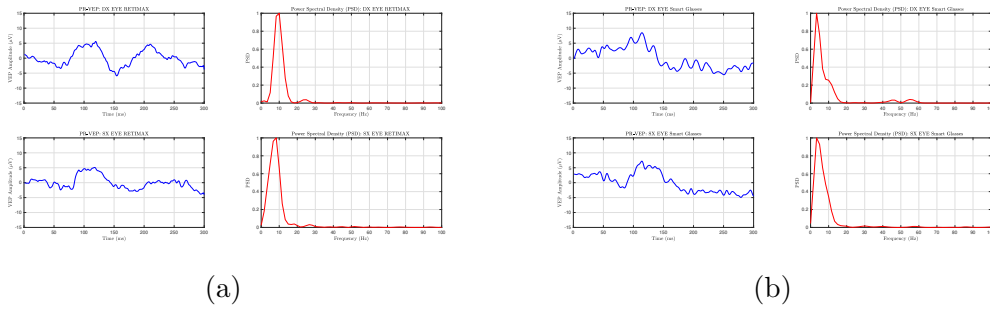


Figure 3.85: Patient GG: (a) PSD of left and right eye signals obtained with Retimax; (b) PSD of left and right eye signals obtained with Smart Glasses.

### 3.4 Comparison between filtered 1-100 Hz and 1-30 Hz signals

As anticipated in the "2.7 Data Post-processing" paragraph, following the frequency analysis it was decided to filter the signals in 1-30 Hz band. Below is an example of signals related to healthy and pathological subjects on which this filtering has been applied.

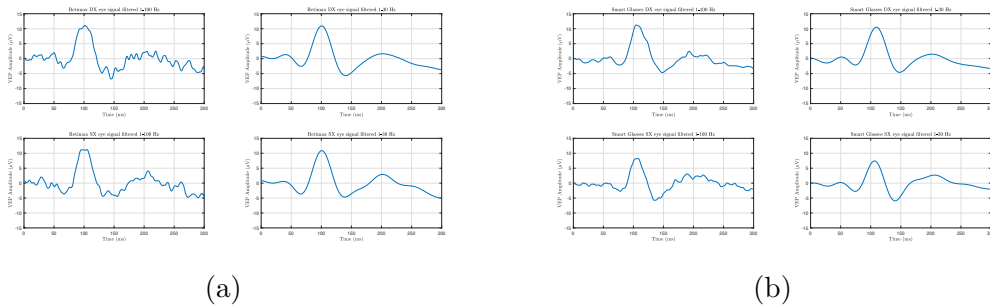


Figure 3.86: Healthy subject: (a) Retimax signals of right and left eye, before and after filtering 1-30 Hz; (b) Smart Glasses signals of right and left eye, before and after filtering 1-30 Hz.

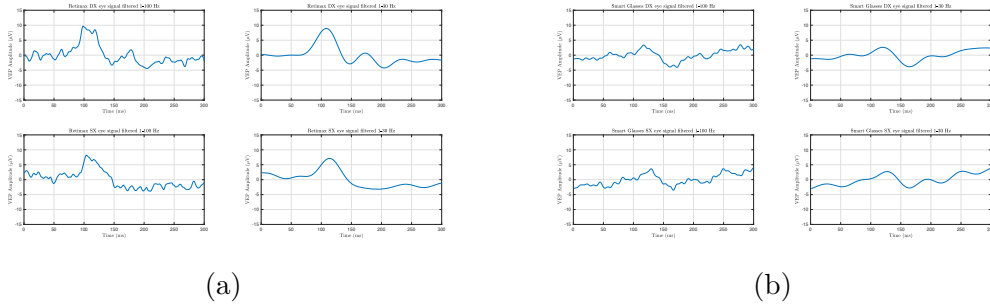


Figure 3.87: Pathological subject: (a) Retimax signals of right and left eye, before and after filtering 1-30 Hz; (b) Smart Glasses signals of right and left eye, before and after filtering 1-30 Hz.

There is a clear improvement in the filtered signal quality in both cases reported: the signal appears less noisy and the typical VEPs waveform is more recognizable, even in the case of pathological subjects.

### 3.4.1 Visual comparison

The overlap of the filtered signals 1-100 Hz and 1-30 Hz is reported, both for the signals obtained through the Retimax system and for those obtained by visually stimulating the patient via Smart Glasses. It is necessary to underline that no significant alterations of the filtered signal in the 1-30 Hz band are visible, neither in amplitude nor in latency.

The representations are related to 5 healthy subjects and 5 pathological ones.

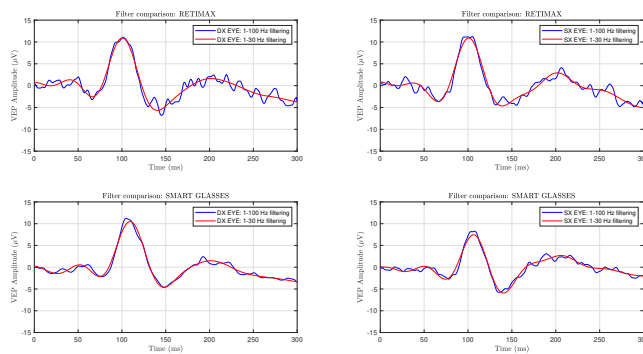


Figure 3.88: Healthy Subject RT: 1-100 Hz and 1-30 Hz filtered signals overlap, for left eye and right one, for the signals obtained from the two different stimulation systems.

### 3 – Results

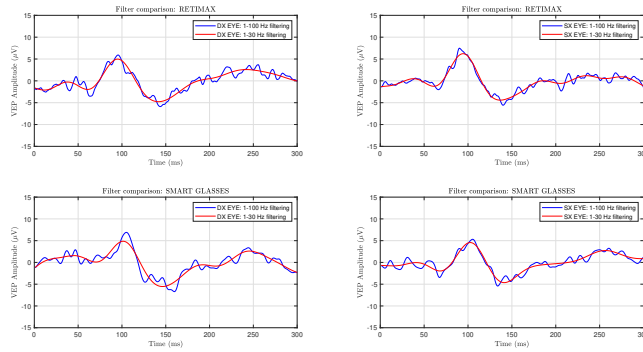


Figure 3.89: Healthy Subject SS: 1-100 Hz and 1-30 Hz filtered signals overlap, for left eye and right one, for the signals obtained from the two different stimulation systems.

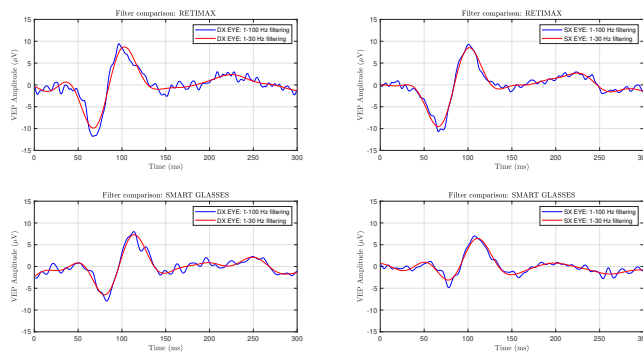


Figure 3.90: Healthy Subject AV: 1-100 Hz and 1-30 Hz filtered signals overlap, for left eye and right one, for the signals obtained from the two different stimulation systems.

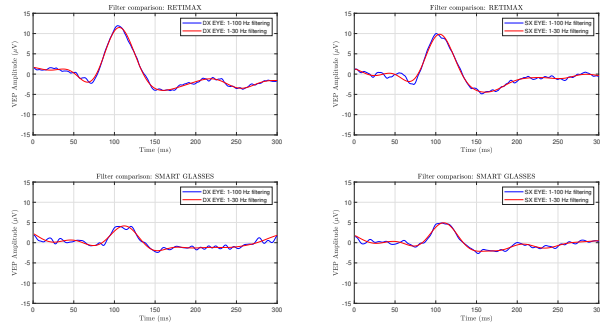


Figure 3.91: Healthy Subject FP: 1-100 Hz and 1-30 Hz filtered signals overlap, for left eye and right one, for the signals obtained from the two different stimulation systems.

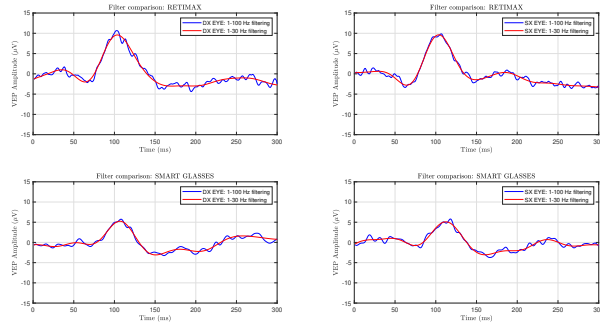


Figure 3.92: Healthy Subject MN: 1-100 Hz and 1-30 Hz filtered signals overlap, for left eye and right one, for the signals obtained from the two different stimulation systems.

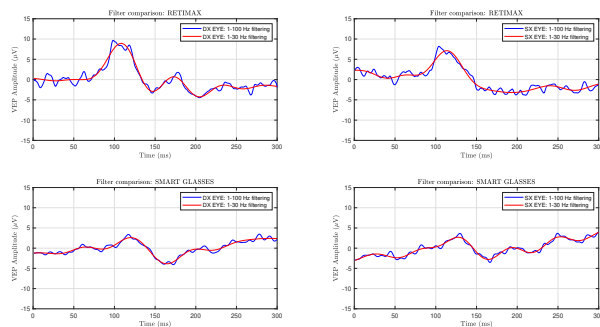


Figure 3.93: Patient AI: 1-100 Hz and 1-30 Hz filtered signals overlap, for left eye and right one, for the signals obtained from the two different stimulation systems.

### 3 – Results

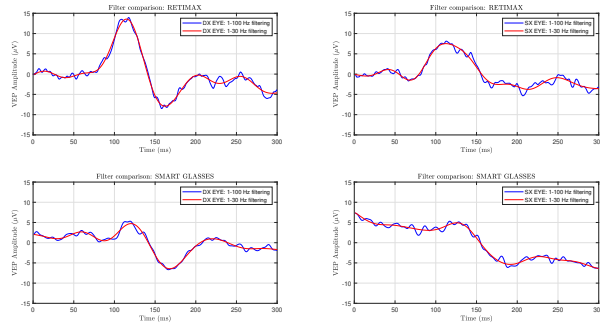


Figure 3.94: Patient BL: 1-100 Hz and 1-30 Hz filtered signals overlap, for left eye and right one, for the signals obtained from the two different stimulation systems.

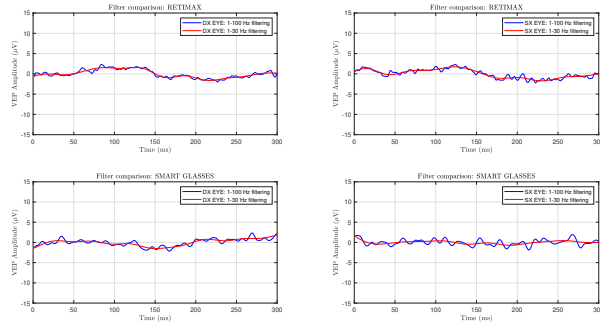


Figure 3.95: Patient FC: 1-100 Hz and 1-30 Hz filtered signals overlap, for left eye and right one, for the signals obtained from the two different stimulation systems.

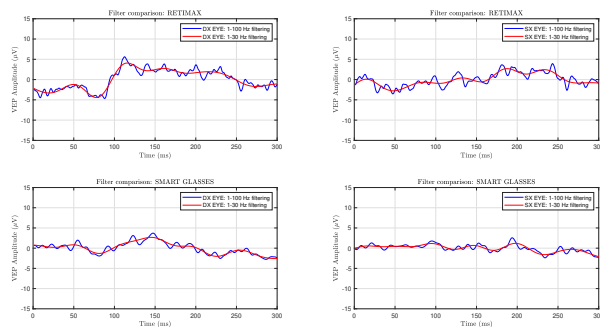


Figure 3.96: Patient LM: 1-100 Hz and 1-30 Hz filtered signals overlap, for left eye and right one, for the signals obtained from the two different stimulation systems.

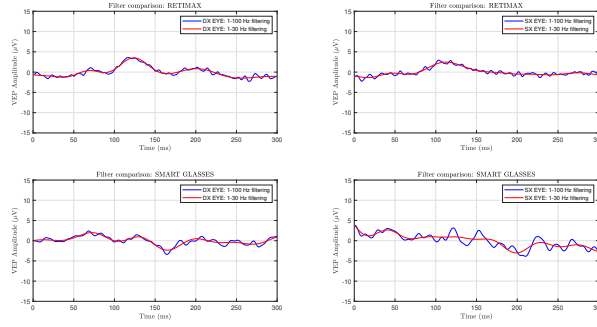


Figure 3.97: Patient LR: 1-100 Hz and 1-30 Hz filtered signals overlap, for left eye and right one, for the signals obtained from the two different stimulation systems.

### 3.4.2 Comparison of the quantity of power

Table 3.5 and Table 3.6 show the average on all signals of the power quantity  $\pm$  standard deviation, before and after filtering in the 1-30 Hz band.

|                         | <b><i>1-100 Hz Filtering</i></b> | <b><i>1-30 Hz Filtering</i></b> |
|-------------------------|----------------------------------|---------------------------------|
| Left eye Retimax        | 7.45 $\pm$ 3.18                  | 7.09 $\pm$ 3.25                 |
| Right eye Retimax       | 9.33 $\pm$ 3.90                  | 8.88 $\pm$ 3.91                 |
| Left eye Smart Glasses  | 5.26 $\pm$ 2.41                  | 4.98 $\pm$ 2.35                 |
| Right eye Smart Glasses | 5.94 $\pm$ 3.15                  | 5.54 $\pm$ 3.05                 |

Table 3.6: Healthy Subjects: average of the power content of the 1-100 Hz and 1-30 Hz filtered signals, of right and left eye, of Retimax and Smart Glasses signals. The values are followed by the standard deviation.

|                         | <b><i>1-100 Hz Filtering</i></b> | <b><i>1-30 Hz Filtering</i></b> |
|-------------------------|----------------------------------|---------------------------------|
| Left eye Retimax        | 4.98 $\pm$ 4.65                  | 4.71 $\pm$ 4.64                 |
| Right eye Retimax       | 6.23 $\pm$ 6.59                  | 5.89 $\pm$ 6.61                 |
| Left eye Smart Glasses  | 2.7 $\pm$ 2.81                   | 2.45 $\pm$ 2.79                 |
| Right eye Smart Glasses | 2.64 $\pm$ 2.69                  | 2.16 $\pm$ 2.47                 |

Table 3.7: Pathological Subjects: average of the power content of the 1-100 Hz and 1-30 Hz filtered signals, of right and left eye, of Retimax and Smart Glasses signals. The values are followed by the standard deviation.

It is interesting to note how the amount of power before and after the filtering of the signals in band 1-30 Hz, has remained almost unchanged. This confirms that through this filtering almost nothing is lost regarding the information linked to the signals, with the advantage of obtaining much cleaner signals.

Moreover, regarding the comparison between the two stimulators, the PR-VEPs evoked with the Retimax Advanced seem to provide a higher information content about power density than the Smart Glasses PR-VEPs.

Finally, the quantity of power relative to the average of the signals of *wet and dry maculopathic* has been calculated. Wet maculopathic power is expected to be the lowest. *Table 3.8* shows the results.

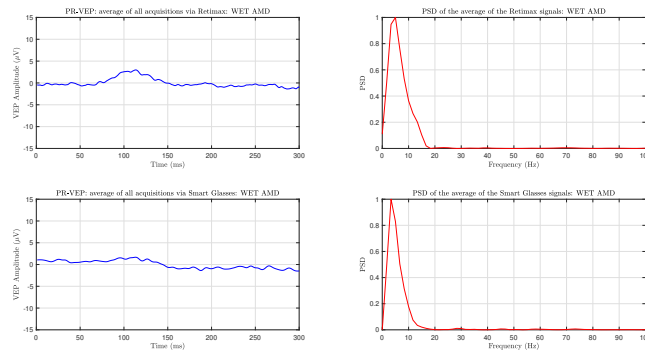


Figure 3.98: PSD of the average of wet maculopathic signals obtained via Retimax and via Smart Glasses.

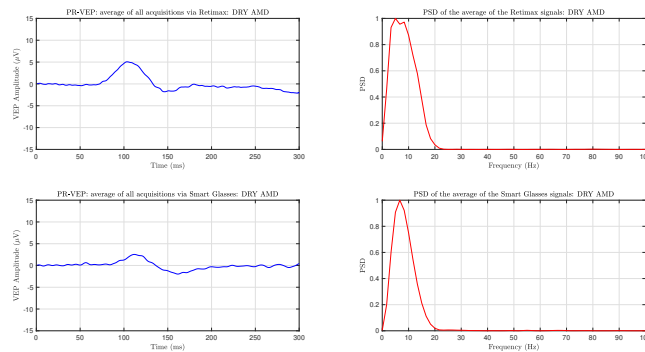


Figure 3.99: PSD of the average of dry maculopathic signals obtained via Retimax and via Smart Glasses.

|               | <i>Wet AMD</i> | <i>Dry AMD</i> |
|---------------|----------------|----------------|
| Retimax       | 0.92±0.02      | 2.51±0.04      |
| Smart Glasses | 0.54±0.01      | 0.96±0.02      |

Table 3.8: Wet and Dry maculopathy: quantity of power of the average of the pathological Retimax and Smart Glasses signals. The values are followed by the standard deviation.

## Summary of this chapter

After the initial calibration on the 10 healthy subjects, the values relative to the characteristic components of the VEP signals (N75, P100 and N135) obtained via Retimax CSO and Smart Glasses, were extrapolated and compared, in terms of amplitude and latency. From this comparison it emerged how the amplitudes of the pr-VEPs obtained through the Retimax system are in general greater than those obtained via Smart Glasses. The latencies, on the other hand, were very similar between the two devices. Then the results of the acquisitions on the 30 subjects suffering from maculopathy were shown. A subdivision between the results of patients with dry maculopathy and wet maculopathy was also reported. This comparison confirmed what the literature suggests: the signals belonging to wet maculopathy are flatter and with less power, as it is precisely the wet maculopathy that causes more damage to the visual pathway. Finally, for all the signals the power spectral density was calculated, with the aim of identifying the frequency band in which the greatest quantity of signal information was concentrated. It emerged that this band corresponds to the 1-30 Hz range. Therefore the power quantity was calculated for each signal, considering the 1-100 Hz band first and then 1-30 Hz. It was shown that 1-30 Hz filtering does not alter the signals of interest. In fact, the amount of power before and after this filtering has remained more or less unchanged, with the advantage of obtaining cleaner and simpler interpretation signals. The chapter concludes with the discovery that signals obtained via Retimax CSO have a greater amount of power than those obtained using Smart Glasses as a visual stimulation system.

# Chapter 4

## Statistic analysis

Once obtained the results for both healthy and pathological subjects, through the two different prototypes compared in this thesis work, a statistical analysis was carried out evaluating the following statistical parameters and algorithms:

- *correlation coefficient ( $r$ ) or Pearson's coefficient;*
- *linear or least square regression line and scatter plot;*
- *Bland-Altman plots.*
- *concordance correlation coefficient (CCC), bias correction factor ( $\chi_b$ ) and intraclass correlation coefficient (ICC) (only for N75, P100 and N135 components.)*

The objective was to establish whether the prototype proposed by us would lead to results quantitatively and qualitatively similar to those obtained with the Retimax CSO system currently in use. This would eventually lead to the validation of the system presented in this work.

### 4.1 Statistic analysis on healthy subjects

For healthy subjects, the statistical analysis was conducted both on the average of the whole signals and on their characteristic components: N75, P100 and N135, evaluated both in amplitude and in latency. A frequency analysis was also carried out, calculating the correlation between the quantity of signals power.

## Correlation Coefficient ( $r$ ) or Pearson’s Coefficient

### Average of the signals

In order to express quantitatively the intensity of the link between two variables it is necessary to calculate a correlation index. Our goal is to estimate the correlation between VEPs acquisitions made through the Retimax CSO system and our prototype.

There are various kinds of correlation indices: in this thesis work it was decided to calculate the **Pearson’s coefficient ( $r$ )**, defined as the covariance of the comparative acquisitions divided by the product of the standard deviations of the two acquisitions.

All correlation indices have some common features:

1. the two data sets are associated to the same individuals or events, or to different but associated subjects from a certain point of view. In our specific case we compare the average of the signals acquired through Retimax CSO with the average of the signals acquired by means of our prototype;
2. the values of the various correlation indices vary between -1 and +1; both extreme values represent perfect relations between the variables, respectively negative and positive, while 0 represents the absence of a relationship;
3. a positive correlation index means that individuals who obtain high values in a given set tend to obtain high values on the second data set. And it’s also true vice versa, ie those who have low values in the first data set tend to have low values also in the second one;
4. a negative correlation index indicates that a low values on a data set correspond high values on the other one.

*Table 4.1* shows the values of the Pearson’s coefficients together with the degree of statistical significance: **p-value**. Generally the p limit value that is indicated as the correlation threshold between the two sets is 0.05: values of  **$p < 0.05$**  represent a good correlation, on the contrary  **$p > 0.05$**  is an index of poor correlation.

|                  | Coefficient $r$ | p-value                 |
|------------------|-----------------|-------------------------|
| <b>Left Eye</b>  | 0.7380          | $3.9309 \cdot 10^{-63}$ |
| <b>Right Eye</b> | 0.7317          | $1.4398 \cdot 10^{-61}$ |

Table 4.1: Pearson’s Coefficient and p-values of the average of the signals: left and right eye, healthy subjects.

From the values of the correlation coefficient, it stresses the existence of a direct correlation ( $r > 0$ ) between the acquisitions made through the two different prototypes. In detail, it is a strong correlation, as  $r > 0.7$ . The p-values confirm these observations.

### N75, P100 and N135 Components

This section shows the correlation indexes between the characteristic components of the VEP signals: for example, the P100 wave of a signal obtained via Retimax CSO is compared, in amplitude and latency, with the P100 wave of a signal obtained by visually stimulating the subject via Smart Glasses. Similarly, the N75 and N135 waves were also evaluated. Components analysis was only possible on healthy subjects, as characteristic waves are often not recognisable in signals belonging to pathological ones.

|                  | Amplitude |        | Latency |         |
|------------------|-----------|--------|---------|---------|
|                  | Left      | Right  | Left    | Right   |
| <b>r of N75</b>  | -0.0088   | 0.6434 | 0.0793  | 0.3077  |
| <b>p-value</b>   | 0.9808    | 0.0447 | 0.8276  | 0.3871  |
| <b>r of P100</b> | 0.5747    | 0.4728 | 0.1445  | -0.5641 |
| <b>p-value</b>   | 0.0822    | 0.1676 | 0.69051 | 0.0894  |
| <b>r of N135</b> | 0.4488    | 0.4602 | 0.3984  | -0.0344 |
| <b>p-value</b>   | 0.1932    | 0.1808 | 0.2542  | 0.9247  |

Table 4.2: Pearson’s Coefficient and p-values of the N75, P100 and N135 components: amplitude and latency, left and right eye, healthy subjects.

From the comparison of the individual components, the results obtained show a weak correlation. In fact, in all cases  $r < 0.7$ . However, as expected, in cases where the Pearson’s coefficient assumes higher values, the p-values decrease.

### Quantity of signals power

It was decided to extract the amount of power from each signal acquired and to use it as a feature to be correlated. Of each signal, for both the right and left eyes, the amount of power was calculated. In this way, 10 power values were obtained for the right eye and other 10 for the left one. Averaging the first 10 values it was obtained the Pearson’s coefficient related to the quantity of power of the right eyes. In the same way, the value relative to the left eyes was also obtained.

|                  | <b>Coefficient <math>r</math></b> | <b>p-value</b> |
|------------------|-----------------------------------|----------------|
| <b>Left Eye</b>  | -0.0270                           | 0.9410         |
| <b>Right Eye</b> | 0.4094                            | 0.2401         |

Table 4.3: Pearson's Coefficient and p-values for the amount of signals power: left and right eye, healthy subjects.

There is a direct correlation, even if weak, only in the case of the right eye. Probably, the acquisitions on the left eye were affected by interference or artifacts, so as to obtain very different amounts of power.

### Signal for signal: average correlation coefficients

Finally, the signals were correlated individually: this resulted in 10 coefficients  $r$  for the right eye (10 healthy subjects considered) and 10 coefficients  $r$  for the left one. Then the average value was calculated, obtaining the two values shown in Table 4.4:

|                  | <b>Average of Coefficients <math>r</math></b> |
|------------------|---|
| <b>Left Eye</b>  | 0.6184  |
| <b>Right Eye</b> | 0.6014  |

Table 4.4: Average of the Pearson's Coefficients: left and right eye, healthy subjects.

From the reported data, it is concluded that the signals compared have a good degree of correlation for both eyes. However, it is not possible to talk about a strong correlation.

Taking into account the values assumed by the Pearson's coefficient, even if a perfectly linear relationship does not exist between the data, it makes sense to determine the equation of a line that approximates the data in the "best possible way". For this reason, the statistical algorithm that will be proposed in the next section consists of the *least squares method*, which allows to determine the equation of the *regression line*.

## Linear or Least Square Regression Line and Scatter Plots

### Average of the signals

The qualitative comparison of the distance between the linear regression line, that is the line that best approximates the data series, and the quality line (bisector line) is shown, in order to evaluate the agreement between the two VEPs acquisition systems. The more similar the regression line and quality line are, the greater the agreement between the results obtained via Retimax and via Smart Glasses.

Furthermore, to visually explore the relationship between two data sets it is useful to represent it through appropriate correlation diagrams, called *scatter plots*. This is a type of graph in which the samples of the two data sets are shown on the Cartesian plane. Generally, the scatter plot is a representation used when one of the two data sets is under the control of the experimenter and is called an independent or control data set.

In this work, the VEP acquisition made by the Retimax system is assumed as the independent data set, whose values are reported on the abscissa axis of the scatter plot. Instead, on the ordinate axis are shown the values of the VEP acquisitions made through our prototype, which represent the dependent data sets.

The overlap between the representation constituted by the regression line and the one constituted by the scatter plot is reported below.

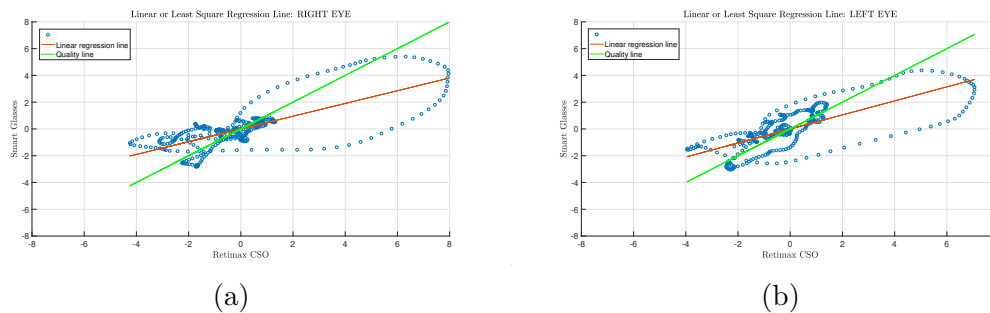


Figure 4.1: Linear Regression Line relative to the average of the signals of healthy subjects: (a) linear regression line for acquisitions on the right eye; (b) linear regression line for acquisitions on the left eye.

From these representations it is possible to make observations in accordance with the values assumed by the Pearson's coefficients. The scatter plots dispersion, in fact, appears more or less concentrated around the regression line (not entirely because the correlation coefficient is not 1). On the other hand, however, this line does not perfectly approximate the quality one: this is due to the fact that there

is a correlation between acquisitions made through the Retimax system and those made through our prototype, but not strictly linear.

## N75, P100 and N135 Components

The same type of statistical analysis was conducted on the characteristic waves of the VEPs signals, as shown below.

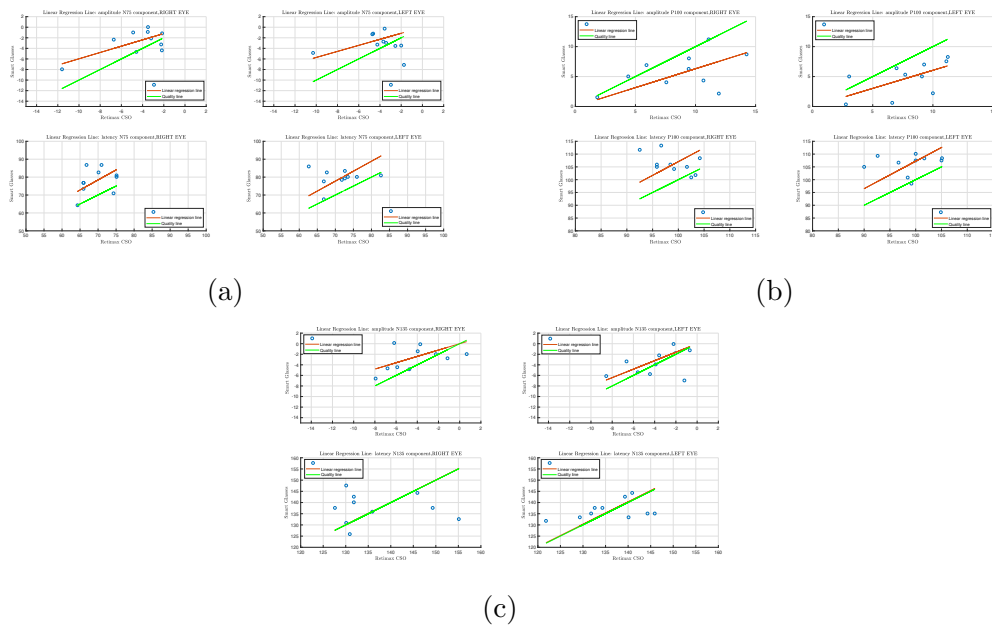


Figure 4.2: Linear Regression Line relative to the signals components, healthy subjects: (a)N75 component: amplitude and latency, left and right eye; (b)P100 component: amplitude and latency, left and right eye; (c)N135 component: amplitude and latency, left and right eye.

In accordance with what was said in *paragraph 3.1* regarding the latency of the N135 wave, we observe the existence of a close linear correlation between the N135 components of the signals, both for the right eye and for the left one. In fact, the regression line approaches the quality line very well.

For the N75 and P100 components, however, what stands out most is the scatter plot scattering: the points that represent the data appear to be particularly concentrated around the regression line, emphasizing a good correlation between the data. The same observation applies to the N135 wave amplitude analysis.

## Quantity of signals power

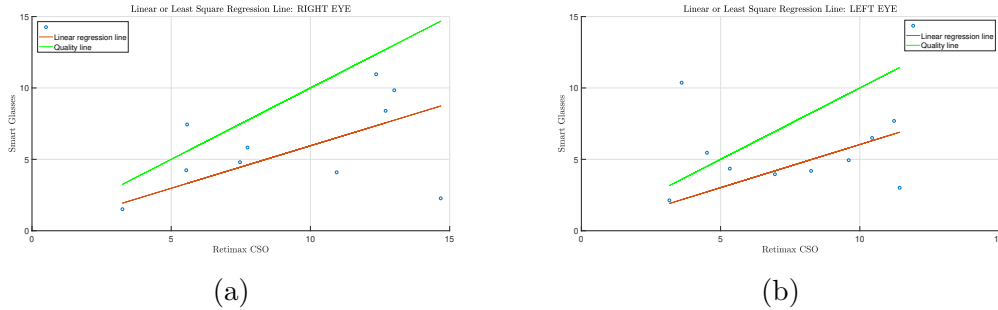


Figure 4.3: Linear Regression Line relative to the quantity of signals power of healthy subjects: (a) linear regression line for acquisitions on the right eye; (b) linear regression line for acquisitions on the left eye.

These representations confirm what is indicated by the correlation coefficients related to the amount of power: in particular for the acquisitions made on the left eye, there is a poor correlation between the data. The scatter plot points, in fact, are dispersed and some ones are very far from the regression line.

## Bland-Altman Plots

### Average of the signals

The Bland-Altman plots allow to compare two measurement methods of the same nature, corresponding, in our case, to the two acquisitions made for each subject through the two different systems.

The graph is a dispersion diagram in which on the ordinates the difference of the two data sets is reported and on the abscissas the reference measure, corresponding to their arithmetic mean.

The horizontal lines represent the average of the difference and the average of the difference  $\pm 2 \times$  standard deviation. The average of the difference makes it possible to estimate whether one of the two methods underestimates or overestimates the measure with respect to the other, while the other two lines constitute the *confidence interval*. If the points of the graph are within the confidence interval, the methods compared provide congruent results, while the points outside this range are cases in which the two methods are not congruent with each other or any *outliers*.

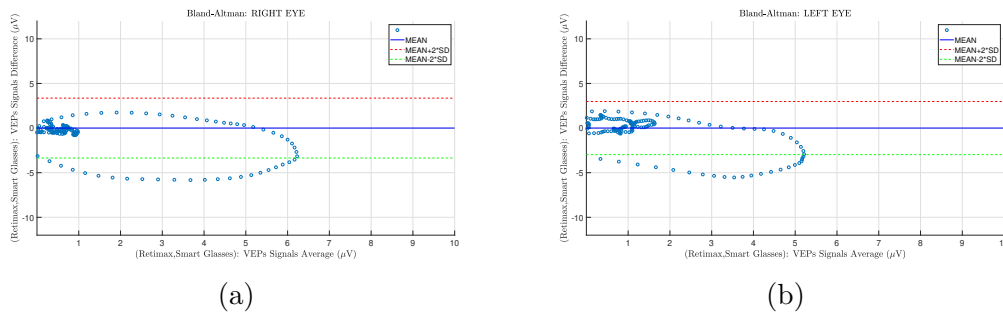


Figure 4.4: Bland-Altman Plots of the average of the signals of healthy subjects: (a) Bland-Altman plot for acquisitions on the right eye; (b) Bland-Altman plot for acquisitions on the left eye.

The absence of a trend in the distribution of values is a symbol of lack of systematic errors. Much of the dispersion lies within the confidence interval, which underlines a good level of congruence between the acquisitions made through the two different systems. Also in this case, these results are in agreement with what is indicated by the correlation coefficients.

## N75, P100 and N135 Components

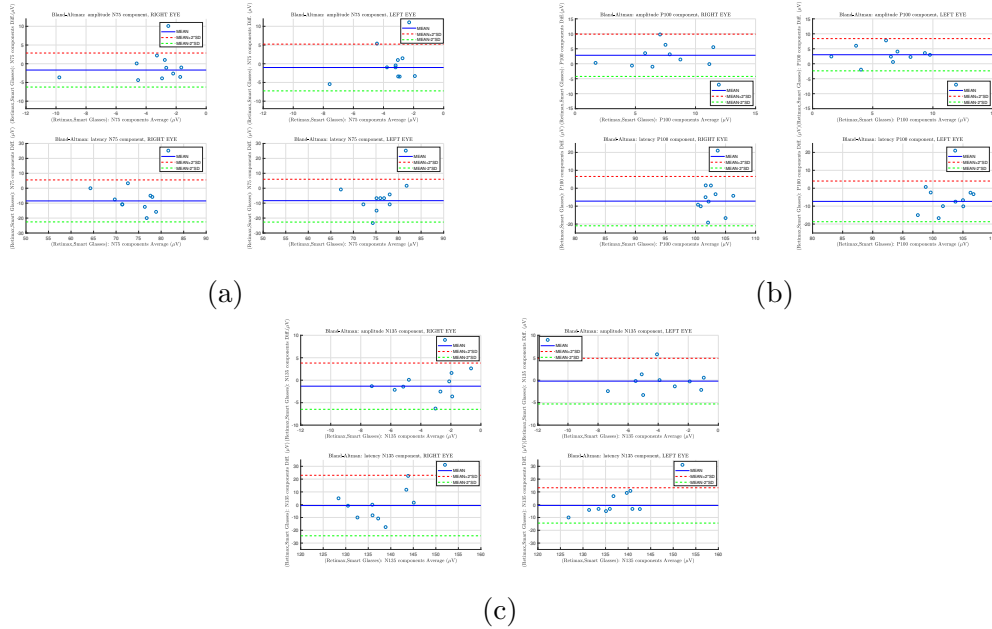


Figure 4.5: Bland-Altman Plots of the signals components, healthy subjects: (a)N75 component:amplitude and latency, left and right eye; (b)P100 component: amplitude and latency, left and right eye; (c)N135 component: amplitude and latency, left and right eye.

In all the representations shown above it is evident that the dispersion of points is entirely part of the confidence interval. There are no outliers. It is also noted that in some cases, as for the latency analysis of the N135 wave related to the left acquisitions, this range is particularly narrow, demonstrating the good congruence between the signal components.

## Quantity of signals power

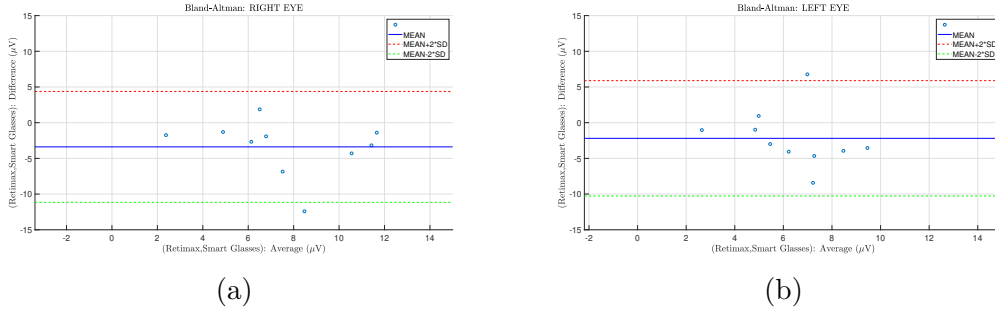


Figure 4.6: Bland-Altman Plots of the quantity of signals power of healthy subjects: (a) Bland-Altman plot for acquisitions on the right eye; (b) Bland-Altman plot for acquisitions on the left eye.

For both right-eye and left-eye acquisitions, the dispersion of the points is within the confidence interval. Confirming the claims made so far, this frequency analysis shows that this range is not very narrow and this is a symbol of a weak correlation.

## Concordance Correlation Coefficient, Bias Correction Factor and Intra-class Correlation Coefficient

At the end of the statistical analysis of the results obtained on healthy subjects, the values assumed by *concordance correlation coefficient* (**CCC**), *bias correction factor* ( $\chi_b$ ) and the *intraclass correlation coefficient* (**ICC**) are reported. These coefficients were obtained by reference to the characteristic components of the VEP signals.

| <b>Left Eye</b>                            |            |                           |            |
|--|------------|---------------------------|------------|
|  | <i>CCC</i> | $\chi_b(\text{accuracy})$ | <i>ICC</i> |
| <b>Amplitude(<math>\mu\text{V}</math>)</b> |            |                           |            |
| N75 Amplitude                              | -0.0071    | 0.8779                    | -0.0079    |
| P100 Amplitude                             | 0.3603     | 0.6268                    | 0.5735     |
| N135 Amplitude                             | 0.4459     | 0.9935                    | 0.4477     |
| <b>Latency(ms)</b>                         |            |                           |            |
| N75 Time Peak                              | 0.0329     | 0.4159                    | 0.0785     |
| P100 Time Peak                             | 0.0540     | 0.3740                    | 0.1402     |
| N135 Time Peak                             | 0.3330     | 0.8360                    | 0.3347     |

Table 4.5: Left eye: CCC,  $\chi_b$  and ICC.

| <b>Right Eye</b>                           |            |                           |            |
|--|------------|---------------------------|------------|
|  | <i>CCC</i> | $\chi_b(\text{accuracy})$ | <i>ICC</i> |
| <b>Amplitude(<math>\mu\text{V}</math>)</b> |            |                           |            |
| N75 Amplitude                              | 0.5158     | 0.8016                    | 0.6317     |
| P100 Amplitude                             | 0.3333     | 0.7049                    | 0.4614     |
| N135 Amplitude                             | 0.3884     | 0.8440                    | 0.4516     |
| <b>Latency(ms)</b>                         |            |                           |            |
| N75 Time Peak                              | 0.1242     | 0.4037                    | 0.2710     |
| P100 Time Peak                             | -0.1948    | 0.3453                    | -0.5639    |
| N135 Time Peak                             | -0.0319    | 0.9267                    | -0.0320    |

Table 4.6: Right eye: CCC,  $\chi_b$  and ICC.

## 4.2 Statistic analysis on pathological subjects

For pathological subjects the statistical analysis has been carried out on the average of the acquired signals and not on the single components: in fact, in the signals relating to maculopathic subjects the characteristic waves are not always easily recognizable. In this case too, frequency analysis was carried out, calculating the correlation between the quantity of signal power.

### Correlation Coefficient ( $r$ ) or Pearson's Coefficient

#### Average of the signals

|                  | Coefficient $r$ | p-value                 |
|------------------|-----------------|-------------------------|
| <b>Left Eye</b>  | 0.8438          | $8.6064 \cdot 10^{-99}$ |
| <b>Right Eye</b> | 0.7901          | $4.3607 \cdot 10^{-78}$ |

Table 4.7: Pearson's Coefficient and p-values of the average of the signals: left and right eye, pathological subjects.

In particular for the acquisitions made on the right eye there is a positive and high correlation coefficient. In both cases, for both the right eye and the left one, the p-values are clearly below the threshold beyond which the correlation would lose statistical significance.

#### Quantity of signals power

|                  | Coefficient $r$ | p-value                |
|------------------|-----------------|------------------------|
| <b>Left Eye</b>  | 0.7006          | $1.6261 \cdot 10^{-5}$ |
| <b>Right Eye</b> | 0.6456          | $1.5557 \cdot 10^{-4}$ |

Table 4.8: Pearson's Coefficient and p-values for the amount of signals power: left and right eye, pathological subjects.

Considering the amount of power of the signals as the characteristic extracted and compared, it is noted that for both eyes there is a good correlation, strong for the left acquisitions.

## Signal for signal: average correlation coefficients

|           | Average of Coefficients $r$ |
|-----------|-----------------------------|
| Left Eye  | 0.3579                      |
| Right Eye | 0.3762                      |

Table 4.9: Average of the Pearson's Coefficients: left and right eye, pathological subjects.

Pearson's mean coefficients indicate a weak correlation. This can probably be due to the fact that the average operation has considerably reduced the variability of the signals, which are indeed very different from patient to patient.

## Linear or Least Square Regression Line and Scatter Plots

### Average of the signals

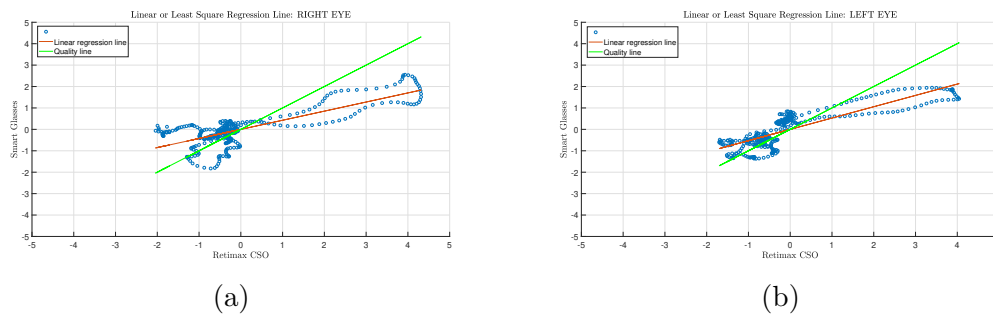


Figure 4.7: Linear Regression Line relative to the average of the signals of pathological subjects: (a) linear regression line for acquisitions on the right eye; (b) linear regression line for acquisitions on the left eye.

To confirm the value assumed by the Pearson's coefficient on the average of the acquisitions made on the left eye, the regression line reported above approximates sufficiently well the dispersion of the data. Again, although the correlation between the two prototypes is confirmed by these evidences, it is not possible to speak of linear correlation, as there is no overlap between regression line and quality line.

## Quantity of signals power

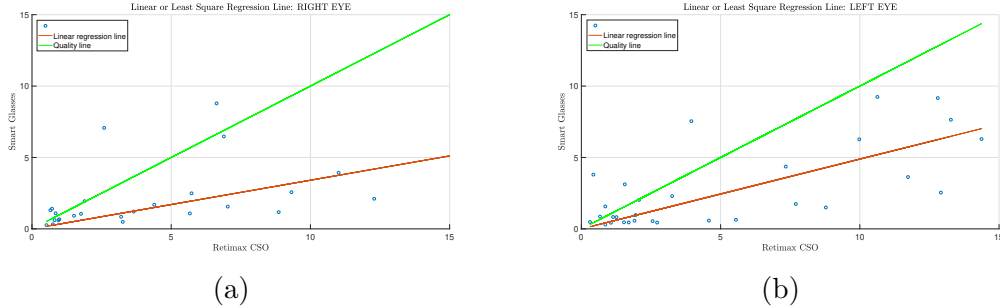


Figure 4.8: Linear Regression Line relative to the quantity of signals power of pathological subjects: (a) linear regression line for acquisitions on the right eye; (b) linear regression line for acquisitions on the left eye.

It is clear that the correlation between the signals obtained from the two different prototypes exists, but it is not linear.

## Bland-Altman Plots

### Average of the signals

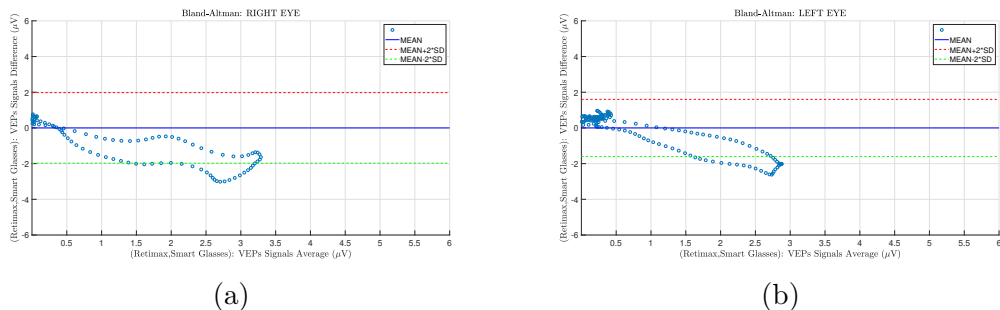


Figure 4.9: Bland-Altman Plots of the average of the signals of pathological subjects: (a) Bland-Altman plot for acquisitions on the right eye; (b) Bland-Altman plot for acquisitions on the left eye.

In both cases, the confidence interval is sufficiently narrow, which indicates a low variability between the data. The data dispersion appears mainly within the confidence range and this indicates a good correlation between the acquisitions made through the Retimax system and through the prototype proposed by us. We highlight some outliers, probably related to subjects whose maculopathy status is particularly advanced. In these cases the two prototypes have small differences.

## Quantity of signals power

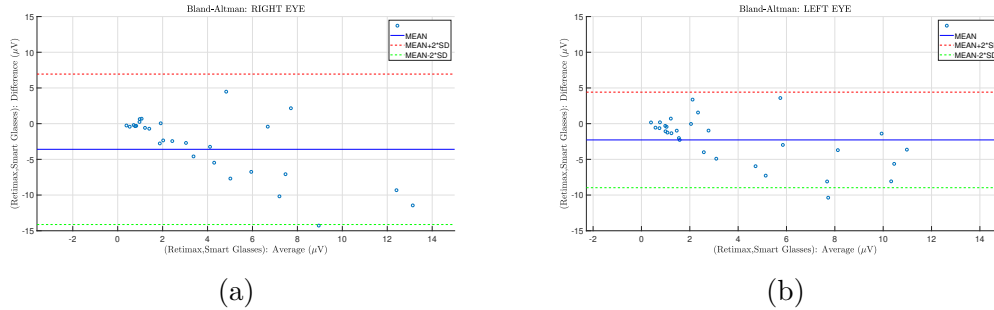


Figure 4.10: Bland-Altman Plots of the quantity of signals power of healthy subjects: (a) Bland-Altman plot for acquisitions on the right eye; (b) Bland-Altman plot for acquisitions on the left eye.

The dispersion of the points is part, for both eyes, of the confidence interval, which is evidently narrower in the case of the left eye.

## Summary of this chapter

The statistical analysis of the healthy subjects signals was conducted on the average of the signals and on the individual characteristic components of the pr-VEPs. Instead, for the maculopathic subjects signals the statistical analysis on the single components was not possible, since in most cases it was not possible to identify them. For both categories of subjects a frequency analysis was then carried out to calculate the correlation between the power quantity of the signals obtained through the two stimulation systems. Both for the healthy subjects signals and those of pathological ones a good correlation emerges between the devices, especially in terms of latency. However, taking into account in particular the performance achieved on pathological subjects, it is still necessary to process the prototype presented in this work. On the whole, there is a direct correlation between the results obtained, even if not linear. Also the standard deviations calculation confirms promising results.

## Chapter 5

# Conclusions, Critical points and Future goals

In this thesis work a portable and low-cost device was presented as a system for carrying out pr-VEPs tests: the *Smart Glasses*.

Born in the field of virtual reality, this device has been used for the visual stimulation of subjects (healthy and pathological), through the most common checkerboard stimulus. The crucial point of this thesis was the performance comparison between the prototype we proposed and the commercial stimulation and acquisition *Retimax CSO* system. Therefore Smart glasses offer the possibility to set the parameters of stimulation, such as the spatial and temporal frequency, in order to adapt them to the parameters of the Retimax system. The *International 10/20 Standard* was followed for electrode positioning. The pr-VEPs signals resulting from the stimulation have been acquired in real time by the bio-potential amplifier *g.HIamp* and finally sent to a laptop for analysis, through *special software*, and post-processing, via *Matlab*.

The choice to propose our prototype as a system for pr-VEPs is linked to the several *advantages* that result. Thanks to their portability, in fact, the Smart Glasses offer the possibility of subjecting even bedridden or motion-impaired patients to the test. Through our device, therefore, the pr-VEP exam can also be done at the patient's home. Another particularly interesting aspect concerns the low cost of the presented system. While the current and commercial equipment required for pr-VEPs tests requires between 20.000 and 70.000 €, our prototype has an estimated price of around 1.200 €.

In view of the intended objective, before using our prototype for clinical tests on maculopathic patients, it was necessary to calibrate it on a set of 10 healthy subjects. Once calibrated, the system was tested on 30 patients whose visual integrity

was more or less damaged.

The results obtained from stimulation via Smart Glasses have been compared with those related to the Retimax system. A first visual comparison was possible by superimposing the signals of the two stimulation systems. The tracks were analyzed both in time and in frequency, through the calculation of *Power Spectral Density* (PSD). From this last analysis it emerged that the greatest informative contribution of the signals is in the 1-30 Hz band. Finally, a *statistical analysis* was conducted using correlation coefficients, such as the Pearson's coefficient ( $r$ ) and the Concordance Correlation Coefficient (CCC), and statistical algorithms, such as linear regression, scatter plots and Bland-Altman graphs.

Although this thesis work is still only a preliminary evaluation, to be extended to a larger number of patients, the conducted analyses show a good congruence between the results of the two systems. In terms of amplitude and latency of the three characteristic waves of VEP signals, the pathways belonging to pathological subjects show greater differences than those relative to the calibration subjects. These differences may be due to the overlapping of the low amplitude signal typical of the maculopathic with the random noise present during the acquisitions, towards which our prototype appears to be particularly sensitive.

In view of these results, I think that the proposed prototype can have a *significant diagnostic value*, to be increased by continuing to test it and improve it with both hardware and software modifications.

For future developments, we can start by trying to find a solution to the following critical issues:

- sensitivity to 50 Hz network interference, a reason of difficulty in analyzing the signal;
- not being able to know exactly the value of the luminance of the Smart Glasses, as it is not indicated as a numerical value but as a "minimum", "medium" and "maximum" luminance;
- difficulty in focusing the Smart Glasses display. This disturbance could be caused by the presence of prisms in the lenses of the glasses, created for viewing 3D movies;
- Smart Glasses wear. Our system has been used in many previous experiments and is therefore not in very good condition. The patient has sometimes been distracted from having to keep the glasses with his hands in the most optimal position, thus not paying attention exclusively to the stimulation pattern. This

aspect has most affected patients in clinical experiments due to their age and limited knowledge of the test.

## **Future Goals**

### **Hardware Improvements**

- we will try to make the Smart Glasses system more comfortable and stable than the current one;
- it will ensure that the structure of the device perfectly isolates the patient from the outside world, so that it is no longer necessary to perform the test in a darkroom.

### **Software Improvements**

- we want to introduce further stimulation modes, so as to be able to perform flash VEP and on/off VEP tests on the same device;
- we want to implement a real-time analysis of the patient's eye movement, in order to stop the stimulation when the patient no longer looks at the fixation point and resume it when he returns to the ideal stimulation conditions.

## **Future developments: Cardboard**

With the aim of creating a prototype that is not only portable and low-cost, like that of Smart Glasses, but that is also accessible to everyone, acquisitions on healthy subjects have been made using Cardboard as a visual stimulator. It should also be remembered that the pr-VEPs tests are currently performed only in specialized ophthalmology clinics with very expensive tools. A device that allows you to make diagnostics with your smartphone, as Cardboard do, opens the way for a whole range of applications in telediagnosics and telemedicine, including in hospitals where specialist screening, as that achievable with VEPs, would not be possible due to economic scarcity.

As regards the results obtained from the acquisitions, it is observed that the three characteristic waves are all recognizable. In some cases, however, there are changes in latency compared to the expected results. These differences are probably due to the luminance level of the smartphone screen, whose necessary value is not yet well known. With the appropriate improvements and modifications, the Cardboard remain a good solution for future visual stimulation.

## Acknowledgements

Per un ingegnere, che ogni giorno gioca con i numeri, i codici e le formule, non è così semplice lasciare spazio alle parole. E adesso, che sono ingegnere al quadrato, quanto sarà complicato per me? Eppure oggi, che è il mio giorno felice, è l'occasione giusta per mettere da parte la razionalità e fare spazio a dolci pensieri.

È mio desiderio ringraziare chi mi ha dato la possibilità di occuparmi di questo progetto e chi mi ha affiancato nella sua realizzazione.

Grazie allora al mio Relatore, il professor Danilo Demarchi. Auguro a chiunque di incontrare, almeno una volta nella vita, una persona come lui, dalla quale imparare che con l'umiltà, l'impegno e l'ambizione si possono fare grandi cose. Lo ringrazio per la fiducia che ha riposto in me fin dal primo momento, consegnandomi le chiavi di quel laboratorio silenzioso dove ho passato i miei ultimi sei mesi e che adesso già mi manca.

Grazie a te, Rossana, che sei stata la mia stella polare. Ti ringrazio per essere stata sempre il più solido sostegno ogni volta che ho perso l'equilibrio. Sono stata estremamente fortunata ad averti come co-relatrice, come instancabile guida e come amica. Sei una bella persona. Grazie di tutto.

Ringrazio anche te, Alessandro, mio co-relatore e artefice di sane risate. Sei stato per me l'utile e il dilettevole. Grazie per non aver mai innalzato superflue barriere di distanza. Grazie per la tua professionalità, per ogni impagabile consiglio e per ogni momento leggero.

Uno dei ringraziamenti più affettuosi va alla mia compagna di avventura, Francesca. Ti ringrazio per aver condiviso con me questo lavoro con la dedizione e la serietà che richiedeva. Questo percorso mi ha regalato anche te.

Vorrei poi ringraziare il dottore Davide Putignano, del centro oftalmico delle Molinette dove ho svolto la mia sperimentazione clinica. Grazie per avermi fornito le conoscenze mediche di cui necessitavo, con immensa disponibilità e simpatia.

Grazie anche a Sabrina e a tutti i ragazzi del laboratorio Civera, luogo di studio e di ricreazione. Grazie per avermi accolta e per avermi subito fatta sentire parte del gruppo, con l'allegria che vi contraddistingue.

Grazie ad Elena e ad Orlando, colleghi di laboratori sperduti e amici quotidiani. Vi ringrazio per aver alleggerito la mia permanenza tra cavi elettrici e strumentazione varia, per aver sempre parlato di cibo tra i miei alimentatori da banco e i vostri circuiti idraulici.

La mia infinita gratitudine va poi ad ognuna delle mie cavie. Grazie per esservi fidati di me anche quando le vostre espressioni lasciavano intendere altro. Grazie in particolare a te, Andrea, per essere stato la cavia per eccellenza.

*Avevo preannunciato dolci pensieri ed ecco allora ciò che voglio dire ai miei affetti più cari.*

Voglio ringraziare la mia mamma, la donna più forte che io conosca. Il mio raggio di sole. Grazie per aver capito e rispettato i miei silenzi. Grazie per tutto quello che ogni giorno fai per me. Grazie per i tuoi sorrisi. Sei la mia fortuna.

Grazie anche a te papà, mio complice di vita. Grazie per avere sempre creduto in me, come persona e come il buon ingegnere che spero di essere. Voglio ringraziarti per la serenità che provo tutte le volte che ti guardo negli occhi. Sei la mia certezza.

A mio fratello vorrei augurare tanta fortuna. Vincenzo, io voglio dirti grazie per la stima e la fiducia che nutri nei miei confronti. Non me lo dici mai, ma io lo so e per questo spero di continuare ad essere una buona sorella maggiore. Ti chiedo inoltre scusa per tutte le volte in cui non ci sono stata a dividere con te il peso dei nostri momenti poco felici.

La mia immensa gratitudine va ai miei nonni, Pina e Luigi. Siete stati la mia salvezza e siete la mia gioia. Su di voi potrei dilungarmi tanto ma mai nessuna parola sarebbe sufficiente a descrivere l'amore che ho per voi. Grazie di tutto.

Grazie a te, Paola, che sei il mio incontro fortunato. Grazie per aver condiviso con me ogni disastro e ogni gioia universitaria, per aver ascoltato ogni mia confidenza, sempre pronta a dire la tua con l'onestà che ti contraddistingue. Tutte le volte che vorrai, mi troverai. Mi troverai ogni volta. Per mille altri motivi, amica mia, io oggi ti ringrazio.

Vorrei adesso che il mio fiore più bello sapesse quanto è sincera la mia gratitudine. Parlo di te, Ivana. "Tu sei la sola al mondo che sa, del mio cuore". A te

voglio dire grazie per avermi sempre sostenuta. Lo sai che non amo le promesse, ma voglio solo dirti che per te ci sarò, ci sarò sempre, un sempre che non mente e che non mi fa paura.

Non posso dimenticarmi di te, Gigi, che sei il mio portatore sano di felicità. Voglio ringraziarti perché mi hai sempre mostrato tutta la bontà di cui è pieno il tuo cuore. Grazie per ogni sorriso sincero e per essere sempre stato il mio punto di riferimento. Grazie anche a te, mia dolce Serena, per essere sempre stata dalla mia parte.

Un ringraziamento speciale va alle mie bambine, Giuliana e Valeria. Vi ringrazio per la nostra serena quotidianità, per i piccoli gesti di affetto che non mi avete mai fatto mancare. Grazie per la vostra pazienza, per la vostra presenza e la vostra comprensione.

Grazie a te Pino e grazie a te Giuseppe. Ogni volta che vi guardo sento un bene profondo e una stima sincera.

Infine è mio desiderio ringraziare tre persone care e rare, Irene, Paola e Simone. Grazie perché con voi anche la domenica lontana da casa è sempre stata domenica! Grazie per la vostra semplicità e per l'amicizia che mi avete regalato. Grazie Irene per la tua lealtà.

Grazie a chi c'è da sempre e a chi, in punta di piedi, è entrato a far parte della mia vita. Nel ringraziarvi tutti mi rendo conto di quanto io sia fortunata.

*“Altra risposta non posso darvi che GRAZIE, e ancora GRAZIE”.*  
(William Shakespeare)

# Bibliography

- [1] Della Coletta E. *Potenziali Evocati*. <http://m.docente.unife.it/enrico.granieri/materiale-didattico/corso-opzionale-percorsi-diagnostici-innovativi-clinico-neurofisiologici-immunologici-sonologici-di-neuroimaging-e-medicina-nucleare-nelle-malattie-del-sistema-nervoso/potenziali-evocati-somato-sensitivi-pess-potenziali-evocati-visivi-pev-e-potenziali-evocati-acustici-baer>
- [2] Cindy L. Stanfield and William J. Germann. *Fisiologia*. Casa editrice EdiSES, terza edizione.
- [3] Stanzione P. and Pierantozzi M. *Potenziali evocati visivi e patologie neurologiche*. <http://fgeditore.it/relazione/soi/pdf/capitolo1/5Potenz.pdf>
- [4] Human eye anatomy. <https://www.varifocals.net/human-eye/>
- [5] Abrahamas P. *Atlante del corpo umano*. DIX editore, 2016.
- [6] *Anatomia dell'occhio*. <https://www.acuvue.it/salute-occhi/anatomia-occhio>
- [7] Accomodation eye. <https://en.wikipedia.org/wiki/Accommodationeye>
- [8] Visual pathway. <http://aminotes.tumblr.com/post/25518386232/the-crayola-fication-of-the-world-how-we-gave>.
- [9] Kenneth S. Saladin. *Anatomia umana*. Casa editrice PICCIN.
- [10] Structure of the retina. <https://discoveryeye.org/layers-of-the-retina/>
- [11] Raeba Mathew, Sobha Sivaprasad, James J. Augsburger, and Zélia M. Corrêa. *Vaughan and Asbury's GENERAL OPHTHALMOLOGY*, nineteenth edition.
- [12] Maculopatia. <https://it.wikipedia.org/wiki/Maculopatia>

- [13] Progressione della maculopatia. <http://www.bluemedicalcenter.com/cms/maculopatia/>
- [14] Maculopathy: Causes and Symptoms. <https://www.microchirurgiaoculare.com/en/maculopathy/causes-and-symptoms/>
- [15] Healthy eye and eye with AMD. <https://www.healththoroughfare.com/wp-content/uploads/2017/06/AMD-Disease.png>
- [16] Macular degeneration. <https://www.webmd.com/eye-health/macular-degeneration/ss/slideshow-macular-degeneration>
- [17] Dry vs Wet Age-Related Macular Degeneration. <https://www.macular.org/dry-vs-wet-macular-degeneration>
- [18] Degenerazione maculare senile. <https://www.docgenerici.it/patologie/degenerazione-maculare-senile/fattori-di-rischio>
- [19] Vottonen P., Paakkonen A., Tarkka Ina M. and Kaarniranta K. *Best-corrected visual acuity and retinal thickness are associated with improved cortical visual processing in treated wet AMD patients.*
- [20] Potenziali evocati visivi PEV. <https://albertobellone.it/potenziali-evocati-visivi/>
- [21] Terracciano R., Sanginario A., Barbero S., Putignano D., Canavese L. and Demarchi D. *Pattern-Reversal Visual Evoked Potential on Smart Glasses.*
- [22] Odom J.V., Bach M., Brigell M.G., Holder G.E., McCulloch D.L., Mizota A., and Tormene A.P. *Iscev standard for clinical visual evoked potentials: (2016 update).* Documenta Ophthalmologica, 2009.
- [23] Odom J.V., Bach M., Barber C., Brigell M., Marmor M.F., Tormene A.P., and Holder G.E. *Visual evoked potentials standard.* Documenta ophthalmologica, 108, 2004.
- [24] J. Vernon Odom, Michael Bach, Mitchell Brigell, Graham E. Holder, Daphne L. McCulloch, Atsushi Mizota and Alma Patrizia Tormene, International Society for Clinical Electrophysiology of Vision. *ISCEV standard for clinical visual evoked potentials,(2016update).*
- [25] Piscolo R. Università degli studi di Napoli, Federico II. Facoltà di medicina e

- chirurgia. *Potenziali evocati visivi nell'imaging intraoperatorio della funzionalità del nervo ottico.*
- [26] H.B. Barlow. Physiological Laboratory, Cambridge University. *Possible principles underlying the transformations of sensory messages*, 1961.
- [27] Cosenza F. *Realtà aumentata per dispositivi android: lo stato dell'arte.* PhD thesis.
- [28] Moverio BT-200 - Epson. <https://www.epson.it/products/see-through-mobile-viewer/moverio-bt-200>
- [29] g.HIamp-Research 256-Channel Research Amplifier. <http://www.gtec.at/Products/Hardware-and-Accessories/g.HIamp-Specs-Features>
- [30] Extended 10/20-System with 30 channels. <https://www.brainlatam.com/manufacturers/easycap>
- [31] Julie Racine. *Clinical Visual Electrophysiology: Visual Evoked Potentials.* November 15, 2015.